PLASTICITY IN MAMMALIAN SOMATOSENSORY CEREBELLAR MAPS

Thesis by

Josée Morissette

In Partial Fulfillment of the Requirements

for the Degree of

Doctor of Philosophy

California Institute of Technology

Pasadena, California

1996

(Submitted November 22, 1995)

Acknowledgments

The moral is, it hardly need be shown,
All those who try to go it sole alone,
Too proud to be beholden for relief,
Are absolutely sure to come to grief.

Robert Frost
Steeple Bush, 1947

I certainly did not do this alone. Many friends and colleagues have made this work possible and more enjoyable. By attempting to name a few, I am destined to leave out some who have also contributed in important ways. My sincere thanks extend to all those who have made my years at Caltech so memorable.

I would especially like to express my appreciation to my thesis adviser Jim Bower for providing a good research environment and for being there with advice and support when needed. I greatly benefited from his scientific versatility and critical comments. I am particularly grateful to my collaborators Leila González, Peter Gruen, Mitra Hartmann, Dieter Jaeger, Maurice Lee, Caroly Shumway, John Thompson, and all of the Bower lab members for their openness to discussion, for listening and helping; Erika Oller for her artful craftswomanship in her drawing of some figures included in this thesis; Leon Glass, Alvin Shrier, and Michael Mackey for inspiring and encouraging me to continue my studies; Walter Heiligenberg for the Bach sonatas, the sushi, and the words of encouragement; Bill Bing for giving me the opportunity to play with great musicians during my years at Caltech; Wyeth Bair, Ron Benson, Öjvind Bernander, Sylvain Clermont, Jack Hwang, Diane Laflamme, and Nadine Miner for the laughs, great dinners, volleyball, late night talks, and much more; Barbara Bray, Jim Bower, Jerry Pine, and many at Project

SEED for giving me the opportunity to experience and contribute to hands-on science education. Thank you all for your help, support, and friendship.

Finally, I am grateful to my family. A very special thanks goes to my husband John Morris for coping with me at my worst and for being the best friend and listener; our love and the peaceful refuge of your arms give daunting mountains a new perspective. Thank you, Chris, John, Suzy, Scott, and Nikolas for your immediate and constant love and support. Sans ma famille, je n'aurais pas eu le courage ou même l'idée d'entreprendre un projet si long et si loin d'eux. Merci, Papa, Maman, Chantal, Hughes, Rolande, Philippe, Mamie, Hélène, et Richard pour votre amour, soutien, et inspiration.

A mes parents

qui m'ont appris à rêver.

Abstract

The organization of sensory maps in mammalian brains can change following peripheral injury or experience. Such plasticity has been demonstrated for somatotopic somatosensory maps in various cortical and subcortical areas. In contrast to somatotopic maps, whose representation is distorted but nevertheless shows a detectable relationship to the topography of the body surface, cerebellar somatosensory maps have a fractured organization. Fractured cerebellar tactile maps display a mosaic of discrete, irregular patches representing nonadjacent areas of the body surface. This thesis describes the effect of peripheral injury on somatosensory maps in the cerebellum and the influence of their cortical and subcortical afferent structures on the pattern of reorganization.

In normal rats, cerebellar granule cell layer field potentials evoked by a brief tactile stimulus consist of two components at different latencies. We carefully investigated the temporal relationship between the evoked tactile responses of the somatosensory cortex (SI) and the cerebellar granule cell layer, and demonstrated that SI is the primary contributor to the long-latency cerebellar response to peripheral tactile stimulation.

Following lesion of the infraorbital branch of the trigeminal nerve, we investigated the developmental plasticity of the fractured tactile map in crus IIa. The tactile maps in the granule cell layer of crus IIa reorganized, maintaining a fractured somatotopy, after lesions made at all ages (from 1 to 90 days postnatal). The denervated upper lip region was consistently and predominantly replaced by representation of the upper incisors, a surprising result since this pattern does not correspond with plasticity studies in somatotopic somatosensory areas. The age of the animal at deafferentation affected the short-latency component of the cerebellar field potential but not the long-latency component. This suggests a difference in the developmental sensitivity of the cerebellum-related pathways to nerve lesion. Possible cerebellar mechanisms for the reorganization were examined. We

also explored reorganization in SI, an afferent structure, which we found to have a strong influence on cerebellar granule cell activity. The upper incisor representation in SI, which we showed to be adjacent to the upper lip representation in the cortex of normal animals, increased significantly in SI of deafferented rats. Our results suggest that the site of plasticity following deafferentation is not in the cerebellum itself but in its afferent pathways. To explore this possibility, a network model of the major somatosensory pathways to the cerebellum was developed. Computer simulations, assuming plasticity only in the cerebellar afferent pathways, produced patterns of cerebellar reorganization similar to those observed experimentally.

Table of Contents

List of Figures

List of Tables

1

Introduction

> *It is probably safe to say that sensitivity in no animal, with the possible exception of man, has never been investigated as thoroughly as in the rat. The story is, however, not yet complete. Large gaps still exist in our knowledge of certain aspects of sensitivity [...]. There is still much to be done before the precise cortical and subcortical contributions to various senses are disclosed.*
>
> N. L. Munn (1950)

Sensory representations in the brain display a remarkable capacity for reorganization following injury of cutaneous, retinal, or cochlear afferents and following sensory experiences (for reviews see Kaas 1991, 1994; Kossut 1992). This capacity for plasticity has been demonstrated for somatotopic somatosensory maps in various cortical and subcortical areas. Despite many studies, the mechanisms underlying reorganization and the location of such plasticity—whether cortical or subcortical—still remain a subject of considerable debate (for reviews see Snow and Wilson 1991; Kaas 1994).

This thesis describes the effect of peripheral injury on *somatosensory*[1] maps in the *cerebellum* and the influence of their cortical and subcortical afferent structures on the pattern of reorganization. Cerebellar tactile maps differ considerably in topography from

[1] The words "somatosensory" and "tactile" will be used interchangeably throughout the thesis.

their afferent structures. In contrast to somatotopic maps, whose representation is distorted but nevertheless shows a detectable relationship to the topography of the body surface, cerebellar somatosensory maps have a fractured organization. Fractured cerebellar tactile maps display a mosaic of discrete, irregular patches representing nonadjacent areas of the body surface. This fractured organization of cerebellar maps makes it possible to distinguish between central and peripheral adjacency[2], something difficult to accomplish with somatotopic maps. It is known that the cerebellar regions we studied receive direct projections from the trigeminal nuclei and indirect projections from the somatosensory cortex. We show that by identifying the cerebellar responses arising from each, the effects of peripheral injury in both pathways can be inferred without simultaneously recording in several structures. Because of this and their particular topography, cerebellar tactile maps provide a good model system for exploring the mechanisms responsible for reorganization following peripheral nerve lesion.

In this chapter, a brief review of the evidence for plasticity in somatosensory maps is presented, followed by a short description of somatosensory representations in the cerebellum. Finally, the contribution and organization of this thesis is described.

1.1 Plasticity in somatosensory maps

1.1.1 Reorganization of the somatosensory cortex

Reorganization of the tactile representation in the primary somatosensory cortex (SI) following peripheral injury has been demonstrated in several mammalian species including the monkey (Merzenich et al. 1983ab; Wall et al. 1983), the rat (Waite 1984; Wall and Cusick 1984), the mouse (Van der Loos and Woolsey 1973), the cat (Kalaska and Pomeranz

[2] Central adjacency refers to the adjacency of the representations of various body parts within a given tactile map found in the brain. Peripheral adjacency refers to the adjacency of body parts on the skin.

1979; McKinley and Smith 1990), the raccoon (Rasmusson 1982; Kelahan and Doetsch 1984), and the flying fox[3] (Calford and Tweedale 1988).

Various experimental approaches have been used to demonstrate reorganization in SI cortex. Elimination of inputs by amputation, deafferentation of peripheral nerves, or transection of the spinal cord leads to reactivation of deprived portions of SI by the remaining inputs. In an influential series of experiments on monkeys, Merzenich, Kaas, and their colleagues showed that after sectioning the median nerve that innervates part of the glabrous hand, there is a topographic expansion of the hairy part of the hand in area 3b of SI (Merzenich et al. 1983ab). They also demonstrated that amputation of the middle finger, digit 3, leads to reactivation of the denervated area of cortex by the adjacent fingers, digits 2 and 4 (Merzenich et al. 1984a). Similar expansion of intact inputs from adjacent cortical areas into the denervated area has been shown in the rat (Wall and Cusick 1984; Cusick et al. 1990). The extent and limit of reorganization are quite variable. Jain et al. (1995) found no reactivation of cortex in the three months following a dorsal column section that removed afferents from the hindlimb skin in the rat, while Cusick et al. (1990) reported that partial denervation of the hindlimb led to a progression of reactivation of the hindlimb cortex over several months. Following deafferentation of an entire limb and extended recovery, Pons et al. (1991) demonstrated a massive reorganization of SI.

Changes in cortical maps can also be induced by sensory experience. In the monkey, cortical representations of specially stimulated skin surfaces increase in area (Jenkins et al. 1990; Recanzone et al. 1992b) and surgical connection of two fingers results in a fusion of their normally discontinuous cortical representations (Allard et al. 1991). In the rat, change in sensory experience resulting from "whisker pairing" (i.e., leaving two whiskers intact while all others are trimmed close to the skin) for less than three days can alter cortical receptive fields (Diamond et al. 1993). Cortical lesions (Jenkins and

[3] An Australian fruit bat.

Merzenich 1987) and cortical stimulation (Recanzone et al. 1992a) can also reshape the tactile representation in SI.

Comparison of the cortical capacity for reorganization following comparable peripheral lesions in developing and adult animals has yielded contradictory results. Many studies show an increased capacity for SI of younger animals to adjust to loss of inputs (Kalaska and Pomeranz 1979; Waite 1984; McKinley and Smith 1990), some do not detect any difference (Kelahan et al. 1981), while others report a decrease in the size of the cortical reorganization following lesions in neonatal animals (Wall and Cusick 1986) compared to adult lesions (Wall and Cusick 1984).

A special form of cortical reorganization, *structural* plasticity, has been demonstrated in the developing but not in the adult rodent. A number of anatomical techniques, Nissl stain, immunocytochemistry of 5-HT, and histochemistry of succinic dehydrogenase, cytochrome oxidase, and AChE, reveal cytoarchitectonic units called barrels in layer IV of rodent somatosensory cortex (for reviews see Kossut 1992; Killackey et al. 1995). The pattern of barrels in SI is a faithful one-to-one representation of the spatial organization of the vibrissae (Woolsey and Van der Loos 1970). Anatomical changes in the barrel field occur following destruction of input from the vibrissae. This form of plasticity operates only during a critical period that ends a few days after birth (Woolsey and Wann 1976). Beyond postnatal days 5 or 6, anatomical changes to the normal pattern are not seen. Electrophysiological recordings, however, demonstrate a small expansion of intact inputs into the barrel cortex following deafferentation of the vibrissae in the adult rat (Waite 1984).

1.1.2 Mechanisms and location of reorganization

Despite the large body of knowledge on reorganization in the somatosensory cortex, the responsible mechanisms are still a topic of considerable debate. Numerous mechanisms have been proposed for the observed reorganization, such as immediate unmasking of

"silent" projections, potentiation of existing synapses, axonal sprouting, and formation of new synaptic contacts. But it is as yet unclear if the mechanisms underlying cortical reorganization are intrinsic to the cortex, take place in its afferent structures, or occur at several cortical and subcortical levels (for reviews see Snow and Wilson 1991; Kaas 1994).

There is some evidence for intrinsic cortical plasticity (somatosensory: Recanzone et al. 1992a; visual: Gilbert and Wiesel 1992) and, although not as extensively studied as the somatosensory cortical maps, there is also evidence for some plasticity in subcortical maps. There is considerable evidence for *anatomical* changes in the brainstem and thalamus following peripheral manipulations in developing animals (for review see Woolsey 1990). Electrophysiological mapping of the cuneate nucleus after fetal forelimb amputation (Rhoades et al. 1993) and of the trigeminal nuclei following neonatal peripheral nerve lesion (Waite 1984) demonstrate reactivation of most or all of the denervated area by intact adjacent inputs. Following peripheral nerve lesion in the adult rat, however, very limited or no evidence of plasticity could be detected in the trigeminal nuclei (Waite 1984) or the gracile nucleus (McMahan and Wall 1983). In the thalamus, there is evidence for reorganization even in adults (Rhoades et al. 1987; Garraghty and Kaas 1991b; Nicolelis et al. 1993). Following deafferentation of the glabrous hand in monkeys, there is an extensive reorganization of the hand representation in the ventroposterior lateral nucleus of the thalamus (Garraghty and Kaas 1991b) which parallels the reorganization in SI of the same monkeys (Garraghty and Kaas 1991a).

Thus, the general pattern of reorganization observed in SI, where the denervated areas are reactivated by adjacent intact representations, is also found in the thalamus and brainstem, implying that the reorganized cortical maps may simply be a reflection of changes occurring earlier in the sensory pathway.

1.1.3 Constraints on the study of plasticity in somatotopically organized maps

Examination of the neural receptive field or the use of anatomical tracers (in rodents) in the somatosensory cortex reveals a representation of the external body surface on the cortical surface. This map is not an exact representation of the body surface; the projection of the body surface onto the cortical surface is distorted. Further, there are discontinuities in the cortical map between parts of the body that are contiguous; for example, in SI of the monkey the face is separated from the rest of the head (Woolsey 1958). Conversely, adjacent cortical areas sometimes represent disjunctive body areas; for example, cortical representation of the face is adjacent to that of the forelimb in the rat (Welker 1971; Chapin and Lin 1984). In addition, the cortical area occupied by different body parts reflects the density of innervation and the importance of the sensory information from this region. For example, the hand representation is much larger than that of the trunk in humans, other primates, and raccoons (Penfield and Rasmussen 1950; Woolsey 1958) whereas SI of the rat is dominated by the whiskers (Welker 1971; Chapin and Lin 1984). Thus, the cortical representation is distorted, presenting a caricature of the body surface. Nevertheless, there is a detectable relationship between the body surface and its cortical representations. Maps that display such representations are referred to as *somatotopic*. Somatotopic maps have also been demonstrated in the subcortical areas discussed in section 1.1.2 (thalamus: Emmers 1965; Waite 1973; trigeminal nuclei: Nord 1967). Figure 1.1 shows the somatotopic somatosensory representation, also called ratunculus, for the somatosensory cortex, thalamus, and trigeminal nucleus in the rat.

Part of the difficulty in determining if SI reorganization results from mechanisms that are intrinsic or extrinsic to the cortex is that cortical maps and all of their afferent structures are somatotopically organized. Because the general pattern of cortical and subcortical reorganization involves adjacent intact representations expanding into the denervated areas (Wall and Cusick 1984; for review see Kaas 1994), SI reorganization

could, in principle, result from reorganization in any of several locations, including the periphery (Snow and Wilson 1991). Therefore, unambiguously identifying the mechanisms responsible for the reorganization of SI is likely to require simultaneous investigation of SI and its afferent structures.

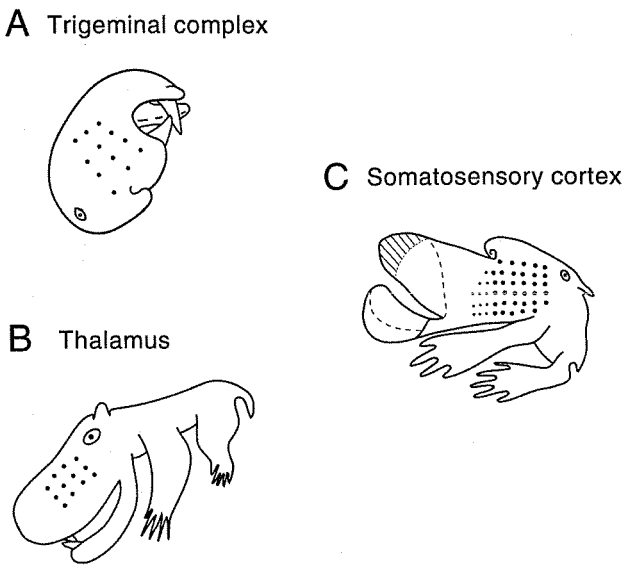

Figure 1.1 Ratunculi, or schematic representations of the somatotopic organization of various cortical and subcortical areas in the rat. **A:** The organization of the spinal trigeminal nucleus Interpolaris is shown in a coronal plane (adapted from Nord 1967). **B:** The thalamic map is shown in a coronal plane (adapted from Emmers 1965). **C:** The somatosensory cortex map is shown in a horizontal plane (adapted from Welker 1971; Chapin and Lin 1984). The dots represent vibrissae; hatched area, furry buccal pad; and broken lines, portions of the upper and lower lip that curve inside the mouth.

1.2 Cerebellar fractured somatosensory maps as a model system to explore mechanisms of reorganization

Unlike cortical and subcortical maps, somatosensory maps found in the lateral hemispheres of the mammalian cerebellum are not somatotopically organized, but rather have a complex, "fractured" somatotopy (for review see Welker 1987). The advantage of studying reorganization in the cerebellar fractured somatosensory maps is that they enable one to distinguish between peripheral and central adjacency. These tactile maps display a mosaic of tiny irregular patches (generally 0.1 to 1 mm^2) representing various parts of the body. Adjacent cerebellar areas often represent nonadjacent body areas. Within a patch, i.e., a cerebellar area receiving input from a particular body structure, the representation for that body structure is somatotopically organized. This fractured pattern of tactile inputs has been demonstrated in rats (Joseph et al. 1978; Shambes et al. 1978ab; Bower and Kassel 1990), cats (Kassel et al. 1984), opossums (Welker and Shambes 1985), and the primate *Galago crassicaudatus* (Welker et al. 1988). As shown in Figure 1.2, the somatosensory projections occupy a large portion of the cerebellum: all the hemispheric folia (except the copula) as well as several folia of the anterior and posterior vermis. Cutaneous projections are predominant in these regions, with some proprioceptive afferents present. All maps presented in this thesis represent the cutaneous inputs exclusively. Each folium receives tactile input from a characteristic set of body structures. For example, the hindpaw is usually represented in the paramedian lobule, PML, but not in crus II. Within a fractured map, there are often several patches representing a specific body structure. Further, a body structure may be represented in several folia (Figure 1.2).

These fractured maps are obtained by detailed, high-density mapping of the tactile projections to the granule cell layer. In that layer, mossy fibers from various regions of the central nervous system (CNS) synapse onto granule cells, the only excitatory and smallest (5–8 μm diameter) cells in the cerebellum. A given mossy fiber can innervate a small

granule cell layer area but can also send branches to several folia (Mihailoff 1983). Although the anatomical spread of individual mossy fibers has not been determined, the examination of horseradish peroxidase-labeled mossy fiber terminals of spinal projections to the rat cerebellar anterior lobe indicates a complex topography analogous in several aspects to the small neurophysiologically defined patch (Tolbert et al. 1993).

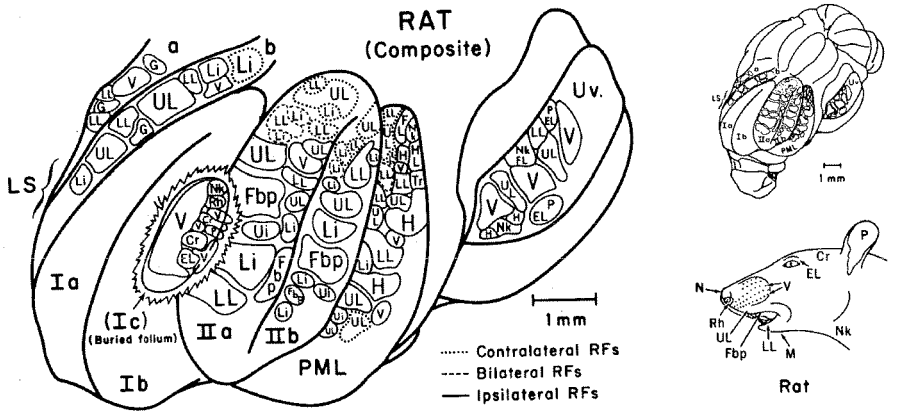

Figure 1.2 Fractured somatotopy in the hemispheres and posterior vermis of the rat cerebellum. *Abbreviations:* LS: lobulus simplex; Ia, Ib: the two surface folia of crus I; Ic: the buried folium of crus I; IIa, IIb: the two folia of crus II; PML: paramedian lobule; Uv: uvula; Cr: crown; EL: eyelid; Fbp: furry buccal pad; FL: forelimb; G: gingiva; H: hand; HL: hindlimb; Li: lower incisor; LL: lower lip; M: mandible; N: nose; Nk: neck; P: pinna; Rh: rhinarium; Tr: trunk; Ui: upper incisor; UL: upper lip; V: vibrissae. (From Welker 1987, with permission.)

Electrophysiological experiments have shown that the fine structure of the tactile projection patterns to the cerebellum appears to reflect the complex but apparently precise branching pattern of mossy fiber afferents. Recent developmental evidence has suggested a possible genetic specificity for some of the cerebellar projections (Sotelo 1995).

Electrophysiological examination of the trigeminocerebellar mossy fiber branching reveals that collaterals from a single trigeminal neuron terminate exclusively in regions of the granule cell layer, within a folium or across folia, that respond to tactile stimulation of the same body area (Woolston et al. 1981). In addition to the direct trigeminal mossy fiber projection, the granule cell layer of the cerebellum also receives equally precise projections from the somatosensory cortex and superior colliculus through the pontine nuclei (Kassel 1980; Bower et al. 1981). Using threshold stimulating current in SI, Bower and his colleagues (1981) showed that the projections from a site in SI responding to a particular skin location influence regions in the cerebellar granule cell layer receiving information from the same skin location directly from the trigeminal nuclei. Similarly, Kassel (1980) demonstrated that projections from the superior colliculus are confined within cerebellar patches of similar receptive field and overlap spatially with peripheral trigeminal projections. In summary, tactile information reaching the cerebellum from the somatotopically organized trigeminal nuclei, somatosensory cortex, and superior colliculus is in register spatially and conforms to the patch-like fractured somatotopy identified in the cerebellar granule cell layer.

1.3 Overview of this thesis

The work presented in this thesis examined the tactile inputs to the crus IIa folium in the cerebellar hemisphere of the rat. We have shown that a detailed analysis of the temporal structure of cerebellar field potentials evoked by tactile stimulation can distinguish between inputs from the trigeminal and the cerebrocerebellar pathways. We thus used cerebellar field potential analysis to draw inferences on the effects of peripheral injury on the trigeminocerebellar and the cerebropontocerebellar pathways without having to record simultaneously from many brain areas.

The upper lip and vibrissae representations occupy a large area in the center of crus IIa. Therefore, deafferentation of the upper lip and vibrissae by sectioning the infraorbital branch of the trigeminal nerve denervates a large portion of the map. We demonstrated that cerebellar somatosensory maps reorganize extensively following peripheral nerve lesion at all ages tested. Our results suggest that the reorganization we observed in crus IIa following nerve section does not arise through intrinsic cerebellar mechanisms but rather appears to be a reflection of reorganization in its afferent pathways.

The following outline briefly summarizes each chapter and indicates references for material that has been published.

- **Chapter 2** describes the temporal relationship between the responses evoked in the somatosensory cortex (SI) and in the cerebellar hemisphere by peripheral tactile stimulation. Cerebellar granule cell layer field potentials evoked by brief tactile stimulations consist of two components at different latencies. We demonstrate that the second component of the cerebellar field potentials is primarily due to input from SI. The results presented in this chapter lay the groundwork for the analysis of the peripherally-evoked field potential in the remainder of the thesis. This chapter has been accepted for publication in *Experimental Brain Research* (Morissette and Bower 1996).

- **Chapter 3** presents the results of deafferentation experiments in which the infraorbital branch of the trigeminal nerve was sectioned in rats 1 to 30 days postnatal. When examined two months later, the cerebellar tactile maps had reorganized extensively but maintained a fractured somatotopy and several other features of normal maps. This is the first demonstration of cerebellar plasticity following peripheral injury. The material presented in this chapter was published in the *Journal of Comparative Neurology* (González et al. 1993).

- **Chapter 4** describes the reorganization of cerebellar tactile maps following deafferentation in *adult* animals. Here we show that cerebellar sensory maps reorganize even in animals deafferented later in development (40–85 days after birth) and that the

pattern of reorganization is similar to that observed in neonates. The pattern of reorganization immediately following nerve lesion, however, does not predict the pattern found two to three months later. The effect of age at deafferentation on the temporal structure of the cerebellar field potential is discussed.

- **Chapter 5** explores the mechanisms of reorganization by contrasting lesion-induced reorganization in the cerebellum and the somatosensory cortex. We show that the expansion of the upper incisor representation in crus IIa is paralleled by a similar expansion in the somatosensory cortex. We argue that this, combined with results from Chapter 4, suggests that cerebellar map reorganization is influenced by the reorganization of its afferents.

- **Chapter 6** describes a network model of the major somatosensory pathways to the cerebellum that was developed to explore the possibility that the site of plasticity following deafferentation is not in the cerebellum itself but in its afferent pathways. Computer simulations, assuming plasticity only in the cerebellar afferent pathways, produced patterns of cerebellar reorganization similar to those observed experimentally.

- **Chapter 7** summarizes the major contributions of this work and discusses directions for future research.

Part of this work was done in collaboration with Leila González (Chapter 3), Peter Gruen (Chapter 4), Maurice Lee (Chapter 6), and Caroly Shumway (Chapters 3, 4, 5).

2

Temporal Relationships of Cerebral and Cerebellar Responses to Tactile Stimulation

You will see something new.
Two things. And I call them
Thing One and Thing Two.

Dr. Seuss
The cat in the hat, 1957

2.1 Abstract

The spatial coincidence of somatosensory cerebral cortex (SI) and trigeminal projections to the cerebellar hemisphere has been previously demonstrated. In this chapter we describe the temporal relationship between tactilely-evoked responses in SI and in the granule cell layer of the cerebellar hemisphere, in anaesthetized rats. We simultaneously recorded field potentials in areas of SI and of the cerebellar folium crus IIa with common receptive fields following peripheral tactile stimulation of the corresponding face area. The response of the cerebellar granule cell layer to a brief tactile stimulation consisted of two components at different latencies. We found a strong correlation between the latency of the SI response and that of the second (long-latency) cerebellar component following facial stimulation. No such relationship was found between the latency of the SI response and that of the first (short-latency) cerebellar component, originating from a direct trigeminocerebellar pathway. In addition, any one of lidocaine pressure injection into SI,

cortical ablation, and decerebration significantly affected the second cerebellar peak but not the first. Further, when tactile stimuli were presented 75 msec apart, the response in SI failed, as did the second cerebellar peak, while the short-latency cerebellar response still occurred. We found a wide spatial distribution of the upper lip response beyond the upper lip area in crus IIa for the long-latency component of the cerebellar response. Our results demonstrate that SI is the primary contributor to the cerebellar long-latency response to peripheral tactile stimulation. These results are discussed in the context of Purkinje cell responses to tactile input.

2.2 Introduction

Tactile projections to the granule cell layer of the rat cerebellar hemispheres are organized in a fine grained fractured somatotopic pattern (Shambes et al. 1978ab; Welker 1987) that is remarkably similar between different individuals (Bower and Kassel 1990). Electrophysiological experiments have demonstrated that the fine structure of these projection patterns appears to reflect the complex, but apparently precise, branching pattern of mossy fiber afferents (Woolston et al. 1981; Welker 1987). Neurons in the trigeminal complex with upper lip receptive fields project exclusively to regions of the granule cell layer that also respond to upper lip stimulation (Woolston et al. 1981). These direct trigeminal projections also appear to be responsible for the short-latency component of the granule cell layer response to peripheral stimulation (Woolston et al. 1981).

In addition to the organized pattern of direct trigeminal projections to the granule cell layer, projections from somatosensory cortex through the pontine nuclei also follow a precise pattern (Bower et al. 1981). These projections are organized such that regions of SI cortex responding to a particular location on the skin influence regions in the granule cell layer receiving information from the same location on the skin directly from the trigeminal nuclei. Therefore, tactile information reaching the cerebellum indirectly through

somatosensory cortex is in register spatially with information received directly from the trigeminal nucleus.

In this chapter we examine in detail the relative timing of these two different influences in the cerebellar granule cell layer by recording simultaneously from SI and the cerebellum. Kennedy, Grimm and Towe (1966) have shown in cats that cerebral cortex has a large influence in tactilely responsive cerebellar regions and that this influence occurs at a later latency than the direct projection. We have confirmed that this is the case for rats, and have extended these previous results to carefully quantify the spatial extent of the influence of SI in the cerebellar regions. We have also documented differences in the variability in the timing of the short- and long-latency cerebellar responses to peripheral stimulation with respect to the SI response. We believe that these different temporal and spatial patterns of the direct and indirect tactile projections to cerebellum (Figure 2.1A) are likely to have important implications for cerebellar cortical processing. An abstract describing these results has been published (Morissette et al. 1991).

2.3 Methods

2.3.1 Animal preparation

Eight adult Sprague-Dawley albino rats (1 male, 7 females) were anaesthetized with sodium pentobarbital (12 mg/kg body weight) and ketamine hydrochloride (50 mg/kg body weight) injected intraperitoneally. Supplemental doses of ketamine (15 mg/kg body weight) were given as needed to suppress reflexive activity. The right cerebral cortex (SI) and the left cerebellar cortex (crus IIa) were surgically exposed and covered with mineral oil following standard procedures (Bower et al. 1981). The trachea was cannulated to facilitate respiration. Rectal temperature was maintained at 36 to 37°C and heart rate was monitored (280–410/min). Further details on surgical procedures can be found in previous

publications (Bower and Woolston 1983; Bower and Kassel 1990). The experiments conformed to the "Principles of laboratory animal care" (NIH publication 85–23, revised 1985).

2.3.2 Electrophysiological procedures

Multiunit activity and/or field potentials were recorded in the granule cell layer (400–700 μm deep) of crus IIa of the cerebellum and in layer IV (600–1000 μm deep) of SI cortex. Glass microelectrodes filled with 2 M NaCl with tip diameter of 5–10 μm and impedance of 1–3 MΩ were used. Neural signals were amplified, selectively filtered (multiunit activity: 300 to 3000 Hz bandpass; field potential: 1 to 1000 Hz bandpass), displayed on an oscilloscope, and made audible via speakers following standard procedures.

As previously noted (Bower and Kassel 1990), multiunit and field potential recordings in cerebellum do not distinguish between electrical activity originating from mossy fibers and that originating from granule cells. We are therefore not claiming that our recordings represent exclusively one or the other source. Instead, in these experiments, we have only attempted to assess the patterns of activity induced by peripheral stimuli at particular locations in the granule cell layer. Previous studies have made it clear that tactile maps obtained using the same procedures as ours actually represent the spatial pattern of mossy fiber inputs to these regions of the cerebellum (Woolston et al. 1981). It has also been shown that these granular cell layer responses are well correlated spatially and temporally with overlying Purkinje cell responses using both extracellular (Bower and Woolston 1983) and intracellular (Jaeger and Bower 1994) recordings *in vivo*. Thus, these physiological studies indicate that activity recorded in the granule cell layer is also correlated with the activation of the synapses of the ascending granule cell axon on Purkinje cells.

2.3.3 Tactile stimulation

In each experiment, controlled tactile stimulation of the facial surface was obtained using a custom-built tactile stimulator based on a Ling vibrator from Gearing & Watson Electronics (Chubbuck 1966). Direct feedback control of the stimulator was achieved by sensing displacement of the probe position. In the current experiments, a square wave (5, 10, or 50 msec width) with a total probe excursion of 0.5 mm was used. The tip of the stimulation probe was less than 1 mm in diameter. Stimulus trials consisted of 5 to 50 sequential stimuli presented with an interstimulus interval of 2 seconds. Timing of stimulus trials was controlled using custom software running on an IBM personal computer. More information on electrophysiological procedure can be found in Chapter 3.

2.3.4 Experimental design

For six of the animals, standard receptive field mapping techniques (Welker 1971, 1973; Shambes et al. 1978ab; Bower et al. 1981) were first used to locate regions of SI cortex and the cerebellar granule cell layer with common receptive fields. As mentioned in the introduction, previous mapping experiments have demonstrated that an SI locus influences cerebellar regions with which it shares overlapping peripheral receptive fields (Bower et al. 1981). In several cases, the influence of these SI locations on the locus of cerebellar recording was directly confirmed by electrically stimulating SI cortex and observing the responses in the granule cell layer (not shown here, see Bower et al. 1981).

Once corresponding regions of SI cortex and the cerebellar granule cell layer had been established, two general strategies were used to determine the specific contribution of SI cortex to peripherally evoked cerebellar responses. In the first, peripheral tactile stimuli were presented, at least 2 seconds apart, while recordings were made simultaneously in SI and crus IIa. The latencies and amplitudes of responses in both locations were then compared: (1) under normal conditions, (2) following a 0.15 cc peritoneal injection of

sodium pentobarbital, and (3) as the time delay within pairs of tactile stimuli was shortened (the time delay between pairs of stimuli was at least 2 seconds).

In the second approach, cerebellar responses were recorded after several different methods were used to interfere with the physiological integrity of SI cortex. In these experiments, cerebellar responses were recorded before and after: (1) local SI pressure injection of 2% Lidocaine HCl (approximately 30 μl) in layer V-VI of SI (1500 to 2500 μm), (2) local ablation of SI cortex (aspiration with a glass pipette), and (3) complete midcollicular decerebration (knife cut at the brachium of the superior colliculus). In order to minimize the number of animals used in these experiments, several of these procedures were performed sequentially in each animal. For example, in one animal, recordings were made following a series of ever larger local ablations of SI cortex and then following a complete midcollicular decerebration.

For the remaining two animals (one shown in Figure 2.6), only the cerebellar cortex was surgically exposed. The tactile stimulator was then positioned at the precise location on the face that elicited the strongest response (bottom inset of Figure 2.6). Fifty peripheral tactile stimuli were given, with two seconds delay between each stimulation, and the field potential responses were recorded. Crus IIa was then mapped by making 40 to 50 electrode penetrations spaced 100–200 μm apart in three medio-lateral columns. At each electrode penetration, the location on the face that elicited the strongest response when stimulated, i.e., the receptive field, was noted, but the tactile stimulator stayed in the same location (circle with the "1" inside, bottom inset Figure 2.6) for the entire experiment. As the electrode was moved away from the center of the upper lip patch, the waveforms occasionally became more complex, for example, they might exhibit a third and/or fourth distinguishable peak within 50 msec after stimulation onset. The first and second cerebellar peaks described in this paper were identified by their latencies. The peak amplitudes of both the short- and the long-latency cerebellar responses to 50 tactile stimulations (2 sec

between stimuli) were measured and averaged. The diameter of each filled circle in Figure 2.6 represents the average value at each electrode penetration.

2.3.5 Map construction

As in previous experiments (Welker 1987; Bower and Kassel 1990), cerebellar tactile maps were constructed by drawing enclosing boundaries around adjacent electrode penetration locations whose receptive fields were from the same body structures. In cases where stimulation of more than one peripheral location could induce a response in a particular penetration, the region eliciting the strongest response was recorded. When responses were of equal strengths, the boundary line was drawn through the site of the electrode penetration.

2.3.6 Data analysis

In order to quantify the effects of the experimental manipulations on cerebellar field potentials, analog responses were digitized and stored on a MassComp 5700 laboratory computer. Off-line analysis was done on a Sun SPARCstation 2. The digitized responses were read by a custom-developed C program that measured the latencies and amplitudes of single responses. The latencies were defined as the time from the onset of stimulator movement to the time at the peak of the evoked response. The amplitudes were defined as the difference between the average of the potential for 100 msec before the onset of the peripheral stimulus and the peak value of the field potential. Comparisons between control and drug applications (sodium pentobarbital and lidocaine) were done using a paired nonparametric Mann-Whitney U test (Ross 1987). All measures of variability described here are standard errors, SE. V is the coefficient of variation, the standard deviation expressed as a percentage of the mean; and r is the coefficient of correlation.

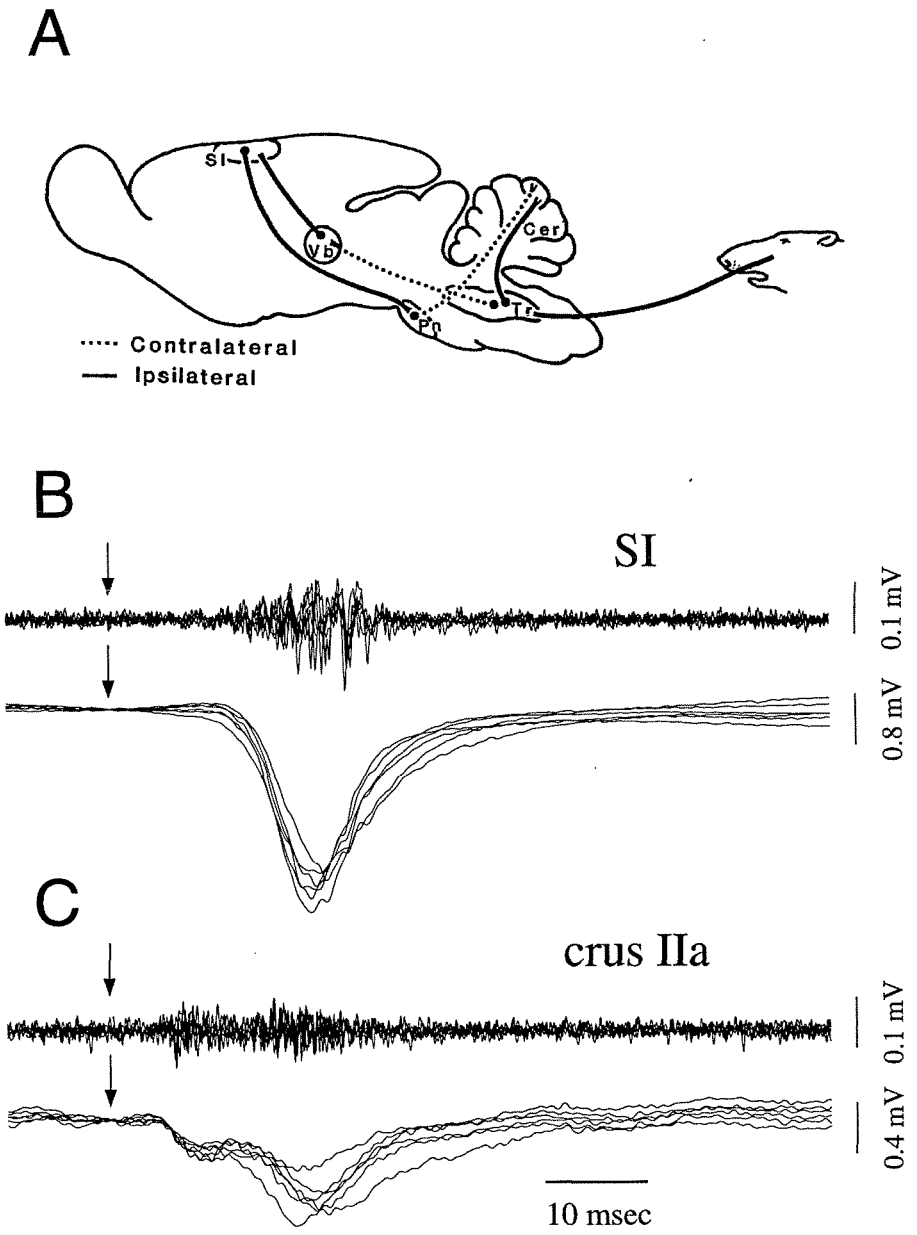
A
SI
Vb
Cer
Pn
Tr
Contralateral
Ipsilateral
B
SI
0.1 mV
0.8 mV
C
crus IIa
0.1 mV
0.4 mV
10 msec

Figure 2.1

Figure 2.1 **A:** Simplified circuit diagram of the tactile mossy fiber inputs to the crus IIa folium in the cerebellar hemispheres. The diagram illustrates the major pathways: a direct path from the ipsilateral trigeminal complex and an indirect path from the contralateral somatosensory cortex via various pontine nuclei. Several other areas not shown, including the superior colliculus, also project to crus IIa (Kassel 1980; Brodal 1981; Huerta et al. 1983; Marfurt and Rajchert 1991). Cer: cerebellum; Tr: trigeminal complex; Vb: ventrobasal complex of the thalamus; SI: somatosensory cortex; Pn: pons. **B–C:** Cerebral (B) and cerebellar (C) cortical responses to a brief (10 msec) peripheral tactile stimulus of the upper lip. Traces show typical field potentials recorded simultaneously in layer IV of the somatosensory cortex, SI (B) and in the granule cell layer of crus IIa (C). Recording electrodes were in an upper lip region in both SI and crus IIa. Responses to six consecutive stimuli, delivered two seconds apart, are superimposed. Arrows indicate the onset of the stimuli. ***Top traces:*** Multiunit activity, bandpass filtered digitally from 300 to 3000 Hz. ***Bottom traces:*** Field potentials, same recordings as in top traces bandpass filtered digitally from 1 to 1000 Hz. Positivity upwards in this and all subsequent figures.

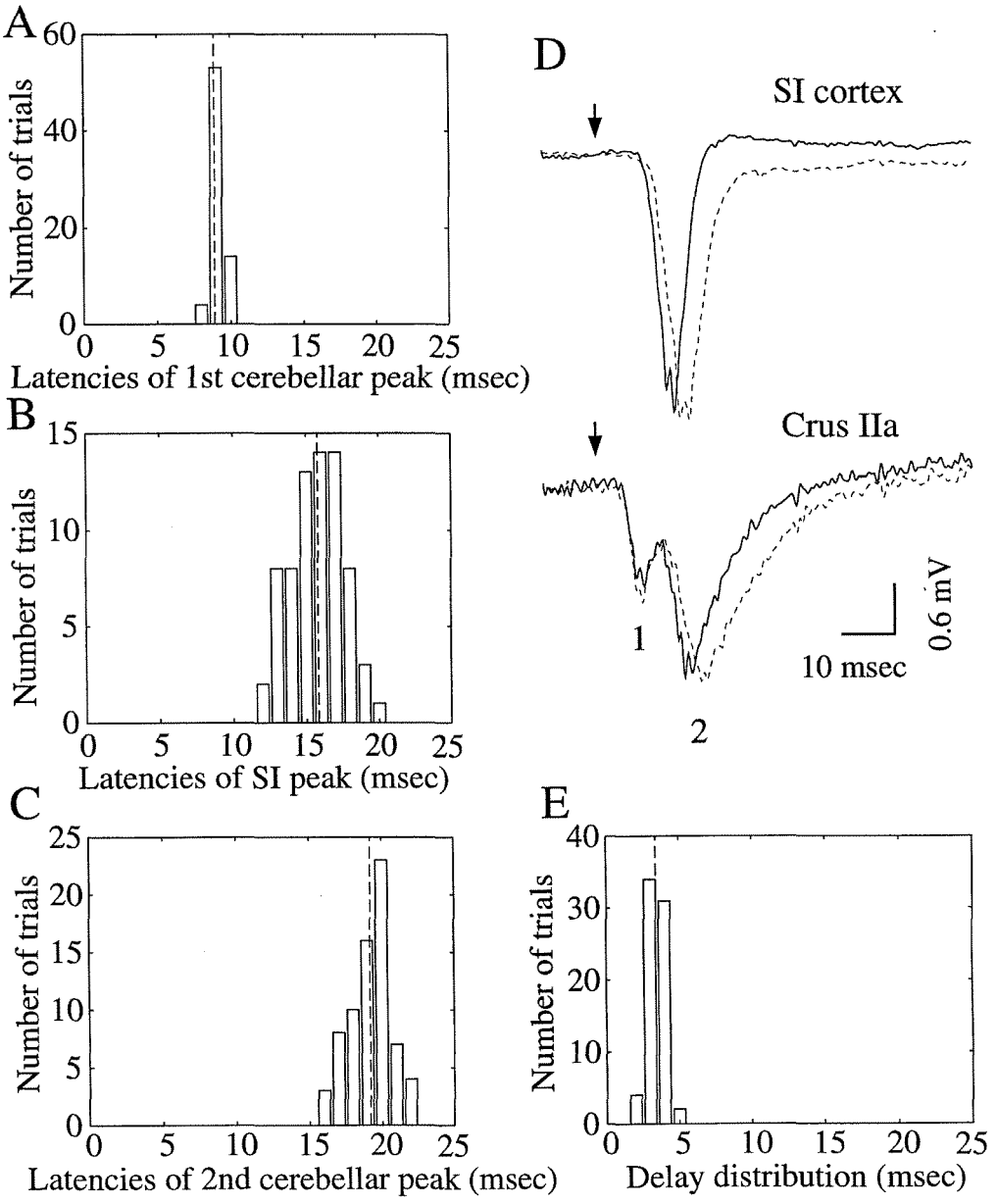
A
Number of trials
Latencies of 1st cerebellar peak (msec)
B
Number of trials
Latencies of SI peak (msec)
C
Number of trials
Latencies of 2nd cerebellar peak (msec)
D
SI cortex
Crus IIa
1
2
10 msec
0.6 mV
E
Number of trials
Delay distribution (msec)

Figure 2.2

Figure 2.2 Histograms of the latencies of the cerebral and cerebellar responses to tactile stimulation of the upper lip. Latencies were measured as the time elapsed from the onset of the stimulus to the time at the peak amplitude of the response. Histograms were constructed from the responses to 71 consecutive peripheral stimulations, at least 2 seconds apart, in one animal. All histogram bins are 1 msec. The dotted line on each graph denotes the mean latency (A, B, C) or mean of latency difference (E). **A:** Histogram of the latencies of the short-latency component of the cerebellar field potentials (shown as 1 in D). **B:** Histogram of the latencies of the SI responses to stimulation of the upper lip. **C:** Histogram of the latencies of the long-latency component of the cerebellar granule cell layer field potentials (shown as 2 in D). Note how the cerebellar first peak latencies (A) are more tightly grouped together than are the SI (B) and second cerebellar (C) latencies. **D:** Simultaneous cortical (*top traces*) and cerebellar (*bottom traces*) field potential responses elicited by peripheral tactile stimulation of the upper lip. Two consecutive responses are superimposed. Peripherally evoked cerebellar field potentials consisted of two components: one with short-latency (peak shown as 1) and one with long-latency (peak shown as 2). Response to first stimulus (*solid line*): cerebellar response peaked at 8.6 and 17.8 msec, cerebral cortex response peaked at 14.6 msec. Response to second stimulus (*dashed line*): cerebellar response peaked at 8.6 and 20.4 msec, cerebral cortex response peaked at 17.0 msec. Arrows denote the time of stimulation. **E:** Histogram of the difference, for each trial, between the latency of the second cerebellar peak and that of the SI response following a peripheral stimulation.

2.4 Results

2.4.1 Cerebellar granule cell layer and SI cortex responses to peripheral stimulation

Punctate tactile stimulation to the face elicited a burst of activity in layer IV of SI and a double burst in the granule cell layer of crus IIa in the rat (Figure 2.1). A brief (10 msec) stimulation of the upper lip led to characteristic bursts of multiunit activity in an upper lip region of both SI and crus IIa (top traces, Figure 2.1 B and C, respectively). Each burst of population spiking was associated with a negative peak in the local field potential (bottom traces, Figure 2.1 B and C). A typical cerebellar response to a tactile stimulus consisted of an initial short-latency response (range: 8–10 msec) followed by a second, long-latency, component peaking in amplitude between 16 to 22 msec. Different animals showed slight differences in the range of latencies (less than 2 msec) for both cerebellar peaks. For a sample of 71 cerebellar and cortical responses to stimulation in one animal, we found that the latency of the first cerebellar waveform, or short-latency response, stayed fairly constant, 8.94 ± 0.05 msec, V = 4.6%; as did its amplitude, 1.10 ± 0.01 mV, V = 8.4% (Figure 2.2A, latency only). In contrast, the second cerebellar waveform, or long-latency response, was more variable in latency, 19.19 ± 0.17 msec, V = 7.4% and amplitude, 2.06 ± 0.03 mV, V = 11.8% (Figure 2.2C, amplitude not shown). The cerebral cortex (SI) response to the same stimulus consisted of a single waveform with latencies ranging from 12 to 20 msec. As shown in Figure 2.2B (latency only), the SI response was highly variable in latency and amplitude, 15.76 ± 0.21 msec, V = 11.3%, 2.77 ± 0.10 mV, V = 31.0%.

2.4.2 Correlation between the latency of the SI response and that of the second component of the cerebellar response

The latency of the second peak in crus IIa was highly variable, as was that of the SI response, but their latencies varied together. This is illustrated in Figure 2.2D which shows

two consecutive pairs of simultaneously recorded cerebellar and cerebral responses to tactile peripheral stimulation of the upper lip. The two cerebellar peaks evoked by peripheral stimulation are denoted as 1 and 2 (Figure 2.2D). We will henceforth refer to the first cerebellar peak (denoted as 1 in Figure 2.2D) as the first, or short-latency, response and to the second cerebellar peak (denoted as 2 in Figure 2.2D) as the second, or long-latency, response. The short-latency responses, 1 in Figure 2.2D, both peaked 8.6 msec after the onset of the stimuli. The long-latency responses, 2 in Figure 2.2D, peaked at 17.8 and 20.4 msec after the tactile stimuli, 3.2 and 3.4 msec respectively after the cerebral cortex response (Figure 2.2D, top traces). The peak of the long-latency response in crus IIa occurred on average 3.44 ± 0.07 msec after the peak of the SI response ($V = 17.8\%$, $n = 71$ in one animal), Figure 2.2E. While varying over a much smaller range than the SI or the second cerebellar responses (compare width of Figure 2.2 E with that of B and C), this delay between the response in SI and the long-latency component of the cerebellar response was not constant. When the latency of the tactilely-evoked SI response was in the later part of the normal range, the delay tended to be shorter than when the SI response was in the early part of the normal range (not shown).

Figure 2.3 compares the latencies of cerebellar and SI responses for four different animals. The latency of the second cerebellar peak and that of the cortical response to stimulation were highly correlated in each case, $r = 0.95$, 0.61, 0.61, and 0.80 (Figure 2.3 A–D respectively, circles), and regression lines fit to the data were significant ($P = 0.0001$). The slopes of the regression lines are $m = 0.7$, 0.5, 0.7, and 0.7 (Figure 2.3 A–D respectively, circles). Note that these slope values are consistent with the delay between the SI response and the second cerebellar component response being shorter when the SI response occurred later, as mentioned in the previous paragraph. In contrast, the latency of the first cerebellar peak was less variable and not correlated with the cerebral peak latency (for all 4 animals shown in Figure 2.3, crosses: $r < 0.2$, regression analysis was not significant, $P > 0.1$).

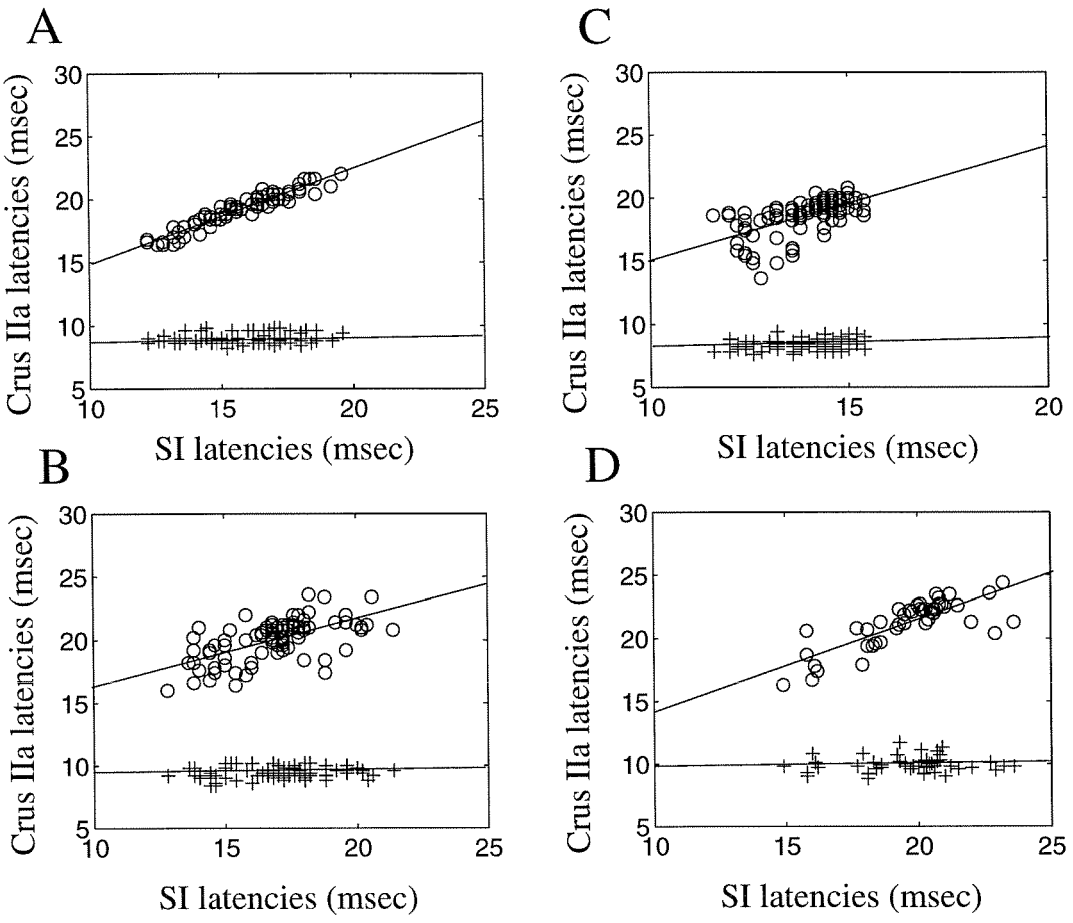

Figure 2.3 Relationship between the latencies of the two peaks of the cerebellar field potential and that of the peak of the cerebral cortical field potential. Crosses represent the cerebellar first peak latencies. Open circles represent the cerebellar second peak latencies. For four different animals (A through D), waveforms were recorded simultaneously in crus IIa and SI following tactile stimulation of the upper lip. The latencies of the second peak of the cerebellar waveforms varied considerably as did the latencies of the peak of the SI cortical waveforms, however, the latencies of these two responses were highly correlated. In contrast, the latencies of the first peak of the cerebellar field potentials were more constant and not correlated with the SI response. Linear regression lines are shown for both cerebellar peaks for each animal; see text for r and P values.

2.4.3 Effects of sodium pentobarbital on SI and cerebellar responses

A 0.15 cc intraperitoneal injection of the barbiturate sodium pentobarbital (Nembutal) caused a significant (as judged by a Mann-Whitney U test, P = 0.0001) amplitude decrease in the cerebral peak as well as in both peaks of the cerebellar field potential (Figure 2.4 B and D). The injection also caused a significant (as judged by a Mann-Whitney U test, P = 0.0001) increase in the latencies of both the cerebral and cerebellar responses (Figure 2.4 A and C). However, the strong correlation between the long-latency cerebellar and SI responses persisted after the sodium pentobarbital injection, before: r = 0.95, after: r = 0.86; the slope of the regression line stayed constant before and after at 0.7 and was significant, P = 0.0001 (Figure 2.4 A and C, circles).

2.4.4 Effects of increased frequency of tactile stimulation

The standard time between each tactile stimulation was at least 2 seconds; however, in some experiments, paired pulses with variable interstimulus intervals (of less than 2 seconds) were given. As shown in Figure 2.5, this had a significant, albeit different, effect on the SI and cerebellar responses. At a 75 msec interstimulus interval, the second stimulus elicited only the short-latency cerebellar response and not the long-latency cerebellar response. At these short interstimulus intervals, cortical traces following the second stimulus also showed very little or no response (Figure 2.5A). Figure 2.5B shows three examples of responses obtained when the interstimulus interval was increased to 85 msec. Following the second stimulation of the pair, in some cases, neither cerebral nor cerebellar long-latency responses occurred (Figure 2.5B, dotted line: a). At other times (Figure 2.5B, solid line: b), a small amplitude cerebral response was observed (7% of the amplitude of the response to the first stimulation) but no cerebellar long-latency response occurred. Finally, some traces following the second stimulation showed a larger amplitude SI response (71% of the amplitude of the response to the first stimulation) as well as a cerebellar long-latency

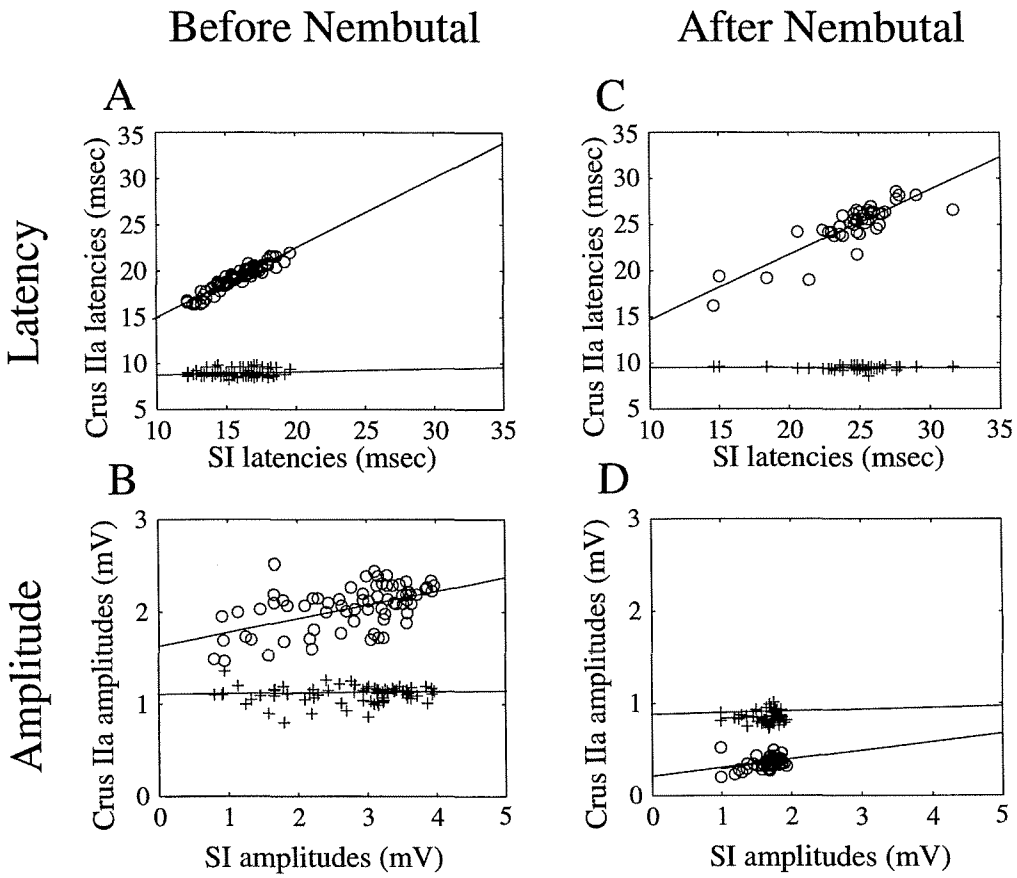

Figure 2.4 Effects of a 0.15 cc intraperitoneal injection of sodium pentobarbital (Nembutal). Results are shown before (**A**, **B**) and 10 minutes after (**C**, **D**) the injection, in one animal. Measurements of the cerebellar first peak are denoted by crosses while those of the cerebellar second peak are shown as open circles. Latencies (A, C) and amplitudes (B, D) of the two components of the cerebellar response are plotted as a function of those of the SI response to tactile peripheral stimulation of the upper lip. **C:** Latencies of both cerebellar peaks as well as that of the SI peak increased significantly ten minutes after a sodium pentobarbital injection. The latency of the second cerebellar peak was still highly correlated to the latency of the cortical peak, while the latency of the first cerebellar peak was not. **D:** Amplitudes of the cerebellar and SI responses decreased significantly after the injection. The significance was judged by a Mann-Whitney U test.

response (Figure 2.5B, dashed line: c). In all cases, the cerebellar short-latency response occurred in response to both stimuli. When the interstimulus interval was decreased from 100 to 75 msec, there was a decrease in the number of long-latency cerebellar and of SI responses to the second pulse of the pair (Figure 2.5C). All cerebellar long-latency responses to the second stimulus occurred in trials where an SI response to the second stimulus was also present. At short interstimulus delay, there was a larger percentage of SI responses than long-latency cerebellar responses to the second stimulus. For paired stimuli with 75 to 100 msec interstimulus delay, when the second stimulus elicited a long-latency cerebellar peak in a trial, the amplitude of the SI response (1.56 ± 0.07 mV, 62% of the amplitude of the SI response to the first stimulus; n = 88) was on average twice as large as when there was no second cerebellar peak (0.79 ± 0.07 mV, 32% of the amplitude of the SI response to the first stimulus, n = 29).

2.4.5 Spatial distribution of the short- and long-latency cerebellar responses

In two animals, we attempted to quantify the spread of activity of both latency responses in crus IIa. In the animal shown in Figure 2.6, we mapped the receptive field at 42 locations in the folium. Recordings were made in each location while stimulating a single location on the rat's upper lip (shown as the circle with the "1" inside, bottom inset Figure 2.6). The largest responses were recorded in locations where the receptive field matched the stimulated upper lip area. However, smaller responses were recorded throughout crus IIa. Comparing the average amplitude of the two components of the response (Figure 2.6 A, B), it can be seen that the short-latency component decreased most rapidly away from the receptive field center, while the amplitude of the long-latency component decreased less, suggesting a somewhat larger projection region. The ratios of the amplitudes of the second and first cerebellar peaks, as seen in Figure 2.6C, indicate that

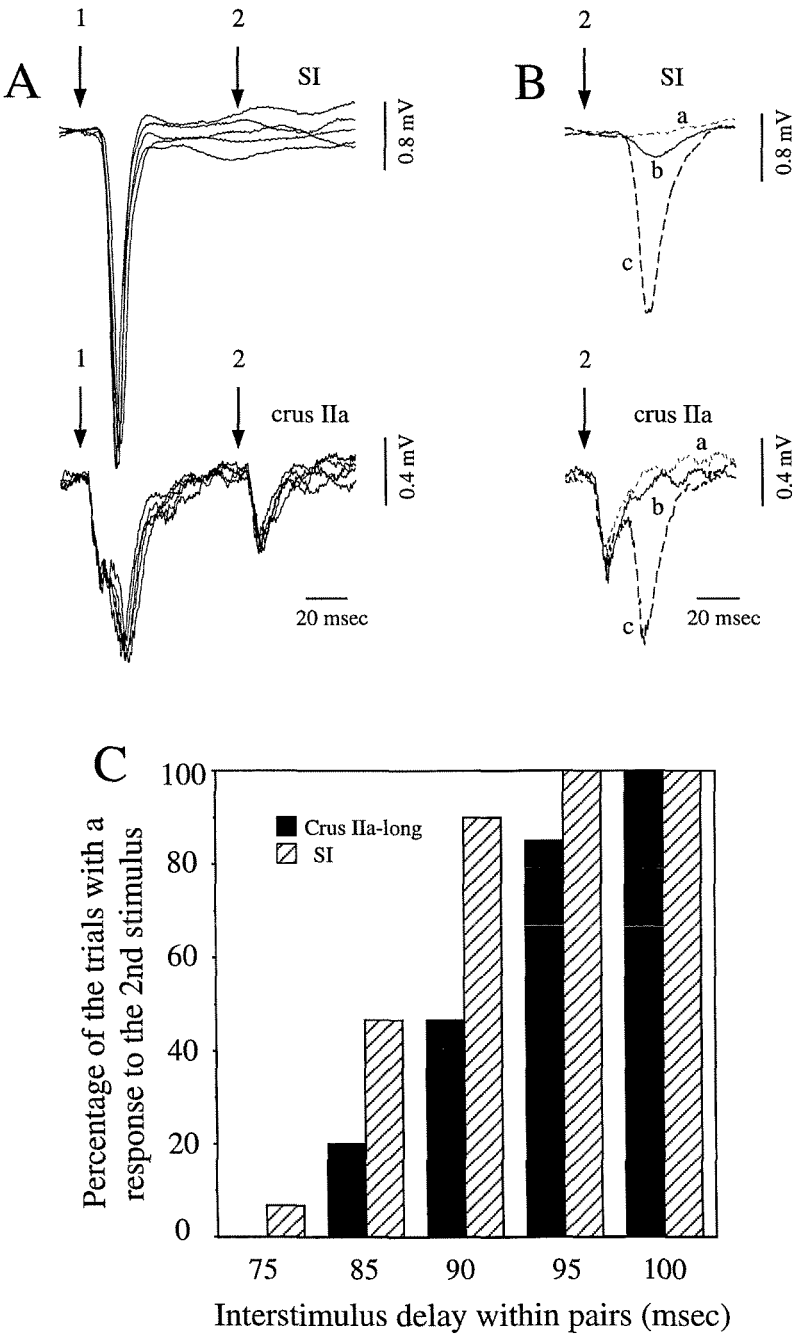
A
1
2
SI
0.8 mV
1
2
crus IIa
0.4 mV
20 msec
B
2
SI
a
b
c
0.8 mV
2
crus IIa
a
b
c
0.4 mV
20 msec
C
Crus IIa-long
SI
Percentage of the trials with a response to the 2nd stimulus
100
80
60
40
20
0
75
85
90
95
100
Interstimulus delay within pairs (msec)

Figure 2.5

Figure 2.5 **A:** Five superimposed field potentials of the responses in SI (top traces) and crus IIa (bottom traces) to a pair of tactile stimuli 75 msec apart. The responses to the first stimulus are typical (compare with Figures 2.1 B, C and 2.2D). When the second stimulus of the pair occurred, 75 msec later, the cerebellar recordings showed only the short-latency response, and the cortical traces showed very little or no response. The arrows denote the onset of the two stimulations. **B:** Responses in SI (top traces) and crus IIa (bottom traces) to the second of a pair of tactile stimuli, 85 msec after the first one. The response to the first stimulus (not shown) was typical, see A. Three different field potential responses are superimposed. The onset of the second stimulus is denoted by an arrow. **C:** Percentage of the trials in which the second stimulus elicited a response as a function of the delay between the two stimuli of paired stimulation. The delay between each pair of stimuli was at least 2 seconds. Percentages are shown for the long-latency cerebellar (black bar) and cortical responses (hatched bar). The short-latency cerebellar response occurred in all but one of the trials (in 164 out of 165 trials) for all interstimulus intervals shown. Each bar represents the percentage of trials with a response to the second stimulus for 30 to 40 paired stimuli.

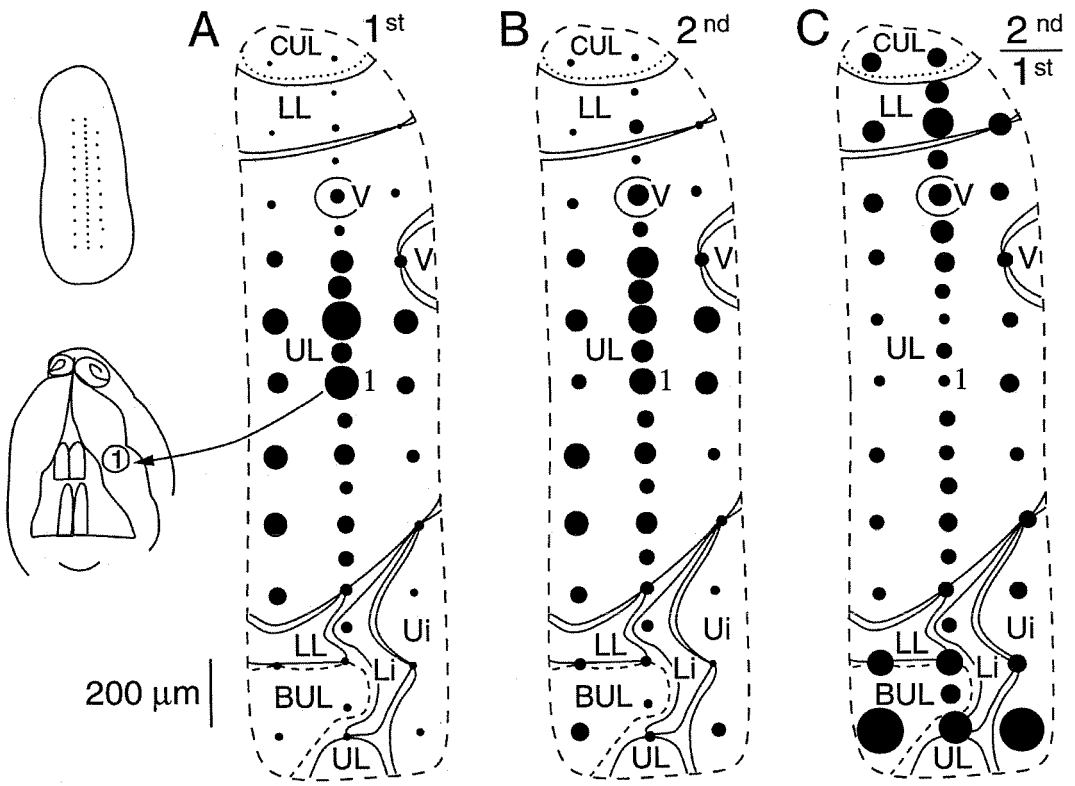

Figure 2.6 Distribution of activity in cerebellar crus IIa following tactile stimulation of the upper lip. Each of the 3 maps (A, B, C) shows a different aspect of the same field potential data obtained in one animal. Each circle represents an electrode penetration and the diameter of each circle is proportional to **A:** the amplitude of the first, or short-latency, component of the response to peripheral stimulation, **B:** the amplitude of the second, or long-latency, component of the response to peripheral stimulation, and **C:** the ratio of the amplitude of the long-latency response to the amplitude of the short-latency response. The diameter of each circle was calculated by averaging the peak amplitude (or ratio of amplitudes) of the responses to 50 stimulations of the upper lip. **Top inset:** positions of electrode penetrations on the surface of the crus IIa folium. **Bottom inset:** circle with the 1 inside indicates the area of tactile stimulation; it was stimulated at each electrode penetration independent of the receptive field at that penetration. This upper lip area was the receptive field at the first electrode penetration shown as 1

on each map. Top is medial; left is rostral. UL: ipsilateral upper lip; BUL: bilateral upper lip; CUL: contralateral upper lip; V: ipsilateral vibrissae; LL: lower lip; Li: lower incisors; Ui: upper incisor. Dotted lines: contralateral structures; dashed lines: bilateral structures; solid lines: ipsilateral structures.

the second cerebellar peak becomes more significant further away from the receptive field relative to the first peak.

2.4.6 Disruption of SI selectively interferes with the long-latency cerebellar response

Several methods were used to interfere with the physiological integrity of the somatosensory cortex to further confirm the influence of SI responses on the cerebellum. Figure 2.7 shows the effects of applying a local pressure injection of 2% lidocaine (approximately 30 µl) in the upper lip region in layer V-VI of SI while recording in a corresponding upper lip patch in the granule cell layer of crus IIa. After the injection, the amplitude of the second peak of the cerebellar response to tactile stimulation of the upper lips was significantly reduced (as judged by a Mann-Whitney U test, $P = 0.0001$). The maximal effect, with the cerebellar long-latency response almost completely vanishing, occurred 5 minutes after the injection. In contrast, the short-latency cerebellar response showed no significant changes (Figure 2.7B). The effect of lidocaine on the second cerebellar peak was repeatable and reversed completely in about 20 minutes (Figure 2.7).

We also examined the effects on cerebellar responses of local ablations of SI (not shown). When the somatosensory cortex was partially ablated, the amplitude of the cerebellar long-latency component fell 48%. A more complete ablation in the same animal resulted in a greater decline in amplitude, 56%; while the amplitude of the short-latency component was not significantly affected.

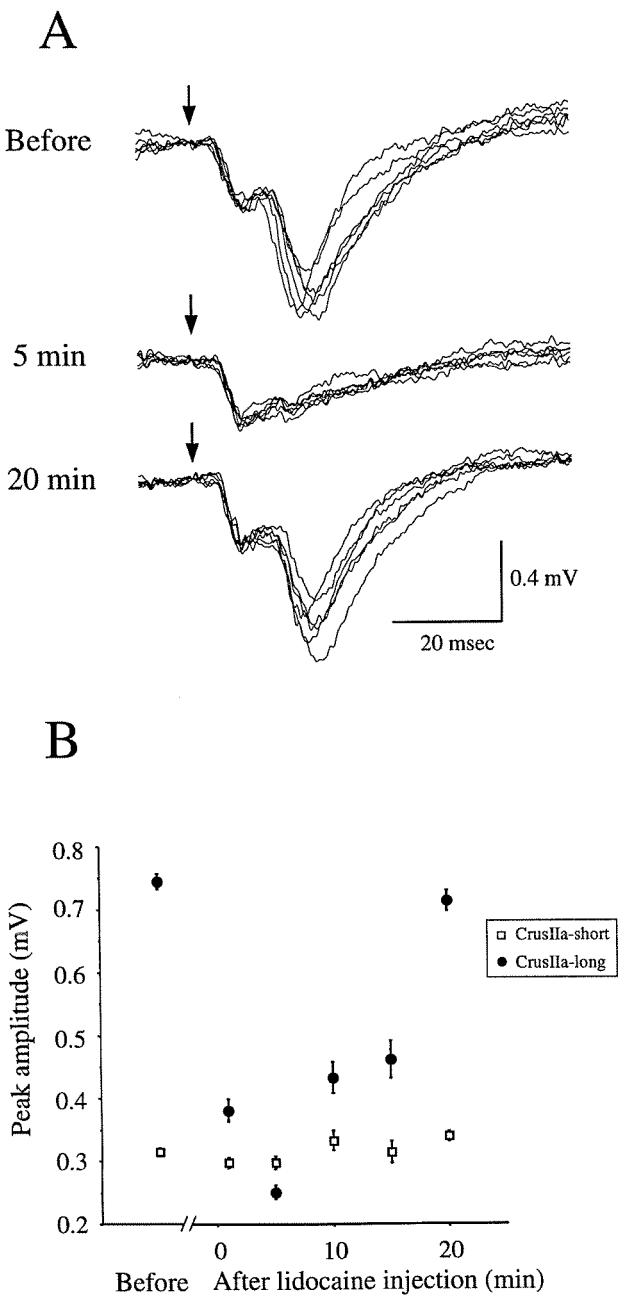

Figure 2.7 Effects of lidocaine injection in SI on the cerebellar response to tactile stimulation of the upper lip. A pressure injection of approximately 30 µl of 2% lidocaine was applied to the corresponding upper lip region in

layer V-VI of the somatosensory cortex. **A:** Six superimposed consecutive cerebellar field potentials are shown before an injection, and 5 and 20 minutes after the injection. Arrows denote the onset of the tactile stimulus. **B:** Amplitude of the two cerebellar peaks as a function of time after the lidocaine injection. Each point represents the mean amplitude ± SE of 50 traces like those shown in A. The cerebellar first, or short-latency, peak is denoted by an open square and the cerebellar second, or long-latency, peak is denoted by a filled circle. Lidocaine injection significantly decreased the amplitude of the cerebellar long-latency responses but had little effect on the amplitude of the cerebellar short-latency responses. Effects were reversed in 20 to 30 minutes. The significance was judged by a Mann-Whitney U test.

The last and most extreme procedure involved a decerebration at the midcollicular level. It resulted in a virtually complete elimination of the long-latency component of the cerebellar response to peripheral stimulation of the upper lip (Figure 2.8). Once more, this procedure affected the second cerebellar peak quite selectively; the first cerebellar peak showed little change (before: 8.51 ± 0.51 msec, 0.64 ± 0.07 mV, n = 97; after: 8.12 ± 0.24 msec, 0.59 ± 0.02 mV, n = 100).

2.5 Discussion

These experiments carefully investigated the temporal relationship between tactilely-evoked responses in the somatosensory cortex and in the cerebellar granule cell layer. Our results were consistent with those obtained in the cat by Kennedy, Grimm and Towe (1966) in showing that the somatosensory cortex is the primary contributor to the long-latency (second peak) cerebellar granule cell layer response elicited by tactile stimulation. By recording from SI and the cerebellum simultaneously, we have demonstrated a strong correlation between the latency of the SI response and that of the second cerebellar peak. Further, as described below, the onset of the SI-related response in

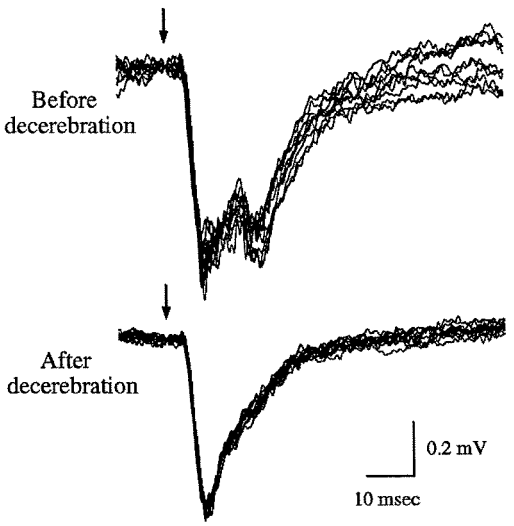

Figure 2.8 Complete midcollicular decerebration abolished virtually all of the cerebellar long-latency response to tactile stimulation. Ten consecutive cerebellar responses to peripheral stimulation of the upper lip are superimposed before and approximately 40 minutes after decerebration. Arrows indicate the time of the stimulus.

the cerebellum appears to correspond with several features of Purkinje cell responses to peripheral tactile stimulation.

2.5.1 Origins of cerebellar granule cell layer responses to tactile stimulation

From 1940 through the late 1960s, a large number of studies of cerebellar afferent systems were conducted using evoked potential techniques (for review see Bloedel 1973; Allen and Tsukahara 1974). These studies used large surface recording electrodes and electrical stimulation of peripheral nerves. These techniques have lower spatial resolution

than the procedures we used, which include recording the afferent potential in the granule cell layer (depth of 400 to 700 μm) and a more natural tactile stimulation of the periphery (for review see Welker 1987). As a result of the lower spatial resolution in the earlier studies, the fine detail of tactile projections to cerebellum was obscured. For example, previous evoked potential experiments were interpreted as suggesting an organized somatotopic projection to the cerebellum (Snider and Stowell 1944; Provini et al. 1968), while Welker and his collaborators, using techniques like those used here, found the projection to be fractured (Welker 1987). Many previous studies also averaged large numbers of individual traces, which would have obscured the timing relationships reported here.

Short-latency component

Our results demonstrated that the first, short-latency, component of the cerebellar response to tactile stimulation was very regular in latency and amplitude. This short-latency response was almost certainly a result of a direct trigeminal projection. A direct projection from the trigeminal nuclei to the lateral hemispheres of the cerebellum has been demonstrated anatomically using HRP, horseradish peroxidase (Watson and Switzer 1978). Further, physiological experiments using antidromic collision techniques have demonstrated direct trigeminal projections to the same regions of the granule cell layer investigated herein (Woolston et al. 1981). It has also been reported that the cerebellar hemispheres may receive projections directly from primary sensory nerves, at least in the case of the teeth (Elias et al. 1987). Whether direct or relayed through the trigeminal nucleus, the short-latency projections clearly provide a large, very fast, and temporally stable cerebellar input.

Contribution of circuits involving SI cortex to the long-latency component

The long-latency response to tactile stimulation was demonstrated to be more temporally variable and distinct from the short-latency response. We have provided clear

evidence that these responses substantially involve the somatosensory cortex. Previous studies (Bower et al. 1981) have shown that direct electrical stimulation of SI cortex induces responses in crus IIa. Numerous studies have described the anatomical properties of projections from cerebral to cerebellar cortex (for review see Allen and Tsukahara 1974; Angaut and Sotelo 1975). With respect to SI cortex and the lateral hemispheres of the cerebellum in particular, a large body of anatomical data shows that the pons receives input from layer V-VI cortical (SI) neurons and sends most of its afferents to the contralateral lateral hemisphere of the cerebellum, including crus IIa (Wise and Jones 1977; Brodal 1979, 1982; Mihailoff 1983; Brodal and Bjaalie 1992). There is also evidence of a secondary projection through the brainstem lateral reticular nucleus (Allen and Tsukahara 1974; Allen et al. 1979), but it projects primarily to the vermis, not the hemispheres (Clendenin et al. 1974; Newman and Ginsberg 1992). Thus, it is most likely that the effects described here are relayed through the pontine nuclei.

Contributions of other mid- and forebrain structures to the long-latency cerebellar response

While SI cerebral cortex clearly has a major influence on tactile regions of the lateral hemispheres, other structures, like the motor cortex (Sharp and Evans 1982; Mihailoff et al. 1985) and the superior colliculus (Kassel 1980), have also been demonstrated to influence these regions of the cerebellum, presumably also through the pons (motor cortex: Mihailoff et al. 1985; superior colliculus: Dean et al. 1988). We have shown that lidocaine injected into SI as well as direct SI cortical ablations substantially reduced, but did not eliminate, the long-latency component of the cerebellar response to peripheral stimulation. Complete midcollicular transection was required to completely abolish the response. This latter procedure should interrupt projections from all forebrain structures and all structures projecting through the pons. Following decerebration, the first cerebellar peak was not significantly affected whereas the second cerebellar peak disappeared. These findings are consistent with those of Kennedy et al. (1966) in the cat,

who also showed a third peak occurring approximately 30-40 msec after the onset of the stimulus that reappeared 30–45 minutes after decerebration. We did not see any such late latency peak reappear after comparable time in our preparation. However, in normal rats, we found a number of responses with a third distinguishable peak when the peripheral area stimulated did not correspond to the primary receptive field of the location recorded from in the granule cell layer, such as when we stimulated the upper lip while recording from a lower lip patch (experiment described in Figure 2.6). Since Kennedy et al. (1966) did not take into consideration the detail of the fine grain input map to the cerebellum, our data suggest that the "third peak" responses they describe may have been recorded from regions outside but near the forepaw receptive field patch. Further experiments will be necessary to determine the origin of that component of the cerebellar response to peripheral stimulation.

2.5.2 Temporal properties of cerebellar and cerebral cortical responses

Timing relationships between responses in SI cortex and the cerebellar long-latency response

Our data demonstrate that the latency of activity in SI cortex and the long-latency cerebellar response are quite variable but highly correlated temporally. This is true both in the regular preparation as well as after the administration of barbiturates (Figure 2.4). While barbiturates result in the lengthening of latencies in all responses measured, probably through a brain-wide increase in the $GABA_A$-induced Cl^- current, and thus inhibition of synaptic transmission (Snyder 1984), the latencies of the SI and long-latency cerebellar responses still remain highly correlated. We have also demonstrated that there is relatively little variability in the delay between activity in SI and the long-latency response in the cerebellum on individual trials (Figure 2.2E). Finally, we have shown that the latency of the short-latency cerebellar response, originating in the trigeminal nucleus, was much less variable and not correlated with the timing of the SI response (Figure 2.3).

Significance of the response timing in cerebellum

After a response has been induced in the cerebral cortex, the information is apparently relayed to the cerebellum rapidly and with essentially fixed latency. This was the case for tactile stimulation given every 2 seconds. Our data showed that when two stimuli were separated by less than 100 msec, the failure rate for SI and SI-related cerebellar responses increased. Previous studies showed similar results at the level of Purkinje cells, which were not capable of following stimuli applied at frequencies of 10 Hz (Bantli and Bloedel 1977).

We have also shown that the forebrain influence arrived in the cerebellum with no consistent temporal relationship to the initial burst of granule cell layer activity. For this reason, we speculate that the detailed timing of information originating in the forebrain and projecting to the cerebellum reflects the temporal requirements of forebrain, not cerebellar, processing. When considering these timing relationships, it is important to keep in mind that stimuli in these experiments were given irrespective of any intrinsic rhythms of the thalamus or cortex. Under more natural conditions, it is entirely conceivable that behaving animals coordinate the acquisition of afferent information so that it is in register with the intrinsic rhythms of their neural circuits. It has been previously proposed that the primary role of the cerebellum may be in the general coordination of sensory data acquisition (Bower and Kassel 1990; Bower 1993). Presumably this coordination would involve not only the spatial but also the temporal use of sensory receptors. Accordingly, it is interesting to consider the timing of this long-latency input with respect to other cerebellar events induced by peripheral stimuli.

Comparison of our granule cell layer responses with extracellular and intracellular recordings from Purkinje cells (Jaeger and Bower 1994) shows that the SI influence on the granule cell layer coincides with two specific transitions in Purkinje cell responses to peripheral stimulation. First, the long-latency granule cell response coincides closely with the termination of the short latency inhibition of Purkinje cells that often results from short

duration peripheral tactile stimuli (Bower and Woolston 1983). Second, the long-latency response coincides with the beginning of a prolonged (50–200 msec) increase in simple spike firing frequency that can result from tactile stimulation. Intracellular work has demonstrated that this prolonged response is due to a prolonged plateau-like Purkinje cell dendritic depolarization that likely also results from the initial activation of the granule cell layer, although it is initially masked by inhibition (Jaeger and Bower 1994). Intracellular recordings have shown that the long-latency granule cell layer response contributes a large part of the intracellular increase in potential in absence of inhibition (Jaeger and Bower 1994). These results suggest a different functional role for the direct and indirect cerebellar projecting tactile pathways, despite their spatial coherence. It has been suggested previously that peripheral and cortical afferents do not converge on common granule cells (Allen et al. 1974). For example, the pontine mossy fibers could activate different mossy fibers – parallel fibers mechanisms than mossy fibers arriving directly from the trigeminal nucleus. Our findings (Figure 2.6) suggest that the SI-related component of the cerebellar responses to tactile stimulation is spatially more distributed than the trigeminal-related component and, therefore, could influence different granule cells.

2.5.3 Proposed role of SI in cerebellar function

It has been known for many years that the cerebral cortex and the cerebellum are very strongly interrelated; the growth of cerebral cortex in mammals is paralleled by the growth of cerebellum (Stephan et al. 1981; Jolicoeur et al. 1984). In the current experiments, we have again demonstrated that SI cortex provides a substantial input to the lateral hemispheres of the cerebellum. Our results, for brief tactile stimulation in anaesthetized rats, showed that the SI response followed the direct sensory response from the trigeminal nucleus. In our data, the first component of the cerebellar response occurs at a latency of 8 to 10 msec, which is before SI is even activated. As it is also known that the initial cerebellar influence on motor output is very fast (Orlovsky 1972), our data suggest

that an initial sensorimotor loop through the cerebellum may very well be completed by the time the response to the tactile stimulus arrives in SI and is relayed back to the cerebellum (Shambes et al. 1978b; Bower and Kassel 1990).

Most theories of cerebrocerebellar interaction focus on the putative role of cerebellum in motor control and, therefore, focus on the influence of motor pathways (Marr 1969; Albus 1971; Houk 1988; Thach et al. 1992). An alternative hypothesis has been proposed: that cerebellar circuits may be involved in monitoring and controlling the active acquisition of sensory information on which the performance of the rest of the nervous system is based (Bower and Kassel 1990; Bower 1993). Specifically, it has been proposed that the cerebellum receives primary tactile sensory information from particular sets of sensory surfaces involved in active exploration, and then, through the motor system, adjusts the position of these tactile sensory surfaces with respect to each other. In this way, it has been proposed that the cerebellum uses the motor system to coordinate the acquisition of sensory data. Such a function for the lateral hemispheres is analogous to the known influence of the flocculus in the vestibulo-ocular reflex (Paulin et al. 1989a). Recent work using functional magnetic resonance imaging in humans (Gao et al. 1995) supports this proposal, demonstrating strong activation of the lateral regions of the cerebellum in tactile discrimination tasks irrespective of the occurrence of overt finger movements.

In the context of this hypothesis, we propose that the long-latency, forebrain-related response in the cerebellum could provide the cerebellum information on the overall state of cortical networks, including information about the appropriate timing of data acquisition. Such information could, in principle, serve to modify Purkinje cell responses to the short-latency, raw afferent input. In this way, ongoing control of sensory acquisition would be dependent both on the raw sensory information and the response of the cerebral cortex to that information. The timing of the SI influence during the plateau phase of the Purkinje cell response set up by the initial direct response to the stimulus is consistent with this idea.

Ultimately, a full understanding of the role of cerebral cortical circuits in cerebellar function, or the cerebellum itself, will require a close examination of neural activity in behaving animals. For example, under natural behavioral conditions, tactile stimuli are likely to be of a longer duration with much more complex timing relationships than those shown here for a single punctate stimulus. However, we would still expect any new stimulus to activate cerebellum first and SI second. Preliminary results from awake behaving animals show cerebellar double peak responses similar those reported here (Hartmann and Bower 1993, 1995).

3

Developmental Plasticity in Cerebellar Tactile Maps: Neonates

All changed, changed utterly:
A terrible beauty is born.
W. B. Yeats
Easter, 1916

3.1 Abstract

Plasticity following deafferentation has been repeatedly demonstrated in somatotopic sensory maps in the mammalian brain. In this study, we investigated the developmental plasticity of the fractured somatosensory map found in the tactile regions of the rat cerebellum. At various stages of postnatal development between postnatal days 1 and 30, we cauterized the infraorbital branch of the trigeminal nerve, which innervates the upper lip, furry buccal pad, and vibrissae that are represented within cerebellar folium crus IIa. The organization of the crus IIa map was then examined two to three months after denervation. We found that tactile receptive fields had reorganized throughout the denervated area but maintained a fractured somatotopy. Comparison of the reorganization in different animals showed that the denervated upper lip region was consistently and predominantly replaced by representation of the upper incisors. Analysis of evoked field potentials revealed an alteration, in denervated animals, of the response of the granule cell layer to brief tactile stimulations. This response in normal animals consists of two

components at different latencies. Animals lesioned later in development were less likely to have the short-latency component. This result suggests a difference in the developmental sensitivity of different cerebellum-related pathways to nerve lesions.

3.2 Introduction

Numerous anatomical and electrophysiological studies have demonstrated that the organization of sensory maps in mammals can be modified during development following peripheral manipulations. To date, however, this work has involved topographically organized cortical and subcortical sensory maps (*somatosensory*: Table 1, Wall and Cusick 1984; Merzenich et al. 1983ab; for reviews see Kaas et al. 1983; Verley 1986; Merzenich 1987; Killackey 1989; Wall 1988ab; Kaas 1991; *visual*: Fraser and Hunt 1980; Fraser 1985; for review see Udin and Fawcett 1988; *auditory*: Knudsen 1983ab, 1985; for review see Knudsen et al. 1987). In somatotopic sensory maps, reorganization generally preserves at least the basic topography of the original map through an apparent expansion of representations of body parts that are both peripherally and centrally adjacent to the denervated peripheral structure (Kaas et al. 1983; Table 1, Wall and Cusick 1984).

Nontopographic, fractured tactile maps have been found in the granule cell layer of the lateral hemispheres of the rat cerebellar cortex (Shambes et al. 1978ab; Welker 1987; Bower and Kassel 1990). In contrast to the somatotopic sensory maps in the cerebral cortex, tactile maps in these cerebellar regions include topographically discontinuous patches, with each patch representing a nonadjacent area of the body surface (Figure 3.1B). Similarly, fractured maps have also been demonstrated in the cerebellum of cats (Kassel et al. 1984), opossums (Welker and Shambes 1985), and the primate *Galago crassicaudatus* (Welker et al. 1988). The overall structure of the cerebellar maps in rats has been shown to be invariant in normal animals (Bower and Kassel 1990). In these animals the fractured representation of peripheral surfaces is also preserved in both the direct trigeminocerebellar

projections (Woolston et al. 1981) and in the cerebellar projections originating from other somatosensory-related regions (somatosensory cortex, Bower et al. 1981; superior colliculus, Kassel 1980).

In this chapter, we examine whether fractured cerebellar tactile maps, like somatotopic sensory maps in other parts of the brain, are capable of reorganizing following peripheral lesions. In addition, if reorganization does occur, we were interested in determining its precise pattern in the expectation that this would shed light on the mechanism of reorganization in the cerebellum. Finally, we were interested in determining whether there is a sensitive period for reorganization in the cerebellum as has been reported for other somatosensory areas (Weller and Johnson 1975; Woolsey and Wann 1976; Durham and Woolsey 1978; Belford and Killackey 1980).

Our results demonstrate that fractured tactile cerebellar maps reorganize in a fractured pattern that is considerably different from other somatosensory regions. The reorganized maps appear remarkably similar across animals regardless of the age of deafferentation, thus supporting the idea that the fractured structure of these maps is important to cerebellar function (Bower and Kassel 1990). Preliminary results of these investigations have been presented elsewhere (Paulin and Bower 1988; Morissette et al. 1990).

3.3 Methods

3.3.1 General experimental design

A total of 26 Sprague-Dawley albino rats of both sexes were used: 12 control and 14 experimental animals. In the experimental animals, the infraorbital branch of the trigeminal nerve was cauterized on various postnatal days, ranging from postnatal day (PND) 1 to

PND 30 (PND 1 (n = 2); PND 2 (2); PND 4 (1); PND 9 (1); PND 12 (1); PND 14 (1); PND 15 (1); PND 16 (1); PND 30 (4)). Two to three months after the nerve was sectioned, the granule cell layer of crus IIa was mapped with multiunit recordings. In 14 of the 26 animals used in determining receptive field maps, recordings of field potential responses to peripheral mechanical stimulation were also taken at all penetration sites (normal controls, (n = 3); PND 1 (1); PND 2 (2); PND 4 (1); PND 9 (1); PND 15 (1); PND 16 (1) PND 30 (4)). The areal extent of each region of the body surface mapped in crus IIa was statistically compared between the normal and experimental animals with a Mann-Whitney U test.

3.3.2 Specific experimental procedures

Nerve cauterization

Cauterization of the infraorbital branch of the trigeminal nerve was performed on young rats deeply anaesthetized with avertine (125 mg/kg body weight). Under a light microscope, an incision was made between the occipital bone ridge and the caudal edge of the vibrissae pad. The infraorbital branch of the trigeminal nerve was exposed by teasing away surrounding muscle. A cautery unit (Sybron) was used to interrupt the nerve for several millimeters. Care was taken to cauterize all of the multiple branches of the nerve. To prevent nerve regeneration, bone wax was inserted under the occipital bone ridge in the nerve's previous location. The wound was bathed with a local anaesthetic, and the skin incision closed with suture. The animals were monitored for two to six hours until they appeared to recover completely from the anaesthetic. They were subsequently placed back with their mothers and returned to the animal care facility.

Cerebellar craniotomy

Two to three months after the nerve cauterization, the rats were prepared for cerebellar mapping. Prior to surgery, each rat was anaesthetized with intraperitoneal

injections of sodium pentobarbital (12 mg/kg body weight) and ketamine hydrochloride (50 mg/kg body weight). Ketamine supplements were given as needed during the experiment to suppress reflexive movement. The head of the animal was immobilized by an acrylic dam bonded to the skull and head-holder. The cranium over the left cerebellar hemisphere was surgically removed. Before removal of the dura to expose the cerebellar cortex, the acrylic dam was filled with warm mineral oil, which was supplemented as needed during the experiment. Rectal temperature was maintained at 36–37°C with a feedback controlled heating pad. The trachea was cannulated to facilitate respiration. The surface of the cerebellum was photographed to allow documentation of electrode recording positions. Animals were sacrificed at the end of the experiment with an overdose of sodium pentobarbital (50 mg/kg IP). Further details of these surgical procedures can be found in Bower and Woolston (1983).

3.3.3 Electrophysiological procedures

Receptive field mapping

Multiple unit activity in the granule cell layer (400–700 μm below the brain surface) was recorded with glass micropipettes filled with 2M NaCl (10 μm in diameter, 1 MΩ impedance). The central region of the exposed folial crown of crus IIa was finely mapped with 60 sequential perpendicular electrode penetrations (3 tracts, 20 punctures per tract; Figure 3.1C). Depending on surface vasculature, the penetrations were spaced 100–150 μm apart mediolaterally (top to bottom on the folium) and 100–200 μm apart rostrocaudally (left to right on the folium). The location of the penetrations on the surface of crus IIa were directly recorded on an enlarged photograph at the time of recording (Figure 3.1C). The central region was selected to avoid difficulties resulting from the downward curvature of the granule cell layer on the rostral and caudal edges of the folium (Figure 3.1). For each electrode penetration, the multiunit granule cell receptive field was determined auditorily

with hand-held glass probes. At least two experimenters independently determined the location of the receptive fields and rated responses subjectively on a scale from 1 (barely detectable) to 5 (maximal). The body region that, when stimulated, elicited the strongest response from the granule cell layer was carefully recorded on standardized figurine drawings of the rat's body surface.

Map construction

As in previous experiments (Welker 1987), maps were constructed by drawing enclosing boundaries around adjacent electrode puncture locations whose receptive fields were from the same body structures. When stimulation of more than one peripheral location could induce a response in a particular penetration, the region eliciting the strongest response was used. In cases where responses were of equal strengths, the boundary line was drawn through the site of the electrode penetration.

Field potential analysis

After auditorily determining the receptive field, the center of the receptive field was mechanically stimulated with the blunt end probe (< 1 mm in diameter) of a custom-built tactile stimulator. The stimulus pulse was a 50 msec square wave, generated by an IBM personal computer. Both the amplitude and duration of the stimulus were monitored from the excursion of the stimulus probe itself which was displayed on an oscilloscope. The field potential response recorded from the granule cell layer (400–700 μm from the cortical surface) was pre-amplified at a gain of 600 (WPI preamplifier) and filtered (1 to 1000 Hz bandpass). To assure proper positioning of the stimulator in the center of the previously determined receptive field, from 5 to 10 single, manually controlled stimuli were initially presented while the granule cell layer evoked response was observed on the oscilloscope. At this time, the presence of one or both normal components of the field potential was also

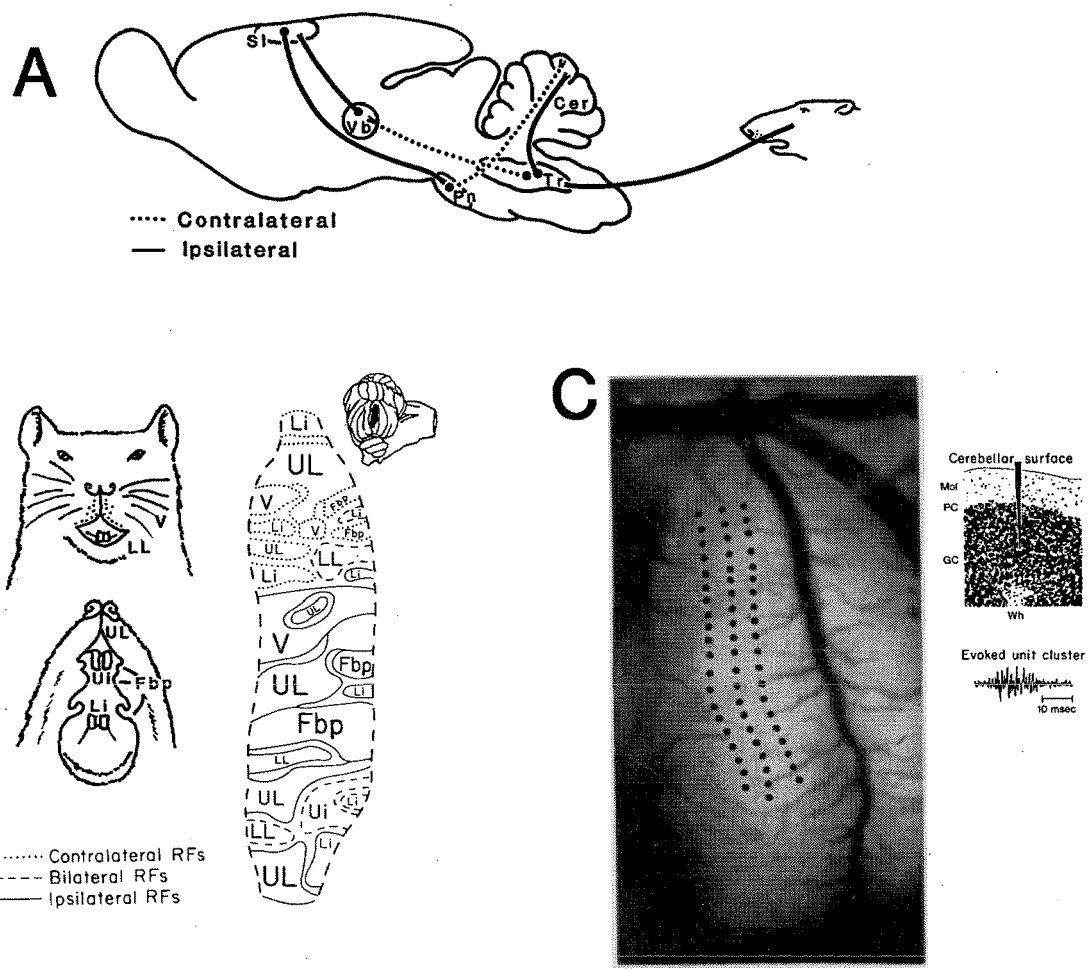

Figure 3.1 **A:** Simplified circuit diagram of the tactile mossy fiber inputs to the crus IIa folium in the cerebellar hemispheres. Several other areas not shown, including the superior colliculus, also project to crus IIa (Brodal 1981; Huerta et al. 1983; Marfurt and Rajchert 1991). Cer: cerebellum; Tr: trigeminal complex; Vb: ventrobasal complex of the thalamus; SI: somatosensory cortex; Pn: pons. **B:** Organization of the tactile map in crus IIa, constructed from the brain of a normal rat (from Bower and Kassel 1990, with permission). The cerebellar map has a fractured somatotopic organization, as demonstrated by numerous authors using high-density electrophysiological mapping techniques. The location of the different receptive fields are shown on the diagram of the rat's head. **Inset**: Location in the folium of the area that has been mapped. **C:** Representation of the 60 electrode penetrations used in this study. The three tracks are 100–150 μm

apart and contain 20 recording sites each. The separation between points is 100 μm. **Inset, top:** Histological section indicating a typical location for the recording electrode within the granule cell layer; **bottom:** Representation of the typical activity recorded from the granule cell multiple units (from Bower and Kassel 1990, with permission). GC: granule cell layer; Mol: molecular layer; PC: Purkinje cell layer; Wh: white matter. Other *abbreviations* in this and all subsequent figures: Fbp: furry buccal pad; Li or LI: lower incisor; LL: lower lip; N: nose; NR: no response; RFs: receptive fields; Ui: upper incisor; UL: upper lip; V: vibrissae.

noted (see below). For further analysis and confirmation of the initial evaluation of the signals, the receptive field was stimulated for an additional 5–10 trials (2 second interstimulus interval) while the granule cell layer responses were digitized and stored on a MassComp 5700 laboratory computer (Concurrent Computer Inc.).

3.3.4 Methodological considerations

Mapping procedures

Tactile receptive fields were determined while manually stimulating the body surface and listening to the evoked response on an auditory monitor. While this is standard procedure for somatosensory mapping experiments (Robertson 1982, 1987; Kaas et al. 1983; Merzenich 1987; Welker 1987), inconsistencies between the mapping criteria of different investigators could, in principle, influence the results. In order to reduce such an effect in the current experiments, the strength of the response was independently assessed by at least two investigators.

Field potential analysis

Field potential recordings were used to quantify changes in the form and extent of granule cell layer responses to tactile stimuli. Field potentials were chosen because of the

difficulties associated with recording from single granule cells and because it has proven difficult to quantify the relatively low amplitude and highly filtered multiunit recordings used in mapping receptive fields.

A possible concern with our field potential analysis involves the ease with which the two components of the peripherally evoked cerebellar response (Figure 3.5) can be identified and separated. In nonlesioned animals, these two components occurred at distinctly different latencies (Chapter 2). However, in some recordings from denervated animals, the field potential appeared as a single broad peak, making it difficult to draw a clear distinction. In these cases, the location was conservatively scored as having both responses present.

3.4 Results

3.4.1 Complete tactile reorganization

In centrally located penetrations in crus IIa of normal animals, on average 64% of responses are from structures related to the ipsilateral upper lip (Figures 3.2C and 3.3; also see Bower and Kassel 1990). Therefore, deafferentation of the infraorbital branch of the trigeminal nerve that innervates these structures eliminates input to a large portion of the crus IIa map. Nonetheless, when neonatally lesioned animals were mapped as adults, most of crus IIa was found to be responsive to tactile stimulation. We did, however, find a tendency for responses in the reorganized maps to be weaker than responses from normal adult mapping experiments (Figure 3.4). Complete reorganization was found in all animals lesioned, regardless of the age of deafferentation (between PND 1 and 30).

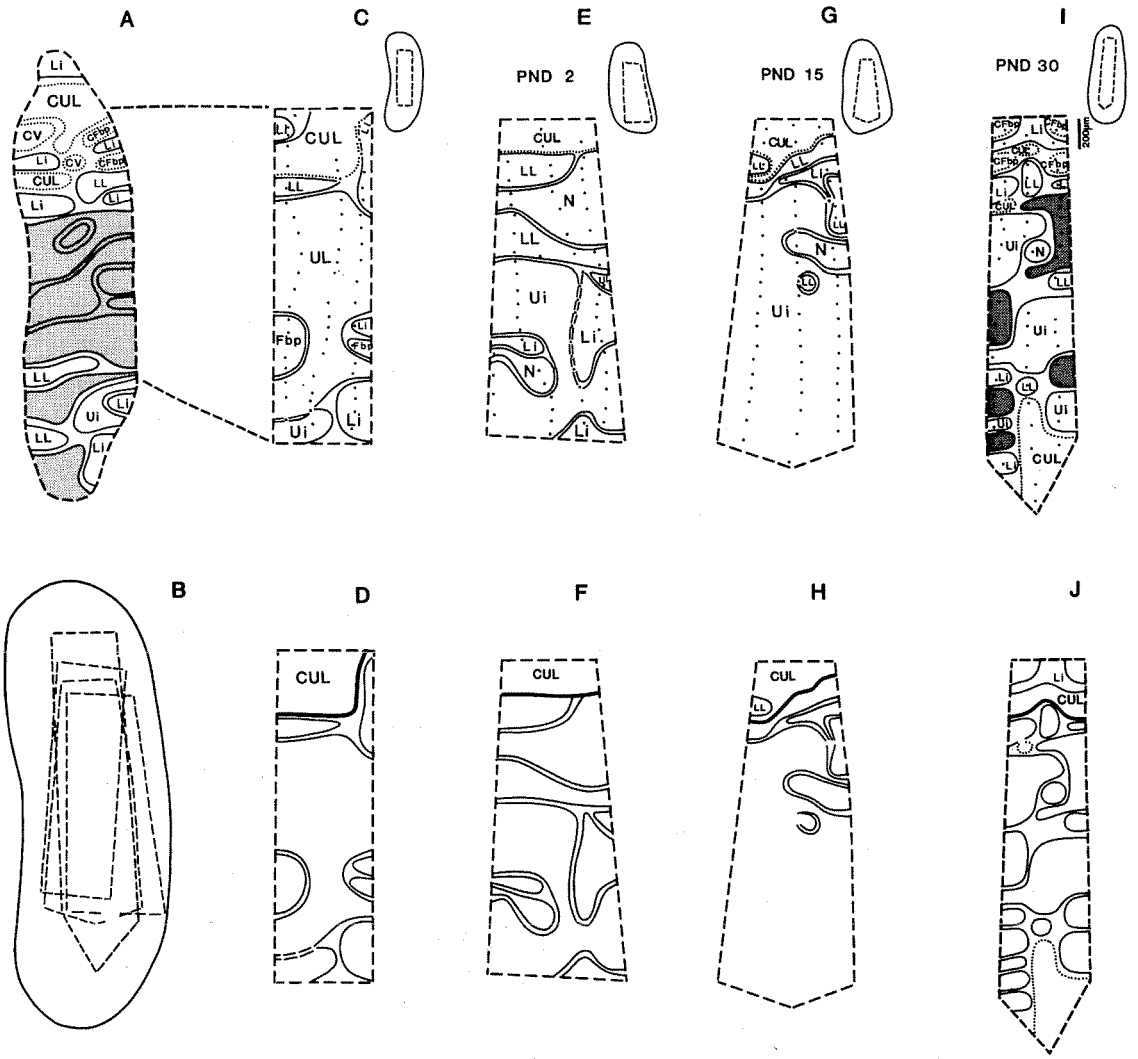

Figure 3.2 **A:** Schematic representation of the complete normal tactile map from Figure 3.1 (modified from Bower and Kassel 1990, with permission), with shaded areas indicating all crus IIa patches receiving input from the infraorbital branch of the trigeminal nerve (ipsilateral upper lip, furry buccal pad, and vibrissae). Solid lines: ipsilateral patch boundaries; dotted lines: contralateral patch boundaries; dashed lines: bilateral patch boundaries. **B:** Superposition of the folial location of the recording sites presented in C, E, G, and I. **C:** Tactile map of crus IIa constructed from the present study from a normal (i.e., nonlesioned) animal. The size and approximate location of this mapped region, relative to the complete crus IIa map (A), is

represented by the dashed lines. **E, G, I:** Maps of crus IIa maps in deafferented animals. Shaded area in I corresponds to nonresponsive regions. **D, F, H, J:** Comparison of the locations of patch boundaries for the corresponding maps in C, E, G, and I. Note the similar location of the patch boundary for the medial contralateral upper lip patch (bold line) in the normal (C) and deafferented (E, G, I) animals. For C, E, G, I, **inset** indicates the location of the recording tracks in the crus IIa folium for each animal. Abbreviations as in Figure 3.1.

3.4.2 Change in representation of body parts

Comparison of the reorganized area in the maps from different animals indicates striking similarities in the replacement structures. As shown in Figure 3.3 and Table 3.1, the perioral structure whose representation consistently invaded most of the area of the denervated region was that of the upper incisor. The upper incisor patches comprised 46% of the map in these deafferented animals ($P < 0.001$, as judged by a Mann-Whitney U test). In contrast, upper incisor patches occupied, on average, only 8% of the map in normal animals (Figure 3.3; also see Bower and Kassel 1990). In lesioned animals, the contralateral upper lip regions also significantly increased in area (from 7 to 19%, $P < 0.002$), as did the lower lip regions (8 to 16%, $P = 0.05$). There was no significant change in areal extent of either the lower incisor or nose representations. Again these results are independent of the age of deafferentation (Table 3.1).

3.4.3 Preservation of fractured somatotopy within denervated regions

The reorganized area retained features characteristic of the normal fractured somatotopy of crus IIa. First, the reorganized area contained a series of patches with typically disjunctive patch boundaries (Figure 3.2). The location of the patch boundaries, however, generally did not correspond to those of the normal upper lip and upper lip-related

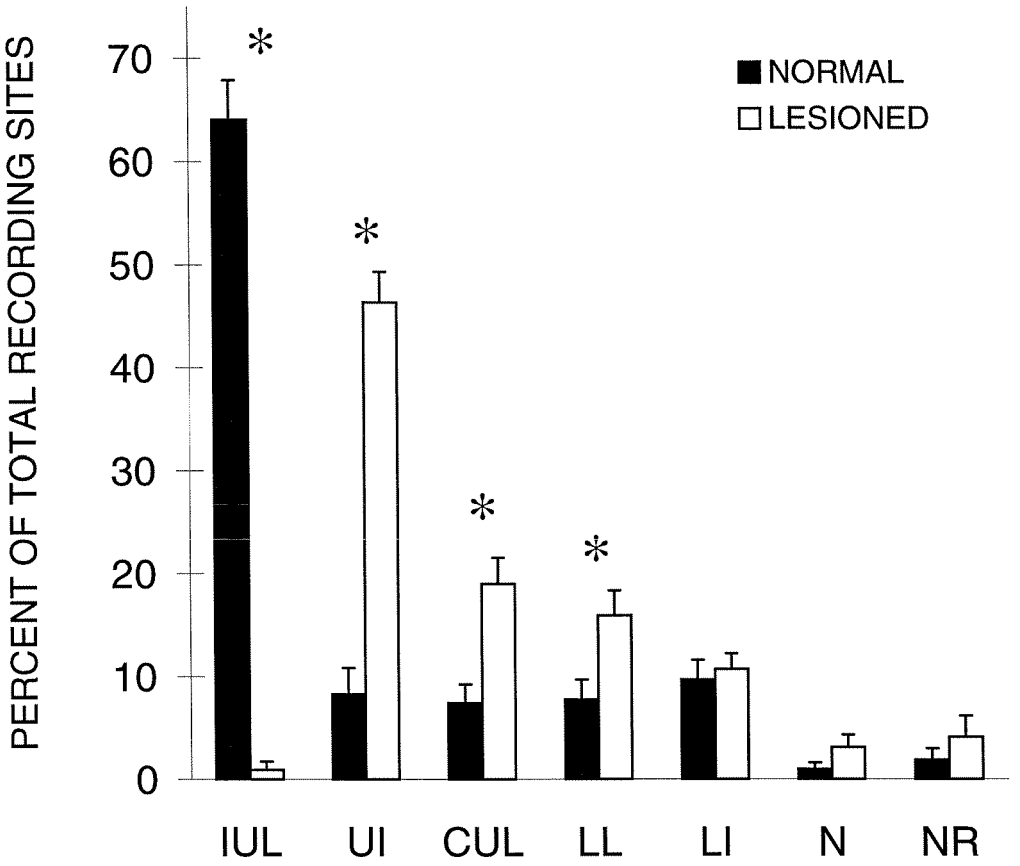

Figure 3.3 Histogram comparing map organization in normal rats (black bars, n = 12) and deafferented rats (white bars, n = 14). Each bar represents the mean ± SE of total recording sites for a given receptive field type. The experimental data from the different developmental stages have been pooled, as the representation of the perioral structures did not significantly differ between the different stages (Table 3.1). Asterisks indicate significant differences between the percentage of representation of a given receptive field type in the normal and experimental animals, as judged by a Mann-Whitney U test. Abbreviations as in Figure 3.1.

patches which they replaced (Figure 3.2 C, E, G, and I). Second, the maps tended to consist of a large (upper incisor) patch surrounded by smaller patches. Ten out of fourteen animals (71%) showed this pattern (Figures 3.2 E and G, 3.5, and 3.7). However, four of the animals showed a more highly fractured pattern, as shown by the PND 30 animal presented in Figure 3.2 I.

	Percent of total recording sites			
		Deafferented developmental stage		
Receptive field type	Normal (n = 12)	PND 1-4 (n = 5)	PND 9-16 (n = 5)	PND 30 (n = 4)
IUL	64.07 ± 3.82	2.22 ± 2.22	0.30 ± 0.30	0
UI	8.27 ± 2.59	44.88 ± 5.38	51.21 ± 5.15	41.97 ± 5.43
CUL	7.41 ± 1.81	15.29 ± 3.34	18.27 ± 5.23	24.65 ± 3.95
LL	7.75 ± 1.94	21.79 ± 5.13	16.05 ± 2.67	8.48 ± 1.05
LI	9.66 ± 1.93	12.03 ± 2.97	9.52 ± 3.00	10.45 ± 2.39
N	0.97 ± 0.61	3.80 ± 3.44	3.16 ± 1.09	2.01 ± 0.77
NR	1.88 ± 1.08	0	1.49 ± 0.50	12.45 ± 5.71

Table 3.1 Comparison of map organization between normal rats and rats with peripheral lesions performed on different postnatal days. Numbers reflect the mean percent ± SE of the total recording sites for a given receptive field type. Abbreviations as in Figure 3.1.

3.4.4 Preservation of other features of crus IIa representations

In addition to the preservation of fractured somatotopy, other general features of the crus IIa maps were maintained within the denervated regions. First, all tactile projections in this area originated exclusively from perioral structures normally projecting to crus IIa. Second, examination of within-patch topography in the contralateral upper lip patches showed that the receptive fields were found to be topographically arranged, as in normal animals (Bower and Kassel 1990).

Finally, the boundary of the contralateral upper lip patch, located in the medial region of the crus IIa folium in normal animals (top of map, Figure 3.2A), was similarly positioned in experimental animals (Figure 3.2 D, F, H, J, delimited by a thick line).

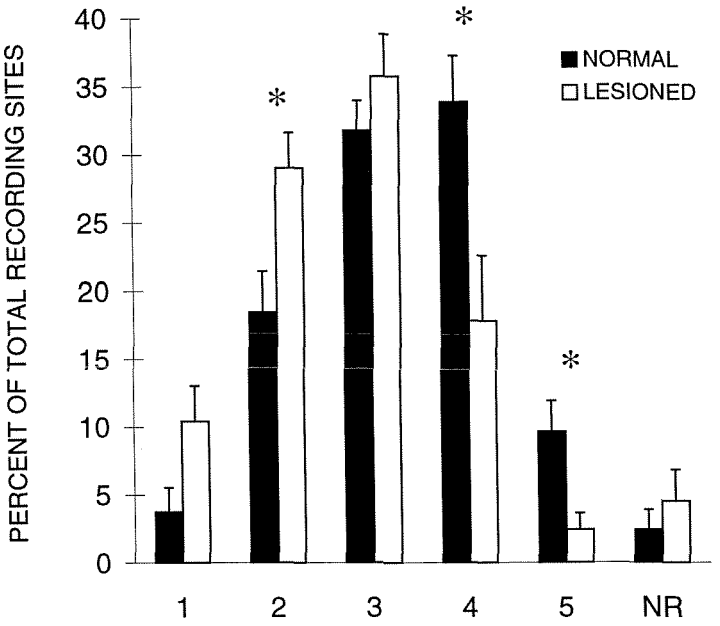

Figure 3.4 Histogram comparing response strength in normal rats (black bars, n = 10) and deafferented rats (white bars, n = 13). Response strength was rated subjectively on a scale from 1 (barely detectable) to 5 (maximal). Each bar represents the mean ± SE of total recording sites for a given response strength. Asterisks indicate significant differences between the percentage of recording sites for a given response strength in the normal and lesioned animals, as judged by a Mann-Whitney U test. NR, no response.

3.4.5 Developmentally-related increase in the number of nonresponsive recording locations

In some experimental animals, penetrations were found that were not responsive to any form of tactile stimulation. The number of these nonresponsive penetrations increased with the age of deafferentation. In normal animals (n = 12), only 2% of the penetrations were nonresponsive. In animals whose nerve had been cauterized between PND 1 and 4, nonresponsive points were also rare, occurring on average in only 1% of the penetrations (n = 5). In animals lesioned between PND 9 and 16, 3% of the penetrations were nonresponsive (n = 5). In the PND 30 animals, the number of nonresponsive points detected was, on average, 10% (n = 4), although there was considerable variability from animal to animal.

3.4.6 Developmentally-related absence of short-latency evoked response

Analysis of the field potential data also demonstrates a change in the structure of recorded field potentials related to the age at the time of lesion. In normal animals, peripherally evoked field potentials always consist of two components, one with short-latency (≈ 8 msec) and one with long-latency (≈ 18 msec); see Chapter 2. In some deafferented animals, however, it is possible to record field potentials that are entirely lacking the first component (Figure 3.5). Further, the percentage of punctures containing only the second component of the response increases with the age of denervation.

Figure 3.6 summarizes these developmental effects. In animals whose nerve had been cauterized between PND 1 and 9, just a few field potentials were found that contained the long-latency component only. This type of field potential occurred, on average, in 3% of the mapped locations (n = 4). In animals operated on PND 15 or 16, the second response was found in 13% of the mapped locations (n = 2). In animals operated on PND 30, the second response was elicited at 20% of the recording sites (n = 4). A regression analysis through these points was found to be significant (P = 0.004).

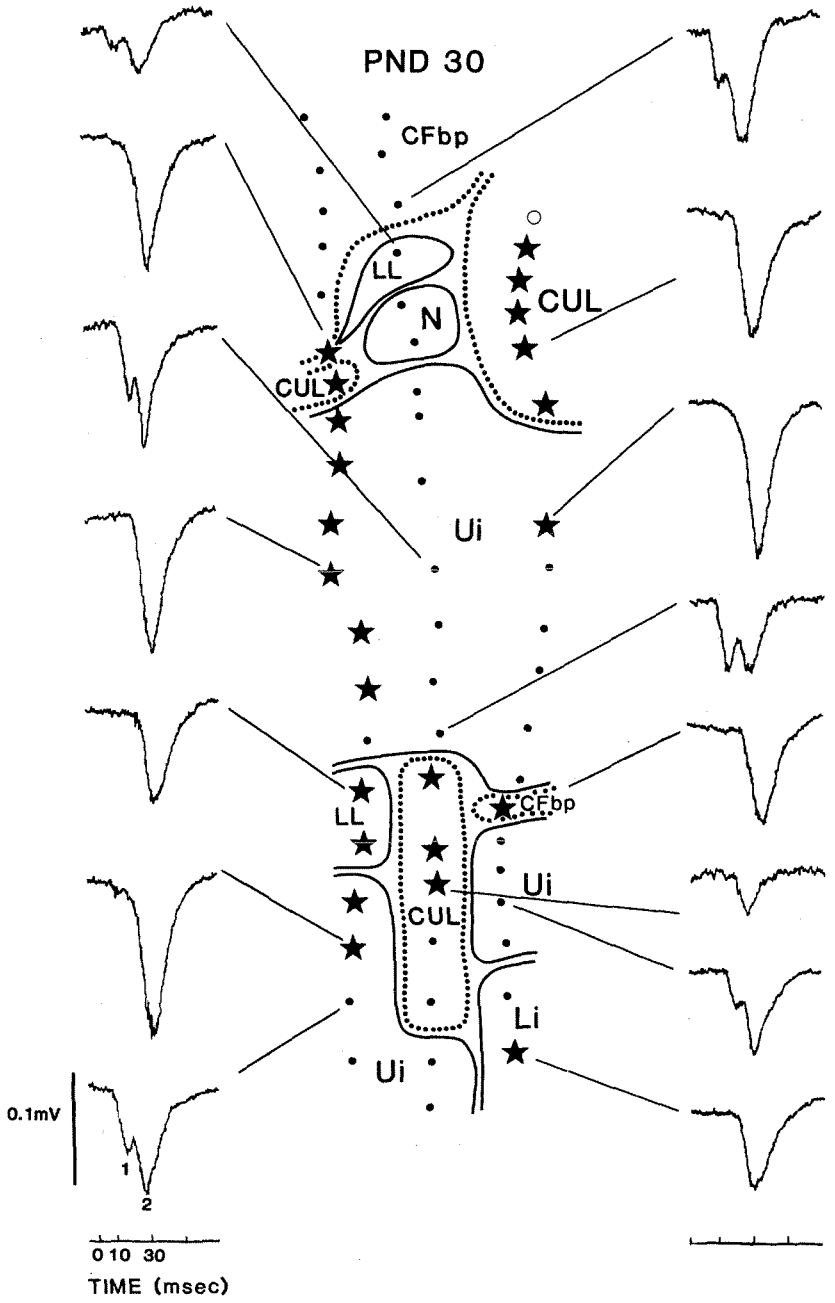
PND 30
CFbp
LL
N
CUL
CUL
Ui
LL
CFbp
Ui
CUL
Li
Ui
0.1mV
1
2
0 10 30
TIME (msec)

Figure 3.5

Figure 3.5 Map from a PND 30 animal showing the location and waveform of the two different types of field potentials that are typically elicited in the deafferented animals upon tactile stimulation of the appropriate receptive field. Solid dots: representative field potentials similar to those in normal animals, which include both short- and long-latency components; stars: representative field potentials that contain only the long-latency component; open circles: penetrations where field potentials were not recorded. Lower left trace shows the peak of the short-latency component from this PND 30 animal at position 1 (x = 10 msec), and the long-latency component at position 2 (x = 21 msec) (n = 8 trials). Dotted lines: contralateral receptive fields. Abbreviations as in Figure 3.1.

3.4.7 Spatial extent of field potential effects

We found no spatial pattern to cerebellar regions that either lack a short-latency response or are nonresponsive to tactile stimulation. Examination of the results in Figures 3.5 and 3.7, for example, shows that it is not unusual for some patches to contain both combined responses (filled dots) and those with the long-latency only (stars). In addition, comparison of these figures shows that evoked potentials lacking a short-latency response can be found in any region of crus IIa. They are even elicited in contralateral upper lip regions of the folium, including both the medial part of the folium and the reorganized area. While changes within the medial part of the folium might at first seem surprising given that neither the area of these medial patches nor the location of the contralateral upper lip border appears to change, it should be noted that, in normal animals, some patches in these locations are actually bilateral upper lip representations (Bower and Kassel 1990), and thus, might be expected to be affected in some fashion by ipsilateral denervation.

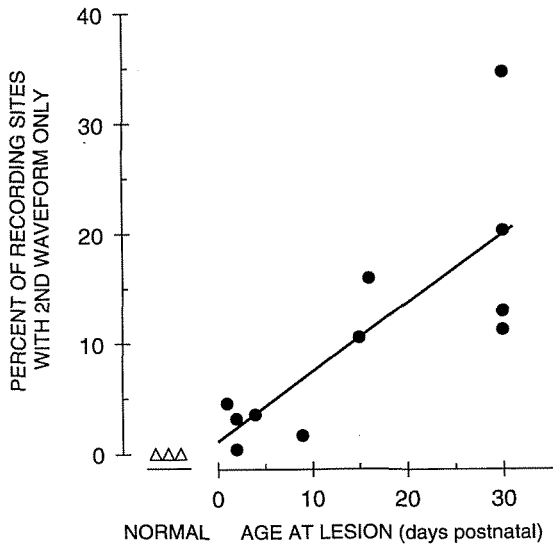

Figure 3.6 Percentage of penetrations with second waveform only as a function of age at the time of the lesion. Each open triangle and filled circle displays data from a single animal and represents the percentage of the 60 recording sites that had field potentials containing only the long-latency component (i.e., second waveform). Open triangles indicate normal animals; filled circles, lesioned animals. Solid line denotes regression line (R^2 = 0.611). The regression is significant as judged by an ANOVA (P = 0.004).

3.5 Discussion

3.5.1 Comparison with reorganization in other somatosensory structures

The results presented in this chapter provide the first demonstration of plasticity in a fractured somatosensory map following peripheral nerve lesions. We have found that tactile responsiveness in the crown of crus IIa is largely restored following lesions made up

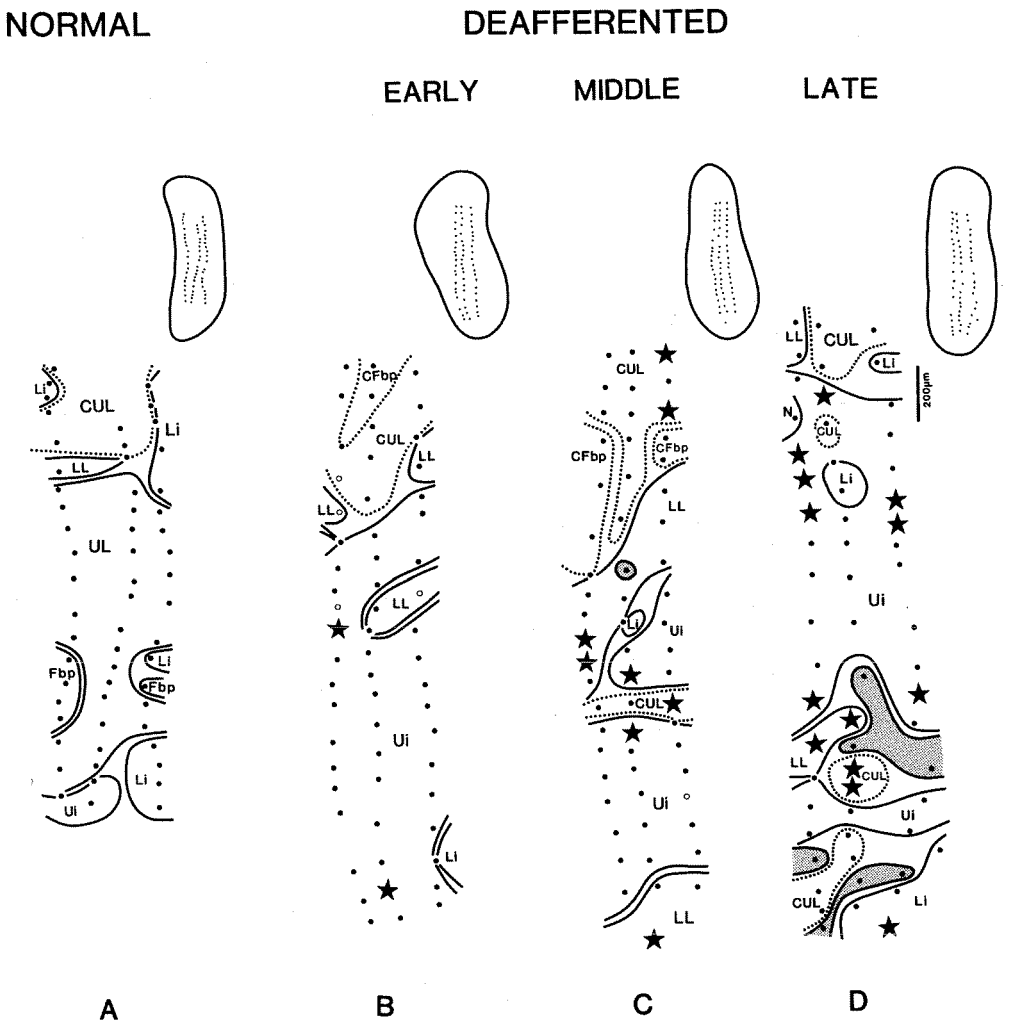

Figure 3.7 A–D: Tactile maps highlighting the location and type of field potential responses in normal animals and animals lesioned at different developmental stages. Recording sites having the normal type of field potential, i.e., including both short- and long-latency components, are represented by filled dots. Recording sites having the long-latency field potential component only are represented by stars. Open dots: recording sites where field potentials were not recorded. Dotted lines: contralateral receptive fields. Shaded regions represent areas that were not responsive to tactile stimulation. **Insets:** Locations of the three recording tracks within the crus IIa folium. Abbreviations as in Figure 3.1.

to 30 days postnatally. Similar physiological experiments in the primary somatosensory region of the cerebral cortex of rats have also demonstrated the ability of tactile maps to reorganize following lesions made postnatally (Waite 1984; Wall and Cusick 1984, 1986; Wall et al. 1986; Delacour et al. 1987) and even in adult animals (Wall and Cusick 1984). Similar results have been found in a variety of other mammals (Kalaska and Pomeranz 1979; Frank 1980; Rasmusson 1982; Kelahan and Doetsch 1984; Jenkins and Merzenich 1987; Merzenich 1987; Pons et al. 1987). Thus, map plasticity seems to be a feature of several mammalian somatosensory regions.

Earlier studies of the cerebral cortex in both neonates and adults have shown that substantial lesions of the periphery leave large nonresponsive cortical areas (Merzenich et al. 1984b; Waite 1984; Wall and Cusick 1984). More recent studies in the cerebral cortex of adult monkeys have shown complete reorganization of the cortical areas (Garraghty and Kaas 1991a; Pons et al. 1991). In the cerebellum, even though the peripheral regions that were deafferented project to a large percentage of crus IIa (64%), we did not find any large nonresponsive location.

3.5.2 Reorganization and cerebellar development

Before discussing possible mechanisms of map reorganization, it is important to point out that the cerebellum was actually being formed during the period when peripheral lesions were made (Altman 1982; Mason 1987). Thus, the process of development of the cerebellar cortex itself potentially complicates the interpretation of our results. In fact, at the earliest lesion dates in our experiments (PND 1 to 4), the cerebellum is quite immature. Mossy fibers are not even recognizable in the granule cell layer until the end of the first postnatal week (Altman 1982; Mason 1987). Throughout the second and third postnatal weeks (PND 7 to 20), the cerebellum continues to form its internal circuitry with the bulk of the granule cells also being formed during this period (Altman 1982; Mason 1987). It is only at the latest lesion dates (PND 30) that the cerebellum assumes anything like its adult

form. Thus, as discussed below, it is entirely possible that different mechanisms or combinations of mechanisms are responsible for the reorganization seen with lesions at different times during this period. Nevertheless, we have shown that the general pattern of reorganization, at least with respect to the distribution of tactile receptive fields, is the same regardless of the date of the lesion.

3.5.3 Mechanisms of reorganization

The particular form of lesion-induced reorganization seen in somatosensory maps has often been used as a basis for speculation on the mechanisms of map reorganization (Kaas et al. 1983). In the somatosensory cortex, for example, such speculations have been heavily influenced by the fact that reorganization consists primarily of the expansion of representations centrally and peripherally adjacent to the area of denervation (Kaas et al. 1983; Table 1, Wall and Cusick 1984; Merzenich 1987). However, the similarity in the organized somatotopy of SI and the structures that project to it (Emmers 1965; Nord 1967; Waite 1978; Belford and Killackey 1979, 1980; Erzurumlu et al. 1980) makes the actual site of reorganization somewhat difficult to determine. For example, Merzenich (1987) has suggested, based on deafferentation studies in the primate somatosensory cortex, that reorganization is primarily intrinsic to the cortex (also the S2 study by Pons et al. 1988). However, others have interpreted the same data to suggest that restructuring of precortical somatosensory areas contributes to, or is entirely responsible for, the observed cortical changes (Kaas et al. 1983; for review see Killackey 1989). Kaas, in a recent review, strongly argues that it is both (1994).

While the cerebellum also receives projections from brainstem and midbrain nuclei whose internal representation of the body surface is somatotopic (for review see Welker 1987), the granule cell layer itself has a fractured topography and the reorganization following peripheral lesions does not appear to be from normally adjacent representations. As discussed in the next sections, we believe that this fractured form of reorganization may

provide a better opportunity for distinguishing between internal (i.e., within the cerebellum) and external mechanisms of reorganization.

Intrinsic mechanisms

One of the most obvious intrinsic cortical mechanisms to consider in attempting to account for somatosensory map reorganization is the physical sprouting of new connections from existing projections (Merrill and Wall 1978; Kaas et al. 1983), although several experimenters have argued that this is an unlikely mechanism for reorganization in the *cerebral cortex* (Merzenich et al. 1983ab, 1987; Merzenich 1987). In the *cerebellum*, physical sprouting is a possible mechanism only for animals older than PND 7 since afferent projections are not even present in earlier stages of cerebellar development (Altman 1982). Even for these older animals, however, we would expect that if the denervated regions were simply being filled in by sprouting from adjacent intact representations, the more heavily represented lower lip, lower incisors, and contralateral perioral regions (as shown in the normal map, Bower and Kassel 1990) would have made a much larger contribution to the reorganized map. Instead, projections from the upper incisor, which is normally minimally represented in the folium (Figure 3.3) and whose representation is often not even adjacent to that of the upper lip in normal animals (Bower and Kassel 1990), predominately fills in for the missing upper lip representation. Accordingly, our observations make sprouting an unlikely explanation for reorganization at any stage of development.

A second intrinsic mechanism of reorganization that has been proposed is the physiological unmasking of existing but previously suppressed or silent connections (Merrill and Wall 1978; Kaas et al. 1983; Devor 1987). This proposal is based on anatomical evidence that the horizontal extent of afferent projections to the somatosensory cortex exceeds the region in which physiological responses from particular afferents are normally recorded (Jensen and Killackey 1987). Unmasking, however, seems an unlikely

explanation in the cerebellar cortex for several reasons. First, the dominance of the upper incisor in the reorganized maps would require that only the representation of this structure be more broadly distributed within the cerebellar cortex. This seems unlikely. Second, previous physiological experiments in crus IIa have suggested that the horizontal spread of trigeminal afferents is restricted only to the region of the granule cell layer that normally responds to those inputs (Woolston et al. 1981). In other words, trigeminal mossy fibers appear not to extend outside the tactile patch to which they project. It is important to note, however, that actual anatomical data on the distribution of mossy fibers with respect to patch boundaries are not yet available.

Extrinsic influences

In sum, it seems unlikely that intrinsic cerebellar mechanisms are primarily responsible for the patterns of map reorganization we have described. Accordingly, reorganization is more likely to be associated with changes in the afferent projections. The strongest experimental support for this interpretation comes from the results of our evoked potential recordings indicating developmentally-related changes in the temporal structure of granule cell responses. These changes are differentially expressed in the two components of the granule cell layer evoked potential. Presumably this reflects the differential modifiability of the pathways associated with these two responses, since a mechanism of reorganization intrinsic to the cerebellar cortex would be most likely to affect both field potential components equally.

The main effect of the age of lesion on cerebellar evoked potentials is a gradual decrease in the areal extent of the cortex responding to peripheral stimulation at short-latency. The decrease begins with lesions made after the first postnatal week and intensifies through at least 30 days postnatal. This result demonstrates a developmentally-related loss of plasticity in one component of cerebellar reorganization. Based on the latency of the shortest granule cell layer response to peripheral stimulation, as well as the results of

previous physiological experiments (Woolston et al. 1982), it is almost certain that the affected response is relayed from the periphery through the trigeminal nucleus.

Our developmental results show that the long-latency evoked response to peripheral stimulation is much more resilient to peripheral lesions than the short-latency response. We demonstrated in Chapter 2 that the primary contribution to this long-latency component comes from a pathway involving the primary somatosensory cerebral cortex. It has also been shown that the somatosensory cortex normally projects to these regions of crus IIa in register with the short-latency direct trigeminal projections (Bower et al. 1981). Accordingly, it seems reasonable to suggest that the resiliency in long-latency responses may be directly related to the demonstrated ability of the somatosensory cortex and/or its related midbrain structures (i.e., the thalamus and pons) to reorganize throughout development (Merrill and Wall 1978; Kaas et al. 1983; Wall and Cusick 1984, 1986; Jenkins and Merzenich 1987; Merzenich 1987; Pons et al. 1987; Killackey 1989).

3.5.4 Significance of the developmental sensitivity of the short-latency component

An obvious question that arises from these evoked potential results is: Which component of the short-latency pathway is responsible for its relative lack of plasticity? There are several locations along this direct trigeminocerebellar pathway that could be responsible. First, the first-order projections from the periphery to the trigeminal nucleus could have a sensitive period for plastic change. Unfortunately, detailed physiological studies of map reorganization in the trigeminal system of the developing rat have not yet been undertaken. However, anatomical experiments with succinic dehydrogenase (SDH) have suggested that the sensitive period for map development in this nucleus ends on PND 3 (Belford and Killackey 1980). More recent anatomical experiments with SDH and horseradish peroxidase (HRP) are also consistent with an early end to trigeminal plasticity (Waite and de Permentier 1991).

A second possible source of reorganization of the short-latency cerebellar response is the second-order projection from the trigeminal nucleus to the cerebellum. It is also not yet known when this part of the pathway completes its development under normal conditions. However, as mentioned previously, trigeminocerebellar afferents do not appear to be present in the cerebellum at the earliest lesion dates of the current experiment (Altman 1982; Mason 1987). Accordingly, it might be expected that this projection completely reorganizes following lesions made at PND 1 and 4.

By the beginning of the second postnatal week, mossy fibers appear to be present in the still undeveloped cerebellum (Altman 1982). However, from their first arrival until the end of the third postnatal week, these afferents terminate directly on Purkinje cells (Mason and Gregory 1984; Mason 1987). Since a similar mossy fiber to Purkinje cell connection has not been reported in the adult, this connection is assumed to be a developmentally-related phenomenon. The timing of these connections, between the second and third postnatal week, is the same time period in which we have found a gradual reduction in plasticity in the short-latency component of the cerebellar granule cell layer response. Accordingly, it seems quite reasonable to suggest that these transient connections may play a role in the establishment of the spatial organization of at least short-latency mossy fiber projection patterns. It is important to note, however, that the bulk of the rest of the cerebellar cortical circuitry is also forming during these early postnatal weeks.

3.5.5 Significance of map reorganization for cerebellar function

Studies of the *somatosensory cortex* have suggested that map reorganization effectively provides a sensory substitution for deafferented regions, i.e., that structural changes reflect functional changes (Jenkins and Merzenich 1987; Merzenich 1987; Pons et al. 1987). For example, Kaas et al. (1983) have shown that intact fingers adjacent to deafferented ones are heavily represented in the reorganized denervated regions of SI cortex in monkeys. Of course, in SI cortex, such structures are both peripherally and centrally

adjacent. The functional significance of map organization is more strongly indicated by recent experiments in intact animal. These experiments have demonstrated that peripheral stimulation alone can alter reorganization within the SI map (Recanzone et al. 1990; Jenkins et al. 1990).

In the cerebellum, the consistency of the upper incisor expansion into the denervated area leads us to suggest that this structure may be functionally substituting for the upper lip. Although the upper incisor representation is often not adjacent to that of the upper lip in crus IIa, the upper incisor is peripherally adjacent to the upper lip in the three-dimensional organization of the rat's perioral region. Thus, through physical contact with the upper lip, the upper incisor may be able to transmit information about contact with the upper lip to the cerebellum. In some animals, responses could be evoked in the new upper incisor patches upon stimulation of the denervated upper lip. The suggestion that this is a functional substitution is further supported by the fact that the pattern of the upper incisor representation, in deafferented animals, is similar to that of the upper lip in normal animals; both representations tend to consist of a large patch in the center of the folium, surrounded by smaller patches from other perioral structures.

In addition to the changes in representation seen in the reorganized cerebellar maps, a striking feature of our results is the persistence of many of the previously reported invariant features of normal maps (Bower and Kassel 1990). Such features include fractured somatotopy; the fact that crus IIa continues to represent the same perioral body parts; and, as noted previously, the fact that the center of crus IIa still primarily consists of one large representation surrounded by adjacent smaller patches.

The invariance of these features in the crus IIa maps of both deafferented and normal animals, and the likely functional substitution by the upper incisor, supports an earlier hypothesis that the detailed arrangement within tactile maps in the cerebellar cortex may be highly significant for their function (Bower and Kassel 1990). Specifically, it was

suggested that those cerebellar regions, which receive somatosensory information following peripheral stimulation faster than the somatosensory cortex (Bower et al. 1981; Welker 1987), are involved in controlling the use of perioral surfaces during sensory data acquisition (Bower and Kassel 1990). By monitoring the information obtained from sensory structures during sensory exploration and by using the motor system to subtly reposition sensory surfaces accordingly, cerebellar circuits might serve to substantially improve the quality of the sensory information obtained. This, in turn, is expected to greatly increase the efficiency of sensory processing by other brain regions (Paulin et al. 1989ab; Rasnow et al. 1989; Bower and Kassel 1990).

4

Developmental Plasticity in Cerebellar Tactile Maps: Adults

[...] but the Spirits inhabiting the cerebel perform unperceivedly and silently their Work of Nature without our Knowledge or Care.

Thomas Willis

Cerebri anatome, 1681

4.1 Abstract

We have previously demonstrated that the fractured tactile cerebellar maps found in the cerebellar folium crus IIa reorganize following deafferentation of the upper lip area in neonatal animals (Chapter 3). Subsequently, we examined the capacity of these same cerebellar granule cell regions to reorganize following deafferentation of the upper lip in *adults*. Two to three months after cauterization of the infraorbital branch of the trigeminal nerve in adult rats, tactile maps in the granule cell layer of crus IIa reorganized with representations of intact structures expanding into the denervated area. The pattern of reorganization was similar to that found previously in neonates in several ways: 1) all representations in the reorganized maps continued to be from perioral structures; 2) the denervated area was predominantly and consistently invaded by a representation of the upper incisor; and 3) the reorganized maps maintained a fractured somatotopy. We also observed several differences in the pattern of reorganization that were related to the age of

the animal at deafferentation. For example, the older the rats at the time of nerve lesion, the more nonresponsive sites were found in crus IIa when mapped two months after the nerve lesion. In addition, and somewhat surprisingly, there was a greater similarity between the pattern of tactilely-evoked field potentials in the adults and animals lesioned at early postnatal days than for animals lesioned between 30 and 40 days postnatal. Finally, we explored possible mechanisms underlying crus IIa reorganization and found that the dominance of upper incisor in the reorganized maps was not due to immediate unmasking of silent projections or expansion of previously weak projections.

4.2 Introduction

This chapter is a continuation of a series of investigations concerning the ability of the tactile maps in the granule cell layer of the rat cerebellum to reorganize following lesion of peripheral nerves. We have previously demonstrated that the fractured somatotopic maps found in this region of the cerebellum do reorganize in a regular and repeatable fashion following peripheral nerve lesions in neonatal animals (Chapter 3).

Over the last several years, numerous studies have examined the ability of somatosensory maps to reorganize following denervation in adults (*somatosensory cortex*: Merzenich et al. 1983ab, 1984a; Wall and Cusick 1984; Calford and Tweedale 1991; *thalamus*: Garraghty and Kaas 1991b; *trigeminal nuclei*: Waite 1984; for reviews see Snow and Wilson 1991; Kaas 1991, 1994). When compared to studies in the same structures following neonatal deafferentation, the spatial extent of adult reorganization is often more variable and restricted. For example, spinal cord or peripheral nerve transection caused extensive reorganization in cortical and/or subcortical areas in neonates, but limited changes in adult rats (Waite 1984; McKinley and Smith 1990). However, Wall and Cusick (1986) reported a more extensive reorganization of the hindpaw region of SI cortex following sciatic nerve section in adults compared to similar section in neonatal rats (Wall and Cusick

1984). While some studies report complete cortical reactivation following injuries ranging from restricted peripheral nerve lesion to extensive deafferentation of an entire limb (Merzenich et al. 1983a; Garraghty and Kaas 1991a; Pons et al. 1991), others report that part of the denervated cortical area did not reorganize even several months after the amputation of two digits in adult monkeys (Merzenich et al. 1984a). Some studies even failed to detect any response in the deafferented cortex following dorsal column section in the rat (Jain et al. 1995). Cortical reorganization can occur within minutes (Calford and Tweedale 1991) and can progress for months (Cusick et al. 1990).

In this chapter, we demonstrate that lesions of the infraorbital branch of the trigeminal nerve in adult rats result in a substantial reorganization of tactile maps in crus IIa of cerebellar cortex. We found extensive reorganization in the brain of adult rats two to three months after the nerve was cut. Moreover, the pattern of reorganization was in many ways similar to the pattern observed when this same nerve was sectioned in neonates. There were, however, several differences in map reorganization related to the age of the animal at deafferentation. The similarity in the overall structure of the maps further supports the idea that the fractured structure of these maps is important to cerebellar function. To explore possible intrinsic mechanisms for cerebellar reorganization, we mapped cerebellar granule cell layer receptive fields before and immediately after lesions, and carefully examined the distribution of weak (subdominant) inputs in normal animals. Our results show that the large expansion of the upper incisor into the denervated area of the cerebellum, observed two months after deafferentation, is not a consequence of *immediate* unmasking of previously weak, or suppressed upper incisor inputs to the region. This, combined with the different effect of deafferentation on the two peaks of the granule cell layer field potentials, suggests that the principal site of cerebellar plasticity following deafferentation is not in the cerebellum itself, but rather in its afferent pathways.

4.3 Methods

4.3.1 Animals used

A total of 35 Sprague-Dawley albino rats were used: 15 adult control animals (3 of which were used in the studies of cerebellar map organization before and immediately after lesion) and 20 experimental animals. The infraorbital branch of the trigeminal nerve of the experimental animals was lesioned at different times after birth, including postnatal day 30 (PND 30, n = 8); PND 40 (3); PND 77 (3); PND 80 (2); PND 85 (3); and PND 89 (1). Since not all experiments were undertaken with each animal, the number of animals used for any given experiment are presented in the results and figure legends.

4.3.2 Deafferentation

The infraorbital branch of the maxillary division of the trigeminal nerve on the left side of the face was cauterized in one to three month old rats. Transection of that branch of the trigeminal nerve removes all sensation from the upper lip, vibrissae, furry buccal pad, and anterior sinus hair on the left side of the face but does not cause any motor deficit. Nerve cauterization was performed on rats anaesthetized with chloral hydrate (420 mg/kg body weight). An incision was made between the occipital bone ridge and the caudal edge of the vibrissae pad, and the wound bathed in 2% lidocaine HCl. The infraorbital branch was then exposed by teasing away surrounding muscle. A cautery unit (Sybron) was used to interrupt the nerve for several millimeters. Care was taken to cauterize all of the multiple branches of the nerve. As an additional precaution against nerve regeneration, bone wax was inserted under the occipital bone ridge in the nerve's previous location. Following another application of the local anaesthetic, 2% lidocaine HCl, the wound was closed with silk sutures. The animals were monitored for several hours until they had appeared to

recover completely from the anaesthesia. They were subsequently returned to the animal care facility.

4.3.3 Cerebellar craniotomy and electrophysiological procedures

Surgical and tactile mapping procedures were identical to those described in section 3.3.

4.3.4 Receptive field mapping immediately following lesion

For three of the normal animals, the central region of crus IIa was mapped in detail as described in section 3.3.3, then immediately mapped again following nerve section. After crus IIa had been completely mapped, the infraorbital branch of the trigeminal nerve was cauterized as described in section 4.3.2. Electrode penetrations following deafferentation were positioned in the same location as the original map, with the aid of the original coordinates and the location of the original penetrations relative to the surface vasculature on the photograph.

4.3.5 Map construction

As in previous experiments (Welker 1987), and as described in section 3.3.3, maps of tactile cerebellar regions were constructed by drawing enclosing boundaries around adjacent electrode penetration locations whose strongest receptive fields were from the same body structure. In cases where responses were of equal strength, the boundary line was drawn through the site of the electrode penetration.

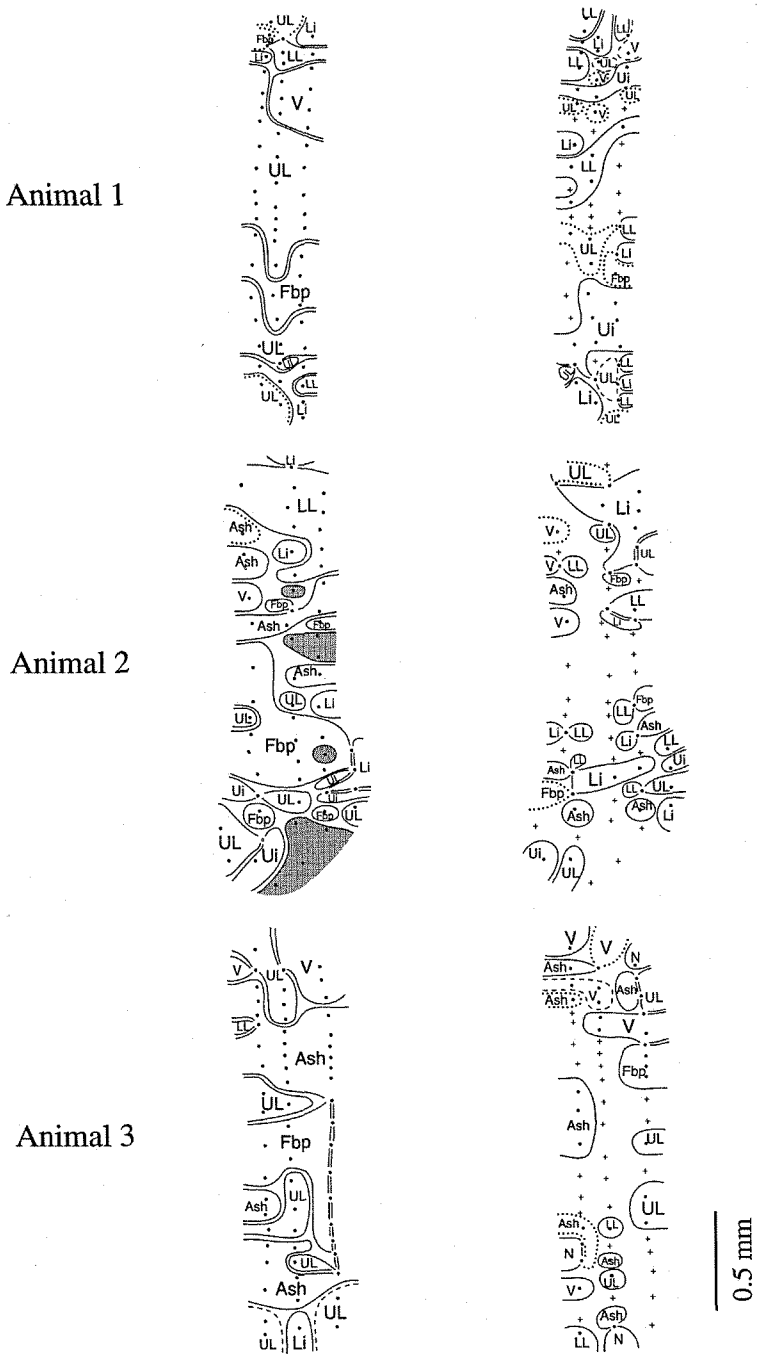
A. Dominant receptive fields
B. Subdominant receptive fields
Animal 1
Animal 2
Animal 3
0.5 mm

Figure 4.1

Figure 4.1 Maps of the tactile receptive fields within crus IIa in three different normal animals. **A:** Dominant receptive fields: the face areas that elicited the strongest response in the granule cell layer following tactile stimulation, are shown. **B:** Subdominant receptive fields: other face areas often elicit weaker responses in the granule cell layer upon stimulation. The strongest of the subdominant receptive fields are shown in B. *For this and subsequent map figures:* Filled dots represent the location of the electrode penetrations; crosses, electrode locations where no subdominant receptive field could be detected. Dotted lines around a patch indicate projections from contralateral structures; dashed lines, bilateral; and solid lines, ipsilateral. Shaded areas indicate cerebellar locations that did not respond to any tactile stimulation (nonresponsive). Ash: anterior sinus hair; Fbp: furry buccal pad; Li: lower incisor; LL: lower lip; N: nose; Ui: upper incisor; UL: upper lip; V: vibrissae.

4.3.6 Statistical analysis of tactile responses

Statistical two-sample comparisons of perioral representations between different experimental groups were conducted with a Mann-Whitney U test. Multiple comparisons of receptive fields within maps were conducted with a one-way repeated measures ANOVA followed by a Scheffé F test. The significance level was set at 0.05. All measures of variability described here are standard errors, SE.

4.4 Results

4.4.1 Tactile organization in normal adult cerebellum

A number of previous reports have described in detail the pattern of perioral representations found in crus IIa of the adult rat (Shambes et al. 1978b; Welker 1987; Bower and Kassel 1990). As shown in Figure 4.1A, the upper lip perioral structures innervated by the infraorbital branch of the trigeminal nerve (i.e., the ventral upper lip,

anterior sinus hair, furry buccal pad, and vibrissae) constitute the largest total representation in the crown of this folium. This is quantified in Figure 4.2 where the average percentage representation of each body structure projecting to crus IIa for 15 animals is shown by the black bars. Note that on average all non upper lip perioral structures are represented in approximately equal proportion in normal adult animals (no significant difference for all pair-wise comparisons, as judged by a Scheffé test).

Subdominant receptive fields

Maps, such as those in Figure 4.1A, are routinely constructed with the perioral structures eliciting the strongest response (Shambes et al. 1978b; Welker 1987; Bower and Kassel 1990). In addition to these "dominant" responses, weaker, "subdominant" responses to stimulation of other perioral structures can often be elicited. The maps in Figure 4.1B show the spatial distribution of penetrations that had receptive fields associated with weaker responses in the granule cell layer. These responses are typically much less robust than the dominant receptive fields and, accordingly, are more difficult to map. Such multiple representations generally have differing strengths of response, which can be due to a number of factors, including differences in the total extent of the input, the width of the axons, the extent of arborization, etc.; further experiments will be necessary to determine what significance, if any, such weak inputs might have for the physiology of crus IIa granule cells. Figure 4.2 compares the mean percentage of the subdominant receptive fields from different perioral regions in normal animals. The data were derived by counting the total number of times a given perioral structure was detected as a subdominant receptive field for each animal and subsequently normalizing this number as a percentage of the total number of subdominant receptive fields for that animal. As this figure demonstrates, the ipsilateral upper lip and its related structures (i.e., furry buccal pad, vibrissae, and anterior sinus hair) tended to be the most common subdominant receptive field type, just as it is the most

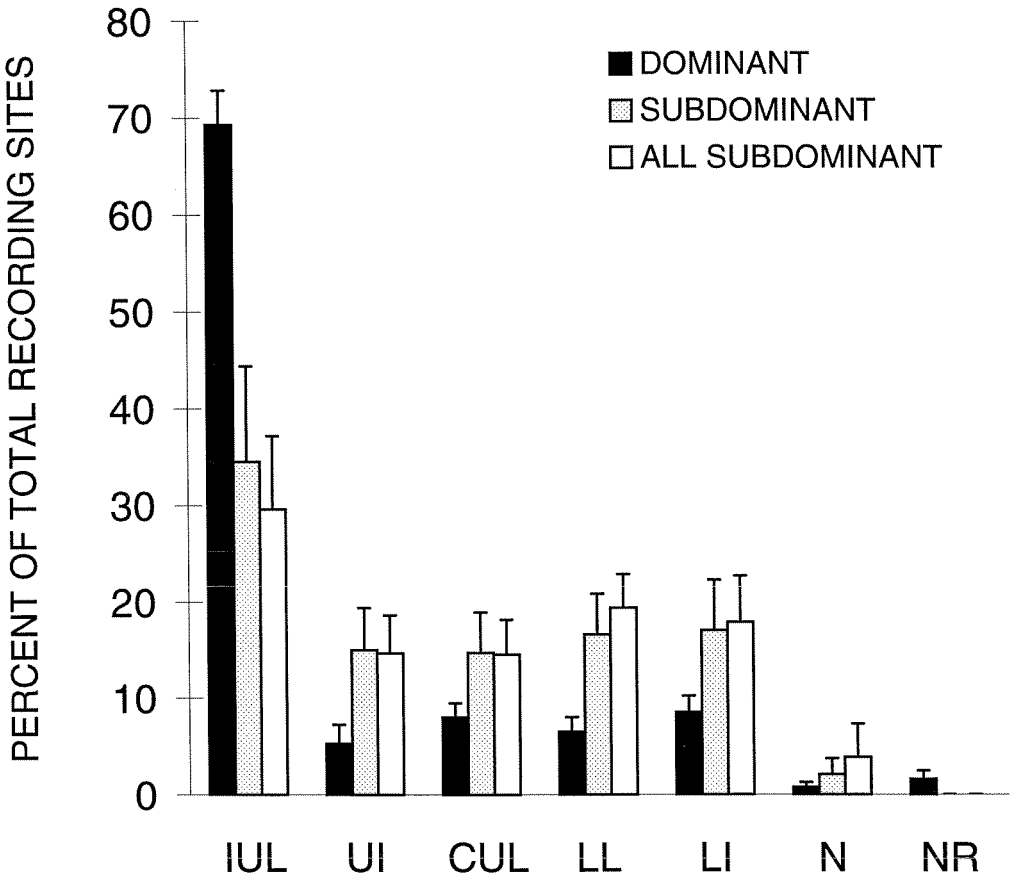

Figure 4.2 Comparison of the proportion of different perioral structures comprising the crus IIa maps in normal animals. Each bar represents the mean ± SE of the total responses elicited by tactile stimulation of a given perioral structure. The dominant responses are shown as black bars (n = 15); strongest subdominant, as stippled bars (n = 6); and all of the subdominant responses, as white bars (n = 6). *Abbreviations for this and subsequent histograms:* IUL: ipsilateral upper lip and related ipsilateral structures (vibrissae, furry buccal pad, and anterior sinus hair); UI: upper incisor; CUL: contralateral upper lip and related contralateral structures (vibrissae, furry buccal pad, and anterior sinus hair); LL: lower lip; LI: lower incisor; N: nose; NR: nonresponsive.

common dominant receptive field type. Of the non upper lip structures, all were represented in roughly equal proportion, with the exception of the nose.

On average, 71% of all responsive penetrations had subdominant receptive fields. Of the penetrations with infraorbital-related dominant receptive fields (i.e., upper lip, vibrissae, furry buccal pad, anterior sinus hair), 52% had noninfraorbital-related subdominant receptive fields. To determine whether some of these subdominant responses could be due to passive electrical spread of granule cell layer activity, we determined how many of the penetrations with subdominant receptive fields were immediately adjacent to a dominant receptive field of the same type. Only the middle mediolateral column of electrode penetrations was used for this analysis in order to ensure that all points had equivalent adjacent penetrations. The results show that 44% of the locations with subdominant receptive fields were adjacent to locations with dominant receptive fields of the same type. Thus, the majority of the subdominant responses (56%) appear to represent actual weak afferent projections.

These subdominant representations, like the dominant, are topographically organized in patches in crus IIa (Figure 4.1). Figure 4.10A compares the "patchiness" of the cerebellar representation for dominant and subdominant responses. Only 9% of the cerebellar sites with dominant responses comprise one electrode penetration, while the majority (81%) comprise three or more adjacent electrode penetrations with common receptive field. In contrast, 32% of the cerebellar sites with subdominant responses comprise one electrode location, 19% comprise two adjacent electrode locations, and 49% comprise three or more. Bearing in mind that these weak receptive fields are difficult to map, these results indicate that subdominant representations are organized in an even finer fractured pattern than those of the dominant, larger amplitude tactile projections to crus IIa.

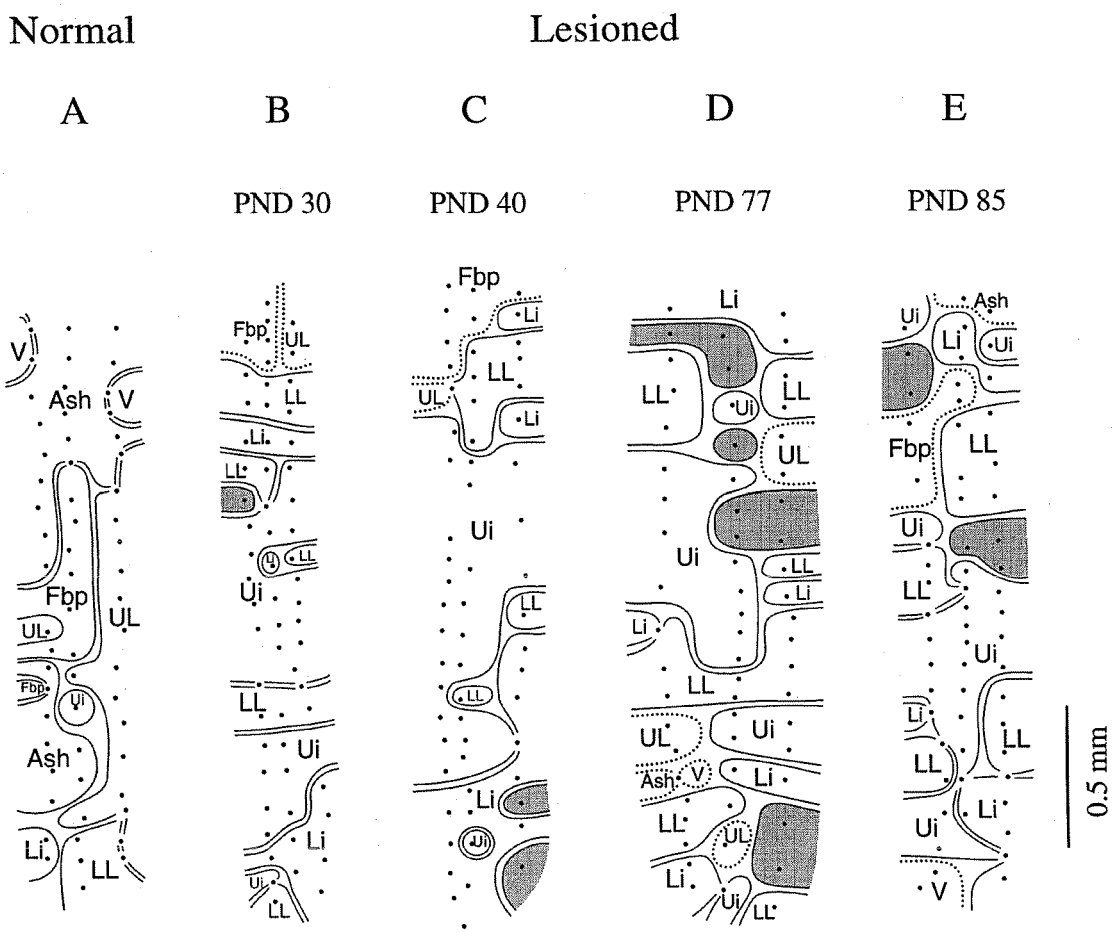

Figure 4.3 Organization of the tactile inputs to the granule cell layers of crus IIa for five different rats. **A:** Tactile map is shown for a normal adult animal. The infraorbital branch of the trigeminal nerve was cut in four animals and the reorganization of tactile inputs mapped two to three months later. The reorganized maps are shown for animals that had their nerve cut at **B:** PND 30, **C:** PND 40, **D:** PND 77, and **E:** PND 85.

4.4.2 Tactile reorganization two months after deafferentation

Figure 4.3 shows the pattern of tactile inputs to crus IIa two months after the infraorbital branch of the trigeminal nerve was lesioned at different postnatal ages (1 to 3 month old animals). This figure shows that extensive reorganization was found in all animals lesioned, regardless of the age at deafferentation. Although there is clear variability between the individual reorganized maps, close examination reveals some striking similarities. In the following sections we describe the pattern of adult reorganization and contrast it with previous data on the reorganization of neonates.

Patchy organization of reorganized maps

It is clear from a comparison of the maps shown in Figure 4.3 that different body surfaces are represented in "patches" within crus IIa of normal animals (A) as well as after peripheral lesions (B–E). Further, the general size and distribution of the patches are similar between normal and lesioned maps. Maps found after neonatal lesions were also generally similar in their patchy structure (Figures 3.2 and 3.7).

Change in representation of perioral surfaces

In each animal mapped, the body surfaces whose representations invaded the denervated region were all perioral regions that are also represented in the crus IIa of normal animals (Figure 4.3). The upper incisor was the predominant structure represented in lesioned animals, covering 44% of the reorganized map. In normal animals, however, the upper incisor was the dominant receptive field in only 5% of the penetrations. As shown in Figure 4.4, in addition to the significant increase in upper incisor ($P = 0.0001$, as judged by a Mann-Whitney U test), there was also a significant increase in the representation of the lower lip (from 6.5% to 20%, $P = 0.0001$). The contralateral upper lip, lower incisor, and nose representation did not increase significantly. The proportion of the various face areas

that invaded the denervated area did not vary significantly whether the nerve was cut 30, 40, or more than 70 days after birth (Table 4.1).

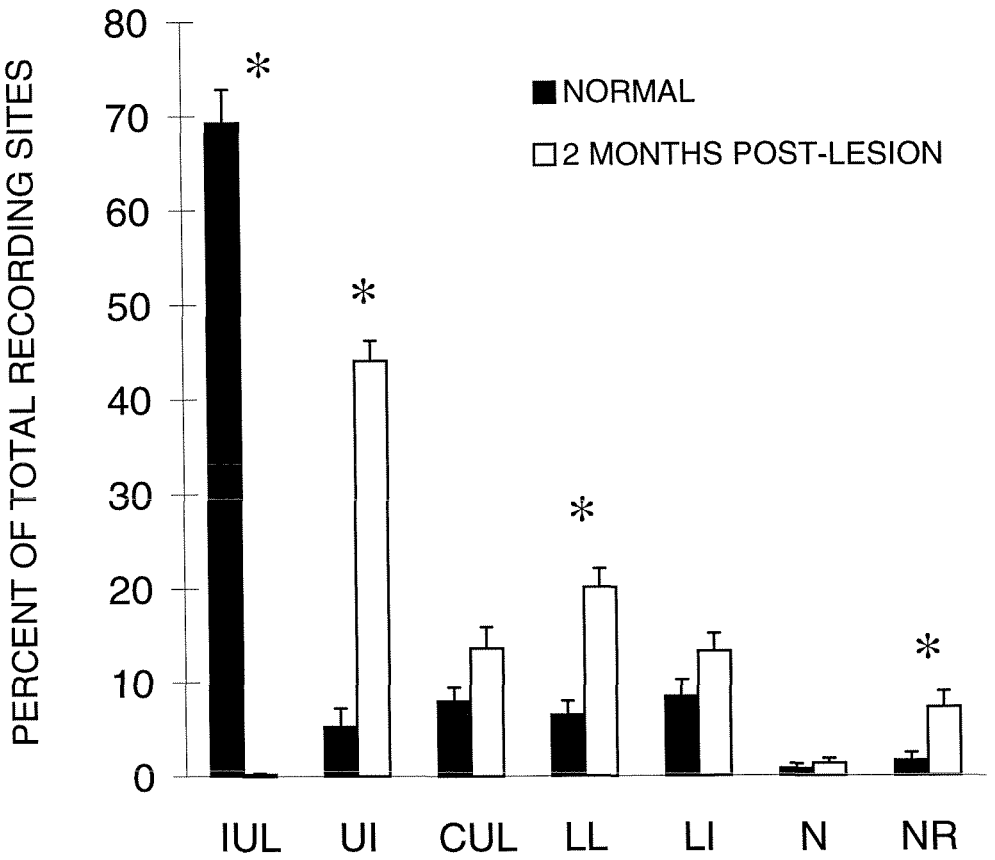

Figure 4.4 Comparison of the percentage of representation for various perioral structures in tactile maps of normal animals (black bars, n = 15) and of lesioned animals (white bars, n = 20). The data from animals lesioned at PND 30 to PND 90 were pooled as there was no significant difference in the body surface representations for these animals (see Table 4.1). Each bar represents the mean ± SE of total recording sites responding to stimulation of a given face area. The upper incisor and lower lip representations were significantly larger in lesioned animals. Asterisks indicate significant differences in the percentage of representation of a particular face area between normal and deafferented animals (as judged by a Mann-Whitney U test, $P < 0.01$).

When Figure 4.4 is compared with Figure 3.3, it can be seen that the proportion of representation for various face surfaces in animals lesioned as adults is very similar to that found in neonatally lesioned animals. In both cases, the largest representation post-lesion is the upper incisor. Neonatally lesioned animals, however, showed a larger expansion of the contralateral upper lip than animals lesioned as adults.

	Percent of total recording sites			
		Deafferented developmental stage		
Receptive field type	Normal (n = 15)	PND 30 (n = 8)	PND 40 (n = 3)	> PND 75 (n = 9)
IUL	69.28 ± 3.53	0.32 ± 0.32	0	0.17 ± 0.17
UI	5.28 ± 1.98	44.18 ± 3.10	44.94 ± 1.89	42.76 ± 3.95
CUL	8.03 ± 1.48	18.54 ± 4.26	7.98 ± 2.51	13.43 ± 3.59
LL	6.54 ± 1.49	16.13 ± 2.69	27.43 ± 4.86	21.86 ± 2.72
LI	8.50 ± 1.74	11.37 ± 3.45	13.85 ± 5.36	13.77 ± 2.40
N	0.77 ± 0.49	1.26 ± 0.53	4.72 ± 2.40	0.18 ± 0.18
NR	1.60 ± 0.87	8.20 ± 2.92	1.08 ± 1.08	7.83 ± 2.42

Table 4.1 Comparison of map organization between normal rats and rats with peripheral lesions performed on different postnatal days. Numbers reflect the mean percent ± SE of the total recording sites for a given receptive field type. Abbreviations as in Figure 4.2.

Increase in the number of nonresponsive sites

In most animals deafferented as adults, no response to peripheral tactile stimulation of any face area could be elicited at some electrode penetrations. Figure 4.3 indicates the locations within each reorganized map that were nonresponsive to tactile stimulation of the body surface. Such nonresponsive penetrations only represented 2% of the total

penetrations in normal animals. The number of nonresponsive penetrations significantly increased to 8% when the nerve was cut in adult animals ($P < 0.05$).

Figure 4.5 compares the number of nonresponsive recordings for all animals lesioned from PND 1 through PND 89. There is an age-of-lesion related increase in the number of nonresponsive recording sites. While the variability from animal to animal at a given age is quite high, a regression line drawn through the lesioned animals is significant ($R^2 = 0.14$, $P = 0.03$).

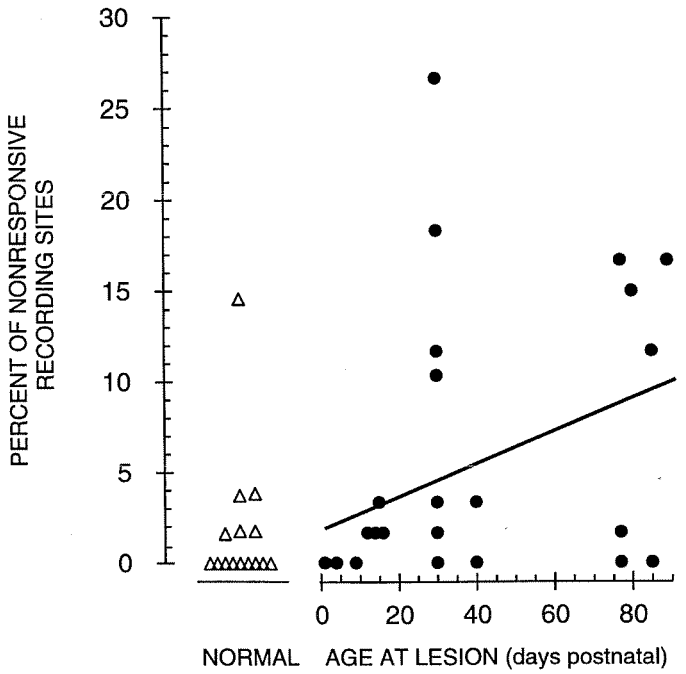

Figure 4.5 Percentage of nonresponsive electrode penetrations as a function of the age at the time of the nerve lesion. Each point displays data from a single animal (open triangles: normal animals; filled dots: lesioned animals) and represents the percentage of the 60 electrode penetrations for which no response could be elicited by tactile stimulation. Solid line denotes regression line ($R^2 = 0.14$). The regression is significant as judged by an ANOVA ($P = 0.03$).

Variation and distribution of field potentials lacking the short-latency component

In our previous studies of neonatal animals, we found that tactilely-evoked field potentials recorded in lesioned animals can sometimes differ from those found in intact animals (Figure 3.5). In particular, peripheral tactile stimulations in lesioned animals sometimes did not evoke the two-peaked field potential responses characteristic of normal animals (Chapter 2). Instead, in some cases, the field potentials consisted of only the second waveform, or long-latency component (Chapter 3). Figure 4.6 shows maps from four different animals lesioned at PND 30 with the locations of such altered field potentials indicated by stars. Note that there appears to be no systematic spatial distribution of the field potential responses with only the second waveform. Those field potentials lacking the first peak, or short-latency component, of the response to tactile stimulation were found for every receptive field type, roughly in proportion to the percentage of representation found within the folium (Table 4.2).

	Percent of total recording sites	
Receptive field type	Sites with 2nd waveform only (n = 17)	All recording sites (n = 17)
IUL	0	0.28 ± 0.20
UI	42.25 ± 9.11	46.78 ± 1.74
CUL	29.84 ± 9.83	16.51 ± 2.94
LL	18.48 ± 6.76	19.73 ± 2.07
LI	3.51 ± 3.20	15.03 ± 2.21
N	5.92 ± 3.63	1.67 ± 0.60

Table 4.2 Comparison of receptive field type for all responsive recording sites and responsive sites with only the long-latency component of the tactilely-evoked field potentials. Numbers reflect the mean percent ± SE of the total recording sites for a given receptive field type. The PND 30 to PND 90 animals were pooled together (n = 17). Abbreviations as in Figure 4.2.

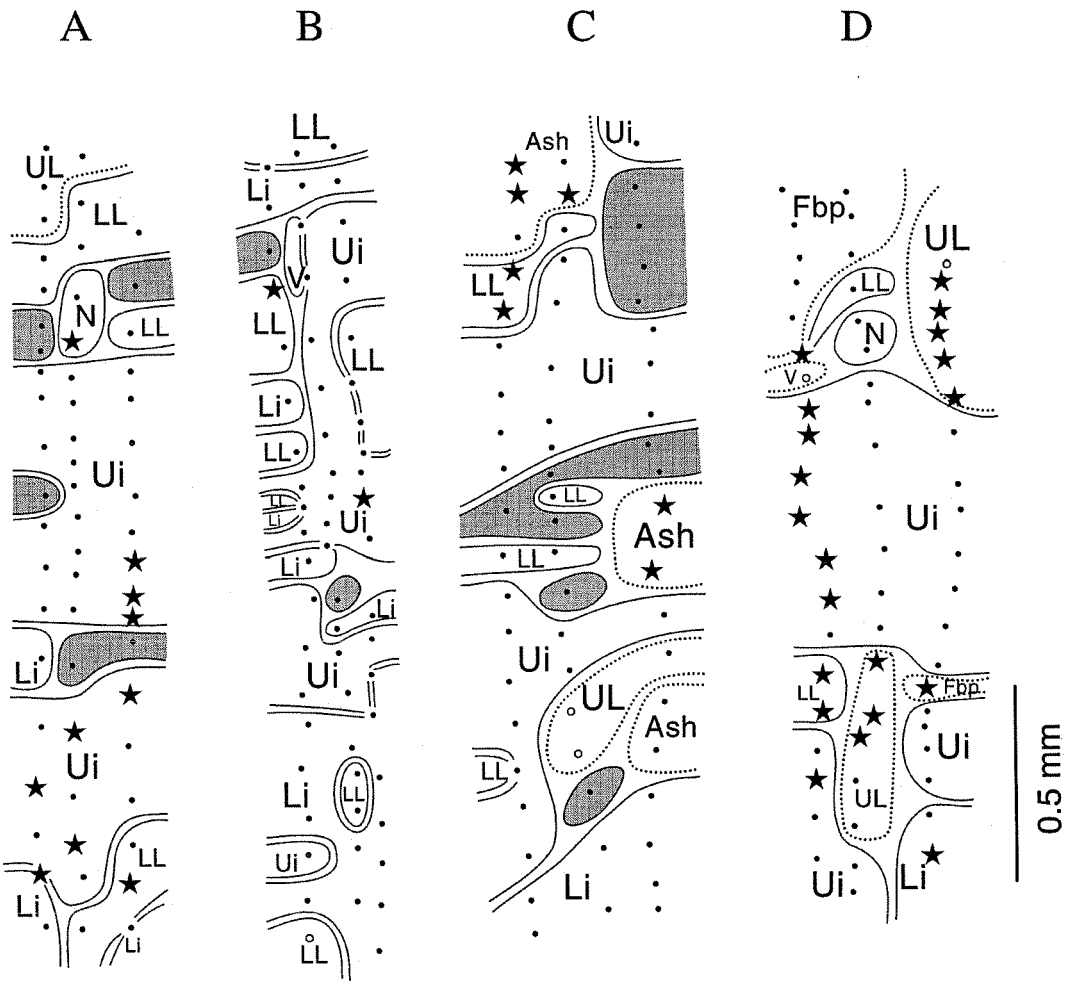

Figure 4.6 Tactile maps from four different animals that had the infraorbital nerve cut 30 days after birth (PND 30). Each map shows the location and distribution of two different types of field potentials seen in deafferented animals following tactile stimulation of the face area corresponding to the receptive field. Solid dots represent field potentials similar to those seen in normal animals, with both a short-latency and a long-latency component (Figure 2.2D). Stars denote electrode penetrations for which the field potentials contained only the long-latency component. Open circles show sites where the field potentials were either not recorded or were not analyzable.

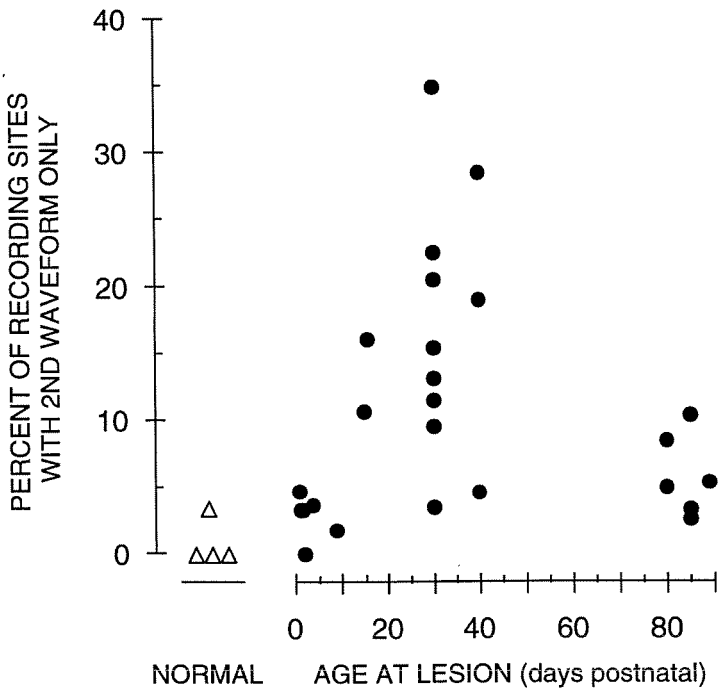

Figure 4.7 Percentage of the 60 electrode penetrations for which the field potentials elicited by tactile stimulation contained only the long-latency component is plotted as a function of the age at the time of the nerve lesion. Each point displays data from a single animal (open triangles: normal animals; filled dots: lesioned animals).

As shown in Figure 4.7 and first discussed in Chapter 3, we found a gradual increase in the number of recording sites with field potentials consisting of only the long-latency component with lesions made from PND 1 to PND 30. The trend in this data made it reasonable to expect that there should be a large percentage of long-latency only responses in adults as well. Surprisingly, as shown in Figure 4.7, this was not the case. Instead, there was a significant drop in the percentage of recording sites with field potentials lacking the first waveform, or short-latency component, from 16.57 ± 2.92% for PND 30 and PND 40 (n = 11) to 5.74 ± 1.24% for PND 77 to PND 89 (n = 6). The significance was judged by a

Mann-Whitney U test (P = 0.02). Animals lesioned 30 and 40 days after birth show considerable variability in the percentage of penetrations with field potentials lacking the short-latency component (Figures 4.6 and 4.7). In contrast, the reorganized maps following adult lesions show less variability and more closely resemble animals with lesions made early in postnatal development. This suggests that PND 30–40 animals are significantly different in this aspect of lesion-related reorganization.

4.4.3 Tactile reorganization immediately following deafferentation

To determine whether the pattern of reorganization observed two months after the nerve section could be due to an immediate enhancement of weak or previously silent inputs to crus IIa, we recorded responses before and immediately following deafferentation of the ipsilateral infraorbital branch of the trigeminal nerve. Figure 4.8 A and B shows the tactile maps obtained in crus IIa prior to deafferentation. The maps in A were constructed from the dominant receptive fields (i.e., the perioral structures eliciting the strongest response). The maps in B represent the strongest subdominant responses that were elicited by stimulation of a facial area not innervated by the ipsilateral infraorbital branch of the trigeminal nerve (i.e., lower lip, lower incisor, upper incisor, nose, and contralateral structures). The thick black line indicates the area normally innervated by the infraorbital branch of the trigeminal nerve, as suggested by the fact that the dominant neural response occurred upon stimulation of the upper lip and its related structures in the intact animal. Shaded areas indicate the regions of crus IIa for which no response could be elicited immediately following deafferentation.

Immediately after deafferentation, on average, 36% of the receptive fields within the denervated area were nonresponsive (n = 3). There was, however, considerable variability among animals (Figure 4.8C). Within the denervated area, 24% of the receptive fields had been previously detected at their penetration sites as either codominant or subdominant

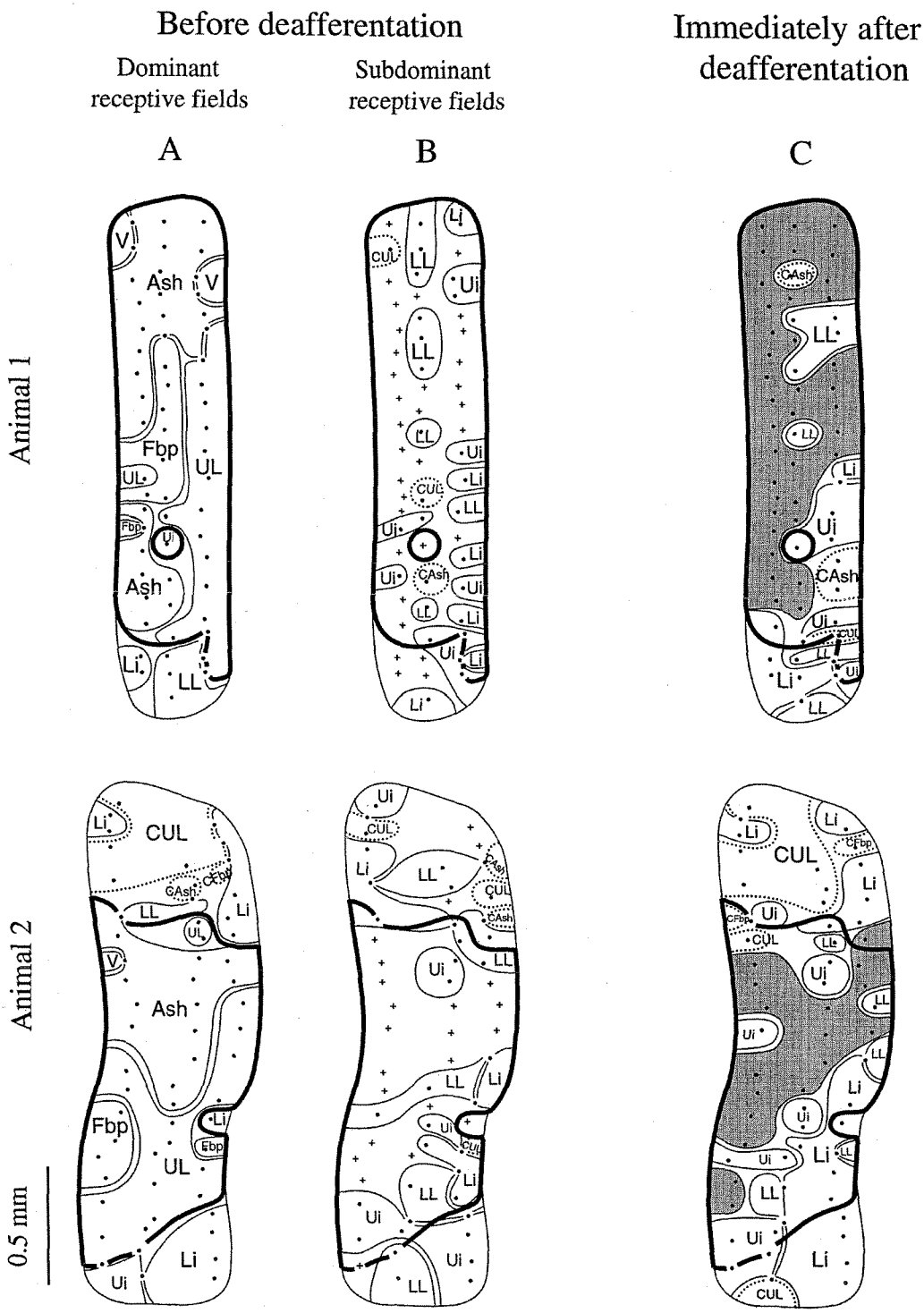
Before deafferentation
Dominant receptive fields
Subdominant receptive fields
Immediately after deafferentation
A
B
C
Animal 1
Animal 2
0.5 mm
V
Ash
Fbp
UL
LL
Li
Ui
CUL
CAsh
CFbp

Figure 4.8

Figure 4.8 Tactile maps in intact animals and immediately following deafferentation. For each of the two animals shown, crus IIa was mapped at 60 recording sites, then the nerve was lesioned and crus IIa was immediately mapped at the same 60 sites in the same animal. Thick black line denotes the area of crus IIa responsive to ipsilateral upper lip and upper lip-related structures (V, Ash, and Fbp); thus, this area presumably gets input from the infraorbital nerve in intact animals. **A:** Maps of the dominant receptive fields. **B:** Maps of the strongest subdominant receptive fields that are not ipsilateral upper lip or upper lip-related structures. **C:** Maps of the dominant receptive fields immediately after the infraorbital branch of the trigeminal nerve was sectioned. Abbreviations and meaning of symbols as in Figure 4.1.

receptive fields, while 40% were considered "new," i.e., representations that had not been previously detected at their penetration sites prior to deafferentation. Outside of the denervated area, 24% of the responsive penetrations were also new, suggesting that some of these new responses might be due to such factors as slight differences in electrode locations during remapping; the difficulty inherent in mapping these very weak subdominant receptive fields; or, possibly, the influence of the upper lip on the normal physiological response of other receptive fields.

To determine whether the new representations within the denervated area result from unmasking of previously silent receptive fields or if they could originate from surrounding receptive fields, the receptive fields adjacent to new representations were examined. Of the 21 new responses out of 38 observed responses (not counting nonresponsive sites) in the middle row within the denervated area from all three animals, 86% (18 of 21) can be explained by adjacency to subdominant or codominant receptive fields. Thus, only 8% (3 of 38) of the observed responses in the middle row within the denervated area appeared to arise via immediate unmasking of previously silent representations (which were not detected previously as codominant or subdominant).

Irrespective of the origin of the observed responses immediately following deafferentation, the upper incisor representation did not occur with any greater frequency than any other perioral region. Comparisons between receptive fields of the entire map recorded immediately after deafferentation indicate similar frequency distributions; all non upper lip perioral structures were represented in roughly equal proportion, with the exception of the nose (Figure 4.9, hatched bars). The mean frequency of representation among these perioral structures was not significantly different, as judged by a Scheffé test.

Comparison with subdominant representation of body parts

The subdominant projections described in section 4.4.1 would be prime candidates for an unmasking mechanism in cerebellar map reorganization. As shown in Figure 4.2, however, the upper incisor was not more heavily represented in these weak responses than the other regions of the face that project to crus IIa. A Scheffé test showed that the upper incisor subdominant representation did not differ significantly from that of the other perioral structures.

Comparison with recovered cerebellar representation of body parts

The pattern of tactile reorganization in crus IIa immediately following deafferentation does not predict the pattern found two to three months later, as shown in the summary histogram in Figure 4.9. Immediately following deafferentation, the intact perioral structures were represented in equal proportion and a large portion of crus IIa was nonresponsive (hatched bars). In contrast, two months later, the upper incisor representation predominated, extending to 43% of the map (white bars) and few penetrations were nonresponsive (8% compared to 31% immediately after). The mean frequency of representation of the upper incisor two months after deafferentation differed significantly from all of the other receptive field types, as judged by a Scheffé test ($P < 0.05$). The nose also differed significantly from all other representation.

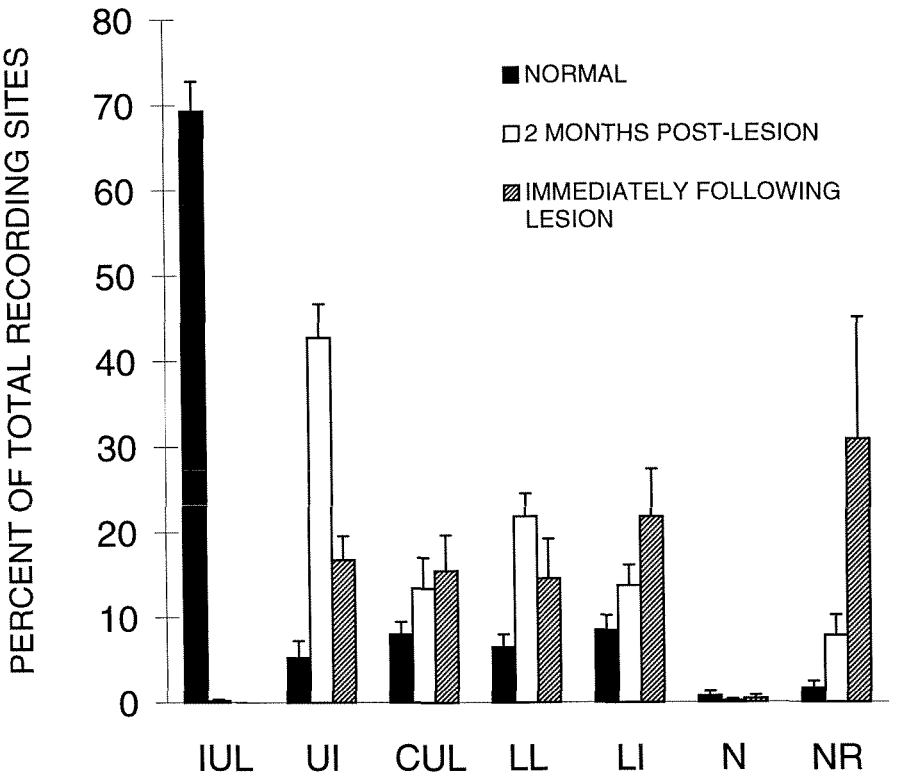

Figure 4.9 Comparison of the map organization in normal adult rats, PND 77 to PND 89 animals, and adult animals that were mapped immediately following lesion. The PND 77 to PND 89 animals were mapped two to three months after the nerve was cut. Each bar represents the mean ± SE of the percentage of total electrode penetrations that responded most strongly to each particular face area. Normal animals are shown as black bars (n = 15), animals that recovered for several weeks following the lesion are shown as white bars (n = 9), and adult animals that were mapped immediately after the nerve was cut are shown as hatched bar (n = 3).

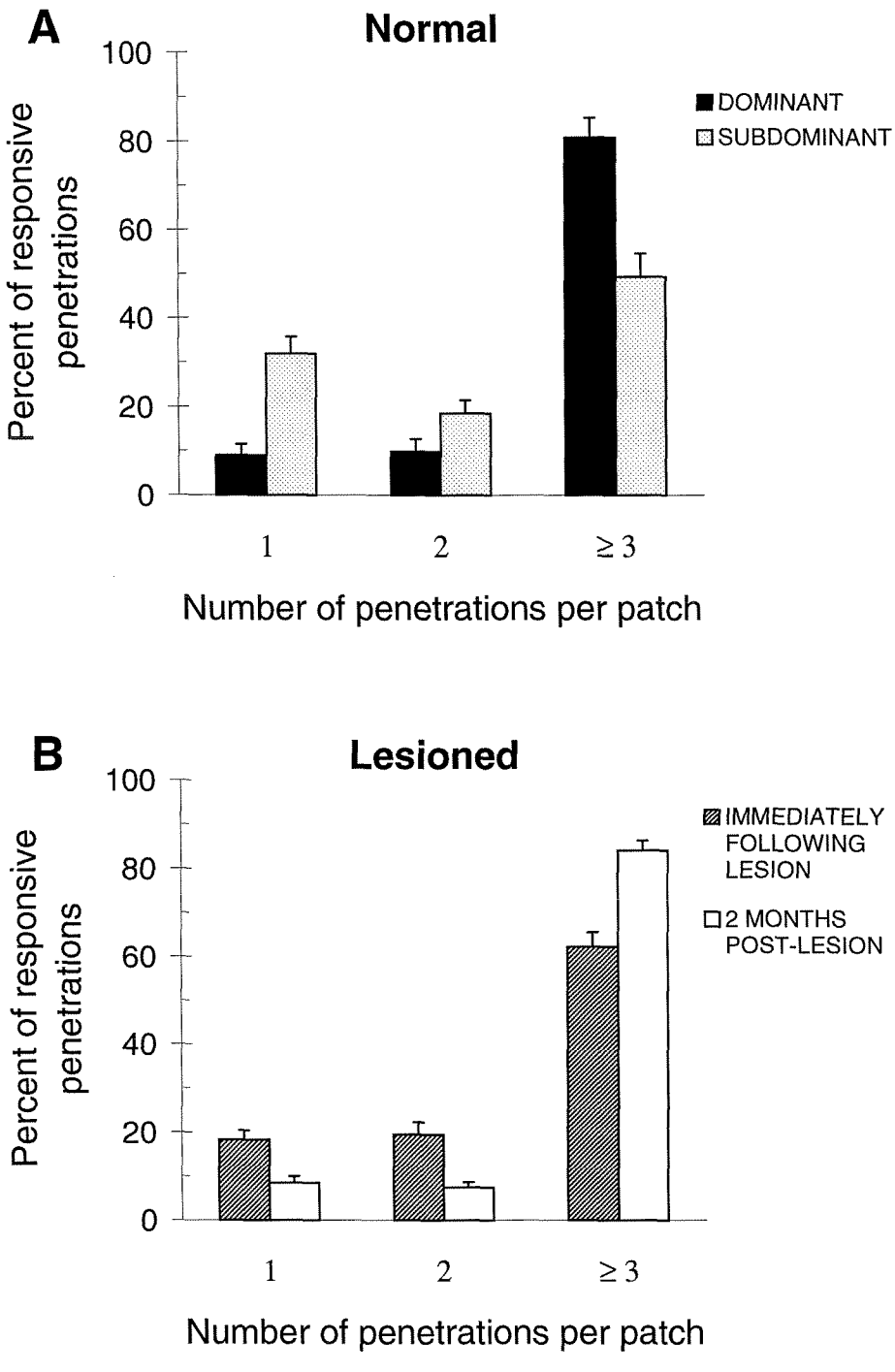
A
Normal
100
80
60
40
20
0
Percent of responsive penetrations
DOMINANT
SUBDOMINANT
1
2
≥ 3
Number of penetrations per patch
B
Lesioned
100
80
60
40
20
0
Percent of responsive penetrations
IMMEDIATELY FOLLOWING LESION
2 MONTHS POST-LESION
1
2
≥ 3
Number of penetrations per patch

Figure 4.10

Figure 4.10 Patch size was examined in normal (**A**) and lesioned (**B**) animals. This was done by counting (i) the number of responsive penetrations with no adjacent penetrations of the same receptive field type (patch consisting of a single electrode penetration), (ii) the number of responsive penetrations in patches consisting of only two electrode penetrations, and (iii) the number of responsive penetrations forming patches with three or more electrode penetrations. Each bar represents the mean ± SE of total responsive penetrations for a given patch size (as measured by the number of equally spaced electrode penetrations, 100 μm apart). **A:** For normal animals (n = 6), the dominant receptive fields are shown as black bars and the subdominant receptive fields, as stippled bars. **B:** For lesioned animals, the hatched bars represent the animals mapped immediately after the nerve was cut (n = 3); the white bars represent the PND 77 to PND 89 animals that recovered for 2 to 3 months before crus IIa was mapped (n = 9).

Comparison of the two different experimental groups showed that the two-fold increase in upper incisor representation between animals examined immediately following lesion and those several months later was significant, as judged by a Mann-Whitney U test ($P = 0.006$). There was no significant change in areal extent of the other perioral structures between the two experimental groups.

Patch size varied between the two experimental groups (Figure 4.10B). A greater diversity of patch size was observed in the rats examined immediately after deafferentation: 62% of the cerebellar sites formed patches comprising three or more adjacent electrode penetrations with common receptive field, 20%, two adjacent penetrations, and 18%, a single penetration. The patch size immediately after lesion showed some similarity to the feature size of the subdominant representation in intact animals (compare the hatched bars in Figure 4.10B with the stippled bars in Figure 4.10A). In contrast, the pattern of patches in rats examined two months later more closely resembled the feature size of the dominant receptive field maps of normal animals—that of a large patch surrounded by smaller

patches (compare white bars in Figure 4.10B with the black bars in Figure 4.10A). Only 8% and 7% of the sites formed patches comprising one and two electrode penetrations, respectively, while the majority, 85%, of the responses comprised three or more electrode penetrations.

When considering all the data together, we conclude that: 1) there appears to be little immediate unmasking of silent upper incisor projections; and, most importantly, 2) neither the immediate unmasking of silent projections nor the expansion of previously weak projections can be responsible for the dominance of the upper incisor in the reorganized cerebellar maps.

4.5 Discussion

4.5.1 Comparison with reorganization in neonatally lesioned animals

Studies of the cortical capacity for reorganization following lesion have reported an increase (Waite 1984; McKinley and Smith 1990), decrease (Wall and Cusick 1986), or no difference (Kelahan et al. 1981) in the reactivation of cortex of younger animals when compared with that of adults. Our results demonstrate that the adult cerebellum consistently reorganized following peripheral injury. In fact, the extent and pattern of the reorganization were extremely similar to what we reported for neonates (Chapter 3), although the adult crus IIa showed a small but significant increase in the number of nonresponsive sites.

The reorganized maps following adult deafferentation, just as those of animals lesioned neonatally, maintained several features of the normal maps. First, reorganized maps showed a mosaic of patches receiving projection from disjunctive body locations. Second, the reorganized maps tended to have a large patch in the middle of the folium surrounded by smaller patches, as in the normal animals. Finally, the medial border above

which contralateral structures are often represented in intact animals (Figure 3.2, also see Bower and Kassel 1990) was maintained in deafferented animals.

4.5.2 Comparison with reorganization of other somatosensory structures in adult animals

Lesions of the infraorbital branch of the trigeminal nerve denervated approximately 70% of the crown of crus IIa. Two months after lesion of this nerve in adult rats, we found that the cerebellar tactile maps had reorganized and that only 8% of the recording sites did not respond to tactile stimulation. Thus, we found only a slight limitation to the extent of reorganization following adult lesion.

The extent of reorganization in the somatosensory cortex following injury also appears to have limitations and seems dependent in a complex way on the overall extent of the lesion and the time between the lesion and remapping. In the somatosensory cortex of adult monkeys, for example, amputation of a single digit causes the representation of the adjacent intact digits to completely fill in the denervated cortical area. If two digits are lost, however, the surrounding skin surface does not fully reactivate the denervated cortex even several months later (Merzenich et al. 1984a). In contrast, removal of inputs to the entire glabrous hand, which deprives a larger cortical area, leads to a complete reactivation of the denervated area by the dorsal hand (Garraghty and Kaas 1991a). At the same time, Jain et al. (1995) reported that inactivation of hindlimb cortex by dorsal column section in rats results in no cortical reorganization while a striking large-scale reorganization has been demonstrated by Pons et al. (1991) who showed that several years after complete deafferentation of the upper limb in monkeys, the denervated cortex is completely reactivated by inputs from the face.

When cortical reorganization does occur, it appears that the intact structures that are represented adjacent to the denervated cortical area will expand to fill in some or all of the denervated area. Subcortical reorganization is consistent with this description (Garraghty

and Kaas 1991b). Recall that in somatotopic maps, body surfaces that are adjacent in the map are also adjacent on the body surface except in a few cases, such as the upper limb - face boundary in SI of the monkey. This is not the case in the cerebellum. The tactile cerebellar maps display a mosaic of patches generally representing nonadjacent skin surfaces. Our results showed that, in crus IIa, the upper incisor representation, which is not necessarily adjacent to the upper lip area, reactivated most of the denervated upper lip area. Thus, crus IIa reorganization, in contrast to reorganization in other cortical and subcortical maps, does not appear to arise by the filling in of adjacent structures.

4.5.3 Significance of the field potentials results

Tactilely-evoked field potentials recorded in the granule cell layer of the cerebellum in normal animals usually consist of two peaks: one occurs approximately 8 msec, the other, about 18 msec after the onset of the peripheral stimulation (Chapter 2). The first peak, or short-latency component, reflects the direct trigeminal input to crus IIa (Watson and Switzer 1978; Woolston et al. 1981). We have demonstrated that the second peak, or long-latency component, is primarily due to indirect input through the somatosensory cortex (Chapter 2). Thus, studying the temporal structure of the field potentials in the granule cell layer of crus IIa allows us to discern the influence of these two input pathways. We have shown that the two components of the cerebellar granule cell layer field potential are affected differently by peripheral injury at different postnatal days. There was a developmentally-related gradual increase in the number of sites lacking the short-latency component for animals whose upper lips were deafferented at different age, from birth to around 30 to 40 days old. Animals deafferented when 3 months old were more likely to lack the first component than were normal animals, but surprisingly, had significantly less sites lacking the first component than animals lesioned at PND 30 and PND 40.

A possible explanation for this result is that the differences in PND 30–40 lesions and those of adults reflect the relative ability of the trigeminal and SI cortex to reorganize

following peripheral lesions at different ages. We have previously interpreted the increase in responses lacking the first component in PND 1 to PND 30 animals as suggesting that the trigeminal nuclei become less plastic earlier in development than the somatosensory cortex (Chapter 3). The increased number of nonresponsive locations in animals lesioned as adults could be interpreted as suggesting that both SI and the trigeminal nuclei were less plastic in adults than at earlier ages. Thus, the possibility exists that locations with only the second waveform in PND 30–40 animals would, in the adult, become nonresponsive locations.

To test this idea, we have taken advantage of the substantial variability in the number of field potential responses with only the long-latency component found in PND 30–40 animals. If the explanation we suggested were correct, one would expect that the PND 30–40 animals with fewer second waveform only responses would have more nonresponsive locations. This turns out not to be the case; there is no significant difference in the number of nonresponsive locations between the PND 30–40 animals with a large number of field potentials lacking the short-latency component and those with few or none (significance judged by a Mann-Whitney U test, $P = 0.2$). Thus, our data suggest that reorganization in PND 30–40 animals is different than in either adults or neonates. Further, the variability in the PND 30–40 data can not be explained by suggesting that some PND 30–40 animals respond as adults while others have an extended neonatal reorganization pattern. Instead, we must conclude that ongoing development in the somatosensory system interacts in complex ways with lesions made at different developmental stages.

4.5.4 Mechanisms for map reorganization

One proposed explanation for cortical reorganization is the "unmasking" of previously ineffective connections and synapses. This hypothesis is supported, indirectly, by the report that thalamocortical arbors are larger than the physiological borders of the cortical neuron's receptive field and overlap each other (Landry and Deschenes 1981;

Garraghty and Sur 1990). It is also supported by the recent electrophysiological evidence of nondominant inputs from the dorsum hand in the SI glabrous hand surface representation of normal monkeys (Schroeder et al. 1995). Following deafferentation of the glabrous hand, the large region of cortex formerly representing that part of the hand becomes responsive to peripheral stimulation of the dorsum hand (Garraghty and Kaas 1991a).

The upper incisor expansion we observed in the cerebellum does not appear to be the result of immediate unmasking. Although the anatomical spread of individual mossy fibers in crus IIa has not been determined, previous physiological studies suggest that the horizontal spread of trigeminal afferents is limited to the regions (patches) of the granule cell layer that normally respond to those inputs (Woolston et al. 1981). In addition, analysis of the subdominant receptive fields showed that all non upper lip perioral structures were represented equally (Figure 4.2). Within the six to ten hours of recording following lesion, we did not observe any preponderant increase in the upper incisor representation. However, reactivation in the cerebral cortex, at least, can occur immediately (Calford and Tweedale 1988, 1991; Byrne and Calford 1991; Schmid et al. 1995). Within minutes of digit denervation in the rat, neighboring intact inputs expand in the deafferented hindpaw area of SI (Byrne and Calford 1991). Reorganization can also progress over weeks to months (Merzenich et al. 1983b; Cusick et al. 1990). These authors concluded that recovered reorganization appears to be determined by or related to the general topography of the immediately unmasked inputs which initially "seed" a large cortical sector. Elsewhere in the somatosensory system, indications of unmasking are less clear. Immediate unmasking has been found in the dorsal root ganglion (Metzler and Marks 1979), but not in the trigeminal brainstem complex (Waite 1984). Studies have reported no immediate change in the thalamus (Wall and Egger 1971; Rhoades et al. 1987); however, Nakahama et al. (1966) did encounter some unmasking there. Unlike reorganization in the somatosensory cortex, the topography that we observed in the cerebellum two months after nerve lesion can not be

explained by immediate unmasking (see Figure 4.9). Neither the pattern[1] of subdominant receptive fields in normal animals, nor the pattern of reorganization immediately following nerve section predicted the pattern observed two to three months after nerve lesion.

Another proposed mechanism for cortical reorganization, especially for large-scale reorganization, is axonal sprouting and formation of new connections. New growth after fetal transection of the infraorbital nerve has been detected in parts of the rat trigeminal complex (Rhoades et al. 1989). Sprouting after peripheral injury in the adult has been harder to demonstrate but was detected in the spinal cord and visual cortex (Florence et al. 1993; Darian-Smith and Gilbert 1994). Sprouting, however, is an unlikely mechanism to explain the pattern of reorganization in the cerebellum following deafferentation of the upper lip. If sprouting were to occur, one would expect the other represented adjacent structures in crus IIa, such as the lower lip, lower incisor, and contralateral upper lip to make as large, or even larger, contribution to the reorganized map than the upper incisor.

Given the evidence from other neural maps, if reorganization were occurring within the fractured cerebellar map, we would expect the deafferented patches to be invaded by afferents from neighboring adjacent patches. However, the upper incisor is not most commonly adjacent to the upper lip; other areas are equally, if not more likely, to be adjacent (Bower and Kassel 1990). Neither can the selective expansion of the upper incisor representation be explained by the size of its neural representation in the normal cerebellum; the upper incisor representation is no larger than that of any of the other perioral structures, whether measured as a dominant or subdominant receptive field (Figure 4.2). We only examined the central portion of crus IIa, but mappings of the entire crus IIa show that the total extent of the upper incisor representation is the smallest of all perioral structures (Bower and Kassel 1990). Thus, our mapping results suggest that the observed reorganization in crus IIa following infraorbital nerve section does not arise through

[1] "Pattern" refers to the proportion of the different perioral structures in crus IIa and the overall organization of the patches.

intrinsic cerebellar mechanisms. Our field potential data also support this suggestion: if cerebellar map reorganization were due to intrinsic mechanisms, one would expect the two components of the cerebellar field potentials to be affected in the same way.

5

Similarities Between Cerebellar and SI Reorganization Following Deafferentation

I shall [...] move with the moving ships,
Change as the winds change, veer in the tide.
A. C. Swinburne

5.1 Abstract

We have shown that fractured tactile cerebellar maps are plastic and maintain a fractured somatotopy following deafferentation at all ages (Chapters 3 and 4). Two to three months after lesion of the infraorbital branch of the trigeminal nerve, the denervated upper lip area in the cerebellar granule cell layer is taken over by intact perioral surfaces, predominantly the upper incisor representation. Unlike the pattern in other somatosensory regions of the mammalian nervous system, however, the representation filling in the denervated area is often not adjacent or even represented in this region of crus IIa of normal adult rats. In this chapter, we explore whether the pattern of reorganization might be related to reorganization in one of the afferent somatotopic structures, the somatosensory cortex (SI) which, through the pons, has a strong influence on cerebellar granule cell layer activity (Chapter 2; also see Bower et al. 1981). We first demonstrate that the upper incisor representation is adjacent to that of the upper lip in SI cortex of normal adult rats. We subsequently show that, in deafferented animals, the upper incisor representation in SI invades the normally adjacent denervated upper lip, increasing over five-fold relative to its

normal area. This result supports the hypothesis that the observed pattern of reorganization in crus IIa following peripheral deafferentation is related to changes in structures that are afferent to it, such as SI.

5.2 Introduction

Numerous studies have demonstrated the remarkable capacity of mammalian somatosensory maps, especially those of somatosensory (SI) cortex, to reorganize following peripheral denervation (Merzenich et al. 1983ab; for reviews see Kaas et al. 1983; Merzenich 1987; Wall 1988ab; Killackey 1989; Kaas 1991, 1994). Nevertheless, the mechanisms responsible for such reorganization still remain a subject of considerable debate. For example, it is unclear whether SI reorganization is due to mechanisms intrinsic to the cortex, such as the immediate unmasking of "silent" projections and/or the sprouting and regrowth of connections within the cortex, or is instead a result of extrinsic effects such as the reorganization of other somatosensory structures afferent to the cortex itself, or a combination of some or all of the above mechanisms (for reviews see Snow and Wilson 1991; Kaas 1994).

One reason for this confusion is that SI and its afferent structures are all somatotopically organized. Because denervated areas of SI are generally "filled in" by adjacent representations (Wall and Cusick 1984; for review see Kaas 1994), SI reorganization could, in principle, reflect reorganization in any of several locations, including the periphery (for review see Snow and Wilson 1991). For this reason, unambiguously identifying the mechanisms responsible for the reorganization of a particular SI locus is likely to require the simultaneous investigation of the afferent structures as well.

The advantage of the fractured somatosensory maps in the cerebellum as a model is that they enable one to distinguish between peripheral and central adjacency. Although

these maps receive somatosensory information from somatotopically organized regions, such as the trigeminal complex, the thalamus, SI, and the superior colliculus (for review see Bloedel and Courville 1981), they have a fractured somatotopy (Shambes et al. 1978ab; Welker 1987; Bower and Kassel 1990). In cerebellar maps, specific locations on the body surface project to small topographically discontinuous patches (bottom of Figure 5.3), resulting in a dissociation between peripheral and central adjacency.

In Chapters 3 and 4, we described the reorganization of cerebellar somatosensory maps in the granule cell layer of crus IIa following lesions of the infraorbital branch of the trigeminal nerve. This branch provides input through the trigeminal nuclei (Waite and Tracey 1995) to a large upper lip representation as well as representations of related upper lip structures (i.e., vibrissae, furry buccal pad, and anterior sinus hair) in the center of the crown of crus IIa (Figure 4.1A). Examination of animals deafferented at all ages showed that the maps reorganized, with the upper incisor representation consistently filling in the cerebellar denervated area. This pattern of reorganization is surprising since it does not correspond with plasticity studies in other somatosensory areas. Specifically, the upper incisor is not consistently adjacent to the upper lip representation in crus IIa of normal adult animals (Bower and Kassel 1990). The purpose of this chapter is to examine the possible contributions of extrinsic influences on cerebellar reorganization. We directly contrast lesion-induced reorganization in the cerebellum and the somatosensory cortex. A comparison of the reorganized maps of SI and cerebellum in the same animals suggests that cerebellar map reorganization is substantially influenced by the reorganization of its afferents. Preliminary results of these investigations have been reported in abstract form (Shumway et al. 1990).

5.3 Methods

5.3.1 Animals used

A total of 49 Sprague-Dawley albino rats were used: 17 adult control and 32 experimental animals lesioned at different stages of development, including postnatal day 1 (PND 1, n = 2); PND 2 (2); PND 4 (1); PND 9 (2); PND 12 (2); PND 14 (1); PND 15 (1); PND 16 (1); PND 30 (8); PND 40 (3); PND 77 (3); PND 80 (2); PND 85 (3); and PND 89 (1). In most animals either crus IIa or SI was mapped. For ten animals, however, *both* crus IIa and SI were mapped during the same recording session (two to three months after the nerve transection). Not all experiments were undertaken with each animal; the number of animals used for any given experiment is presented in the results and figure legends.

5.3.2 Deafferentation

Transection of the infraorbital branch of the trigeminal nerve was performed on rats of various postnatal ages (PND 1 to 89). The younger animals (16 days old and younger) were anaesthetized with avertine (125 mg/kg body weight); the others, with chloral hydrate (420 mg/kg body weight). The procedure was identical to that described in section 4.3.2.

5.3.3 Receptive field mapping

Surgical and tactile mapping procedures were identical to those described in the previous chapters. Briefly, prior to surgery, the rats were anaesthetized with intraperitoneal injections of sodium pentobarbital (12 mg/kg body weight) and ketamine hydrochloride (50 mg/kg body weight). Throughout the experiment, ketamine supplements were given as needed to suppress reflexive activity. The right cerebral somatosensory cortex (SI) and the left cerebellar cortex, crus IIa, were surgically exposed and covered with mineral oil.

Further detail on surgical procedures can be found in sections 2.3.1 and 3.3.2 as well as in previous publications (Bower et al. 1981; Bower and Kassel 1990).

Field potentials were recorded in the granule cell layer of crus IIa (400–700 μm below the brain surface) and layer IV of SI cortex (600–1000 μm) with glass micropipettes filled with 2M NaCl (5–10 μm in diameter, 1–3 MΩ impedance). The central region of the exposed folial crown of crus IIa was finely mapped with 60 electrode penetrations (3 parallel tracts, 20 punctures per tract, as shown in Figure 3.1C). The somatosensory cortex was mapped with as many penetrations as required to determine the areal extent of the upper incisor representation. The location of the penetrations on the surface of crus IIa and SI cortex were directly recorded on enlarged photographs at the time of recording. In crus IIa, penetrations were spaced 100–150 μm apart rostrocaudally and 100 μm apart mediolaterally (or more depending on surface vasculature). In the SI cortex, penetrations were spaced 100–200 μm apart in each direction. Near the apparent border of the upper incisor representation, penetrations were generally spaced 100 μm apart. For each electrode penetration, hand-held glass probes were used to stimulate perioral surfaces and the receptive field was determined auditorily from the multiunit activity. Two experimenters independently rated responses on a scale from 1 (barely detectable) to 5 (maximal).

5.3.4 Map construction and analysis

The cerebellar and cortical maps were constructed as described in section 4.3.5. All measures of variability described in this chapter are standard errors, SE. Statistical two-sample comparisons were conducted with a Mann-Whitney U test. Multiple comparisons of receptive fields within maps were conducted with a one-way repeated measures ANOVA followed by a Scheffé F test. The significance level was set at 0.05.

5.4 Results

5.4.1 Reorganization in the cerebellum

As described previously (Figure 4.1A, also see Bower and Kassel 1990), projections from the upper lip, furry buccal pad, anterior sinus hair, and vibrissae occupy the largest area in the crown of crus IIa. This is quantified in Figure 5.1 where the average percentage of representation for each body surface projecting to crus IIa of intact rats is compared (black bars). Note that all non upper lip perioral structures are represented in approximately equal proportion in normal adult animals (data from 15 animals were pooled, no significant difference for all pair-wise comparisons, as judged by a Scheffé test).

We also reported that the cerebellar upper incisor representation is substantially larger two to three months following deafferentation of the infraorbital branch of the trigeminal nerve in young (Chapter 3) and older animals (Chapter 4) than in normal adults. Figure 5.1 compares the distribution of body surface representations for normal (black bars) and lesioned animals (white bars); the data from 31 lesioned animals, from PND 1 to PND 89, have been pooled together. The upper incisor is much more prominently represented in the reorganized maps, expanding to 45% of the map (from 5% in normal). The lower lip significantly expanded as well, from 7% to 20% of the crown of crus IIa.

5.4.2 Contribution of afferent structures to cerebellar reorganization

Representation of the upper incisor in SI of normal animals

The purpose of this study was to contrast the upper incisor dominated reorganization of cerebellar tactile maps with the pattern of reorganization of the upper incisor representation in SI cortex. It was first necessary to determine the areal extent and position

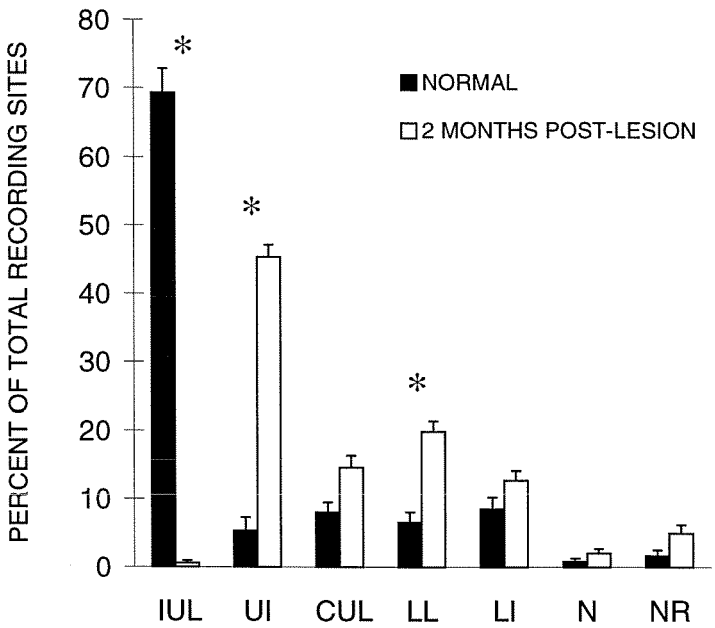

Figure 5.1 Comparison of the map organization in crus IIa of normal (black bars, n = 15) and deafferented rats (white bars, n = 31). Each bar represents the mean ± SE of total recording sites for a given receptive field type. The experimental data from all stages of development tested (PND 1 to PND 90) were pooled. Asterisks indicate significant differences between the percentage of representation of a given receptive field type in the normal and lesioned animals, as judged by a Mann-Whitney U test ($P < 0.0001$). *Abbreviations:* IUL: ipsilateral upper lip and related ipsilateral structures (vibrissae, furry buccal pad, and anterior sinus hair); UI: upper incisor; CUL: contralateral upper lip and related contralateral structures (vibrissae, furry buccal pad, and anterior sinus hair); LL: lower lip; LI: lower incisor; N: nose; NR: nonresponsive.

of the SI upper incisor representation in normal animals since these data had not been reported previously for the rat (for maps of other perioral structures in rats see Welker 1971; Chapin and Lin 1984; for maps of the incisors in area 3b and 1 of SI in squirrel monkeys see Cusick et al. 1986). Maps of the upper incisor representation in SI of two normal animals are shown in Figure 5.2. In our SI maps of normal animals, the upper incisor representation was found immediately adjacent to the ipsilateral upper lip representation, specifically the rostroventral surface of the upper lip. This is also the region of the upper lip most heavily represented in crus IIa of the normal adult rat cerebellum (Chapter 4, also see Bower and Kassel 1990). Note that the crus IIa maps are from the left cerebellar hemisphere (which mostly represents the left side of the body) whereas the SI maps are from the right hemisphere (which mostly represents the left side of the body). In this chapter, a face area is termed ipsilateral if it is on the left side of the rat's face, i.e., if it is ipsilateral to the nerve lesion.

Expansion of the upper incisor representation in both SI and crus IIa of lesioned animals

We compared the reorganization in the upper incisor area in SI following deafferentation with that found in the granule cell layer of the cerebellum. This comparison was made for animals lesioned at different postnatal days and mapped two to three months later. Figure 5.3 shows SI (A) and cerebellar (A') representations mapped in a normal animal and in four animals lesioned at different developmental stages (B–B' to E–E'). The upper incisor representation (hatched areas) clearly expands in both structures following peripheral lesions.

When the data for SI and crus IIa are each pooled across age of lesion, as in Figure 5.4, there is a statistically significant increase in the area of the upper incisor representation in both brain structures (as judged by a Mann-Whitney, $P < 0.02$). The data

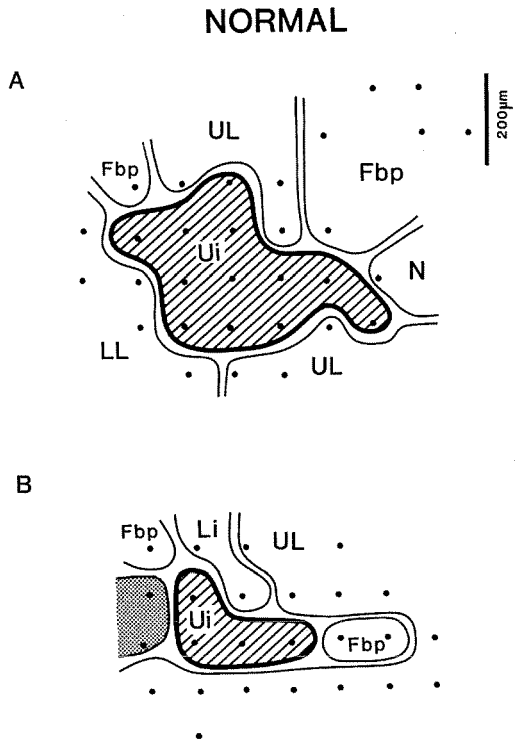

Figure 5.2 Portion of the tactile representation in the right somatosensory cortex for two different normal rats (A and B). The extent and location of the upper incisor representation is shown (hatched area). Top is lateral; left, rostral. Filled dots represent electrode penetrations. Shaded areas indicate nonresponsive regions of SI. *Abbreviations:* UL: upper lip; Ui: upper incisor; Li: lower incisor; LL: lower lip; Fbp: furry buccal pad; N: nose.

from the different developmental stages were pooled because there was no significant difference in the upper incisor area at different ages. On average, the upper incisor area increased 13.2-fold in the cerebellum and 5.4-fold in SI compared to normal animals. In fact, regardless of the age of lesion, the upper incisor area in crus IIa was larger in any given lesioned animal than any given normal: in other words, the range of upper incisor areas for lesioned animals showed no overlap with the range for normal animals (normal: 0 to

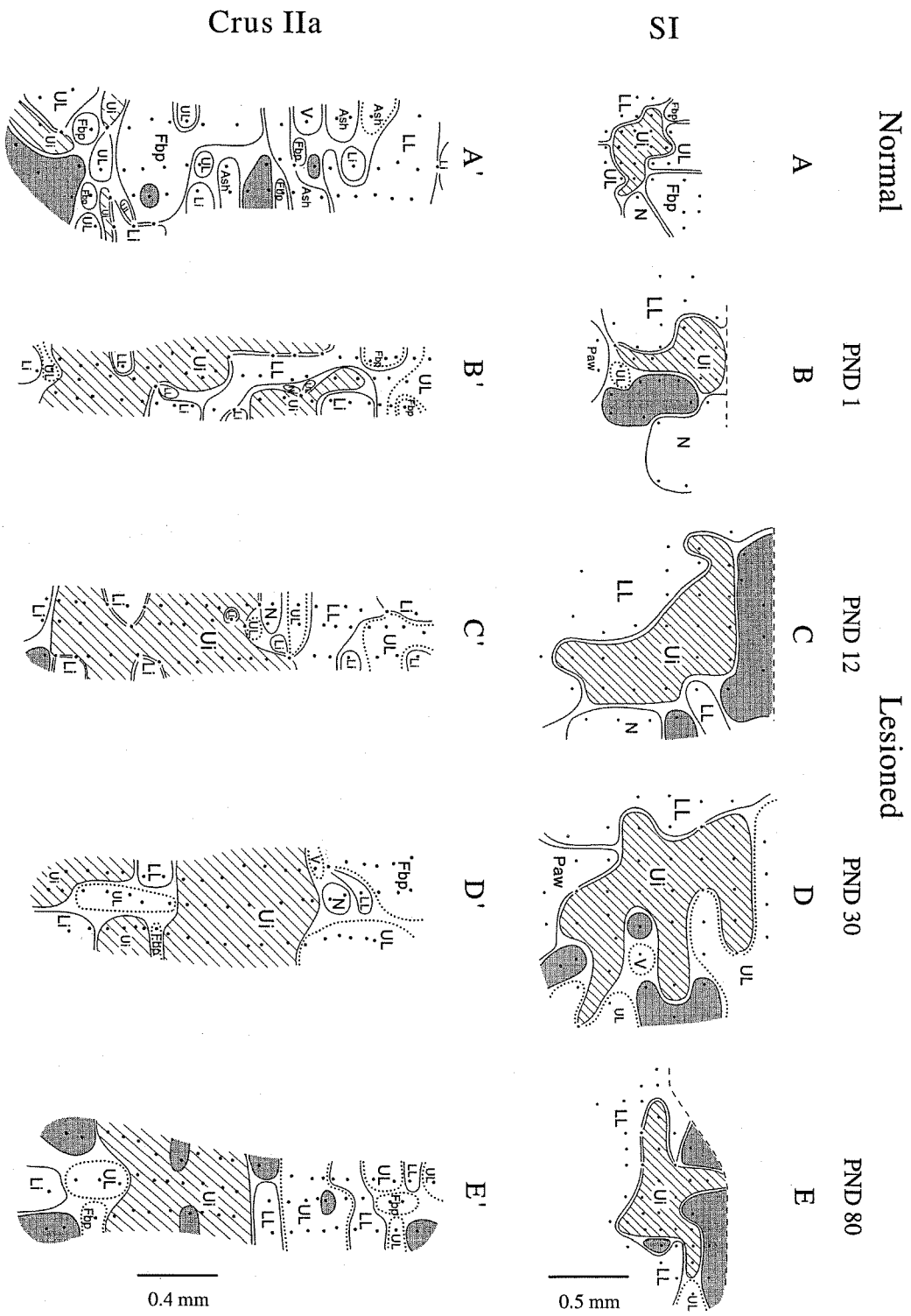
Crus IIa
SI
Normal
Lesioned
PND 1
PND 12
PND 30
PND 80
A
B
C
D
E
A'
B'
C'
D'
E'
0.4 mm
0.5 mm

Figure 5.3

Figure 5.3 Tactile maps in the right somatosensory cortex (top) and left cerebellum (bottom). **A–A':** Normal animal, **B–B':** PND 1, **C–C':** PND 12, **D–D':** PND 30, **E–E':** PND 80. The two brain regions, SI and crus IIa, were mapped in the same animal (i.e., A and A' are from the same animal but from a different animal than B and B'). The upper incisor representation is indicated by the hatched areas. Shaded areas indicate nonresponsive regions; filled dots, electrode penetrations. Solid line around a patch indicates projections from the left side of the rat's face (the side ipsilateral to the cut IO nerve); dotted line, right side. Dashed line at top of SI map indicates the lateral edge of the brain. For all maps, left is rostral; for SI maps, top is lateral; for crus IIa maps, top is medial. Note the difference in the scale for SI and crus IIa maps. *Abbreviations* as in Figure 5.2, V: vibrissae; Ash: anterior sinus hair.

9.7×10^4 μm^2; lesioned: 17.2×10^4 to 100.7×10^4 μm^2). For SI, all but one of the ten experimental animals showed an increased upper incisor area relative to the normal animals, regardless of the age of lesion (normal: 6.1×10^4 to 19.2×10^4 μm^2; lesioned: 18.2×10^4 to 128.8×10^4 μm^2).

5.5 Discussion

Previous analysis of the latencies of granule cell layer responses to peripheral stimuli in reorganized maps suggested that a long latency pathway through SI cortex might be contributing directly to reorganized responses in the cerebellum (Chapters 3 and 4). In this chapter, reorganization in SI was contrasted with that in crus IIa to determine if the pattern of cerebellar reorganization might reflect the reorganization of afferent somatosensory structures. By mapping both SI and crus IIa in animals with peripheral lesions made at different postnatal days, we showed that the upper incisor representation expands significantly in both structures. The overall pattern of reorganization within each

structure was similar regardless of the developmental stage at which the lesion was made. The reorganization in SI appears to be consistent with the "filling in" by adjacent representations that has been reported previously (Wall and Cusick 1984; Kaas 1994) since the upper incisor is adjacent to the upper lip representation in normal adult animals. In the cerebellum, however, the upper incisor representation is not consistently adjacent to the upper lip. Comparing the specific pattern of reorganization in cerebellar and SI maps suggests that the pattern of cerebellar reorganization may be influenced by changes in SI cortex and/or other somatotopic structures afferent to the cerebellum.

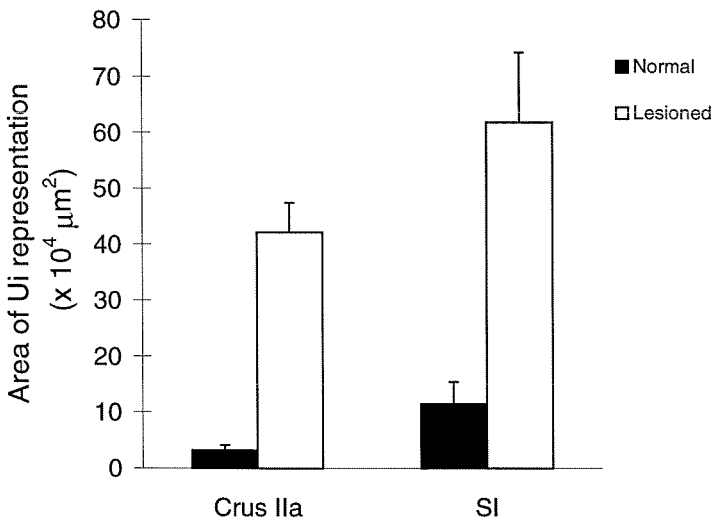

Figure 5.4 Mean area ± SE of the upper incisor representation in the somatosensory cortex and the cerebellum of normal animals (black bars, n = 3 for SI, n = 11 for crus IIa) and lesioned animals (white bars, n = 10 for SI, n = 14 for crus IIa). Data for the lesioned animals were pooled from all ages at deafferentation, as there was no significant difference between the upper incisor area at different ages. In both brain regions, the area of the upper incisor representation is significantly larger in lesioned animals than in normal animals. Significance judged by a Mann-Whitney U test (SI: $P < 0.02$; crus IIa: $P < 0.0001$).

5.5.1 Map reorganization and brain development

These experiments involved lesions made at different stages during the development of the rat brain. Accordingly, the final adult pattern of the maps following the lesion is almost certainly the result of the complex interplay between lesion-induced changes and developmental mechanisms. Interpretations of lesions in the adult, in contrast, can assume that reorganization is based on adult morphological and physiological patterns. Another potential complication in interpreting the results is that the developmental pace of SI and the cerebellum differ; SI cortex achieves its adult morphology earlier than the cerebellum. For example, in the cerebellum, although a two to four cell deep granular layer is found at PND 5, the bulk of granule cells are formed between PND 8 and 15 (Altman 1972), with mossy fiber terminals not forming before PND 7 (Schoen et al. 1991); while most SI cortex neurons are generated between embryonic day 14 and 20 (Bayer and Altman 1991), with thalamocortical projections arriving in SI as early as PND 1 to PND 3 (McCandlish et al. 1993).

The timing of the development of connections in the cerebellum and SI gives further weight to the idea that the main site of reorganization is extrinsic to the cerebellum, possibly in the cerebrocerebellar pathway. We have shown that increases in the upper incisor representation in crus IIa were observed with lesions as early as PND 1, when the cerebellar circuitry is not yet developed. While the reorganization of cerebellar and SI cortical maps in response to early postnatal lesions undoubtedly reflects a complex interaction between normal development and abnormalities caused by the lesion, our results indicate that the pattern of reorganization in both structures is generally the same regardless of the animal's age at deafferentation, even adults. We did not find any significant developmental change in the expansion of the upper incisor in crus IIa or SI, although there was a large variation in the total area representing the upper incisor (see section 5.4.2). This large range might be related to variation in the maps of different individuals (crus IIa: Bower and Kassel 1990; SI: Merzenich et al. 1987; Riddle and Purves 1995).

5.5.2 Mechanisms of reorganization

A number of mechanisms have been invoked to explain sensory map reorganization, including unmasking of previously silent representations in the denervated area (via shifts in the balance of excitatory and inhibitory connections); spreading of adjacent undamaged afferents within the CNS; sprouting of afferent axons, dendrites of adjacent cells, or the migration of adjacent cells; peripheral branching of intact nerve fibers distal to the peripheral nerve damage; and cell death (Merrill and Wall 1978; Kaas et al. 1983; Merzenich et al. 1983ab; Pons et al. 1991; and Kaas 1994 for discussion of the above mechanisms). Various neurotransmitters (such as acetylcholine, norepinephrine, GABA) and receptors (NMDA) have also been shown to be involved in reorganization (for review see Kaas 1994). The underlying mechanisms generating the cortical pattern of reorganization are still under investigation by many laboratories.

Differences in the pattern of map reorganization

Our data and that of many others indicate that the typical pattern of SI reorganization involves the expansion of intact cortical representations that are adjacent to the denervated cortical area (see section 1.1.1 for a brief review; also Merzenich et al. 1983ab; Wall and Cusick 1984; Pons et al. 1991; for review see Kaas 1994). This pattern of reorganization is also found in the thalamus and brainstem, implying that the new cortical maps may simply reflect changes occurring earlier in the processing sequence (Waite 1984; Garraghty and Kaas 1991b; for review see Woolsey 1990). There is, however, some evidence for cortical changes as well (somatosensory: Recanzone et al. 1992a; visual: Gilbert and Wiesel 1992). Given the evidence to date, cortical reorganization likely reflects changes that occur at all levels of the sensory pathway.

In the cerebellum, however, the reorganization is not a result of an intrinsic expansion of normally adjacent representations. Often, the upper incisor is not adjacent to

the upper lip in normal animals, and when it is present, has no greater representation than other non upper lip structures such as the lower lip and lower incisor (Figures 5.1 and 5.3). Our suggestion that the reorganization observed in the cerebellum reflects reorganization of its afferent pathways is based on the following: 1) the upper incisor expansion observed in the cerebellum can *not* be explained by (i) a larger upper incisor subdominant cerebellar representation (section 4.4.1) or (ii) immediate unmasking of the upper incisor in the cerebellum (section 4.4.3); 2) the upper incisor *is* commonly adjacent to the ipsilateral upper lip in somatotopic afferent structures, such as SI cortex and the trigeminal complex; and 3) the same changes in organization that occur in crus IIa following infraorbital nerve lesion—specifically, the expansion of the upper incisor representation—occur in SI. Although we did not compare expansion of other body surfaces, previous investigators have reported that infraorbital nerve lesions also result in increased representation of the lower jaw, digits, and the vibrissae over the eyes in SI (Waite 1984). It is important to note that infraorbital lesions denervate large sections of SI, since two-thirds of SI receives projections from the head and neck; vibrissae alone constitute about a fifth of the total SI area (Welker 1971).

Our proposal is that the afferent projections to the cerebellum are hardwired and that the information they carry is dependent on the somatotopic organization of afferent structures. Thus, the changes in the information carried by these afferents is due to a shift in the representations in afferent structures. The demonstration that the SI upper lip area projects to the cerebellar upper lip patches by Bower et al. (1981) is consistent with this hypothesis.

Contribution of afferent projections

In order for our hypothesis to be correct, we would expect that there should be some orderly relationship between the shift in SI maps and those of other major cerebellar afferents. While the cerebral cortex, via the pontine nuclei, provides a substantial projection

to cerebellar cortex (Bloedel and Courville 1981; Bower et al. 1981), other somatosensory structures have also been shown to influence the lateral hemispheres of the cerebellum (Brodal 1981, Huerta et al. 1983; Marfurt and Rajchert 1991). Perhaps the most substantial noncortical influence is from the trigeminal complex, which sends afferents directly to the granule cell layer of the cerebellum (Watson and Switzer 1978; Woolston et al. 1981). The lateral regions of the cerebellum even receive a minor projection directly from primary afferents, at least in the case of the teeth (Elias et al. 1987). In addition, deep layers of the superior colliculus provide mossy fiber input to the cerebellum (through the pons), which, like the direct projections from the trigeminal complex (Woolston et al. 1981) and the indirect cerebrocerebellar projections (Bower et al. 1981), respects the fractured somatotopic maps in the granule cell layer of crus IIa (Kassel 1980).

We have demonstrated that careful analysis of the responses generated in the granule cell layer distinguishes between direct trigeminal input to the granule cell layer and input relayed through forebrain structures, principally SI (Chapter 2). Our previous analysis of the granule cell layer field potentials induced by peripheral stimulation of lesioned animals indicates that the new upper incisor representation is carried by both direct and indirect pathways following denervation (Chapters 3 and 4). Lesion-induced reorganization in the trigeminal nucleus, as in SI, led to a reactivation of the denervated area by intact adjacent inputs, at least in young animals (Waite 1984), which supports the suggestion that it is changes in afferent maps that dictate changes in cerebellar responses.

6

A Systems Level Topographic Model of the Somatosensory System

We dance round in a ring and suppose,
But the Secret sits in the middle and knows.

Robert Frost
The Secret Sits, 1942

6.1 Abstract

Our detailed physiological mapping of the tactile inputs to the lateral hemisphere of the cerebellum demonstrated that these regions reorganize following peripheral nerve lesion (Chapters 3 and 4). Analysis of cerebellar and cortical reorganization patterns and of the temporal structure of tactilely-evoked cerebellar field potentials to infer the influence of afferent projections suggested that the principal site of plasticity following deafferentation is not in the cerebellum itself but in its afferent pathways (Chapters 4 and 5). We developed a network model to explore this possibility. Parts of the trigeminal complex, thalamus, SI, and crus IIa were represented in a simplified fashion based on known anatomical and physiological features of the system. The network connections were established based on the published receptive field size properties and topography of the various brain areas.

The model was intended to test the hypothesis that the observed pattern of reorganization in the cerebellum following peripheral deafferentation is related to changes

in afferent structures and not due to intrinsic cerebellar plasticity. Computer simulations of this network connectivity model support this conclusion by producing reorganized cerebellar tactile maps that were similar to experimental maps without assuming any intrinsic cerebellar plasticity.

6.2 Introduction

Reorganization of cortical structures following peripheral manipulations has been convincingly demonstrated in a large number of studies (Merzenich et al. 1983ab; Wall and Cusick 1984; for reviews see Kaas et al. 1983; Merzenich 1987; Wall 1988ab; Killackey 1989; Kossut 1992; Kaas 1994), but whether cortical plasticity reflects an intrinsic cortical capacity for reorganization, reorganization occurring in its afferent pathways, or a combination of both, is still a topic of debate (for reviews see Snow and Wilson 1991; Kaas 1994). We have demonstrated that cerebellar somatosensory maps reorganize after peripheral injury and our results suggested that the particular pattern of cerebellar reorganization is due to changes in structures that send projections to crus IIa. This suggestion was based on the following results: 1) We found no evidence that cerebellar reorganization arose through intrinsic cerebellar mechanisms; the predominance of the upper incisor representation in the reorganized cerebellar maps could not be explained by immediate unmasking of silent projections or expansion of subdominant projections (Chapter 4). 2) The expansion of the upper incisor representation in crus IIa was paralleled by a similar expansion in the somatosensory cortex (Chapter 5). In addition, the pattern of reorganization we observed in SI (expansion of the upper incisor representation into the adjacent denervated upper lip area) was consistent with the "filling in" by adjacent representations that has been reported previously (Wall and Cusick 1984; for review see Kaas 1994). In contrast, the upper incisor representation was not consistently adjacent to the upper lip in the cerebellum (Chapter 5). 3) The two components of the tactilely-evoked

cerebellar field potentials, which reflect a direct trigeminal and an indirect cerebral influence (Chapter 2), were present at most recording sites, suggesting reorganization of the afferent pathways; moreover, they were sometimes affected differently by nerve lesions—if cerebellar reorganization were due to intrinsic mechanisms, one would expect the two components of the cerebellar field potential to be affected in the same way (Chapter 4).

This chapter describes simulation results based on a network model we developed to explore reorganization in the somatosensory system. Because trigeminal, thalamic, cortical (SI), and cerebellar tactile maps have different topographies, even a small change in one of the early afferents could lead to extensive reorganization in the cerebellum. The simulation results support the suggestion that cerebellar reorganization is substantially influenced by reorganization of its afferent pathways.

6.3 Major somatosensory pathways to the cerebellum

The cerebellum receives two major excitatory afferent projections, the climbing fibers and the mossy fibers. The climbing fibers originate from the inferior olive and synapse on Purkinje cells. The mossy fibers arise from various nuclei and excite granule cells whose axons project towards the cerebellar surface, bifurcate to form the parallel fibers, and synapse on Purkinje cells (for review see Bloedel and Courville 1981). Figure 6.1 illustrates two major mossy fiber input pathways to crus IIa in the cerebellar lateral hemisphere: the direct trigeminocerebellar pathway (dashed line) and the indirect cerebrocerebellar pathway (solid line). Figure 6.1 also indicates the topography of each brain area. Thus, the cutaneous inputs from the face are represented somatotopically in the trigeminal nuclei (Nord 1967, Waite 1984). The trigeminal nuclei send projections to the ipsilateral cerebellum as well as topographical projections to the contralateral thalamus.

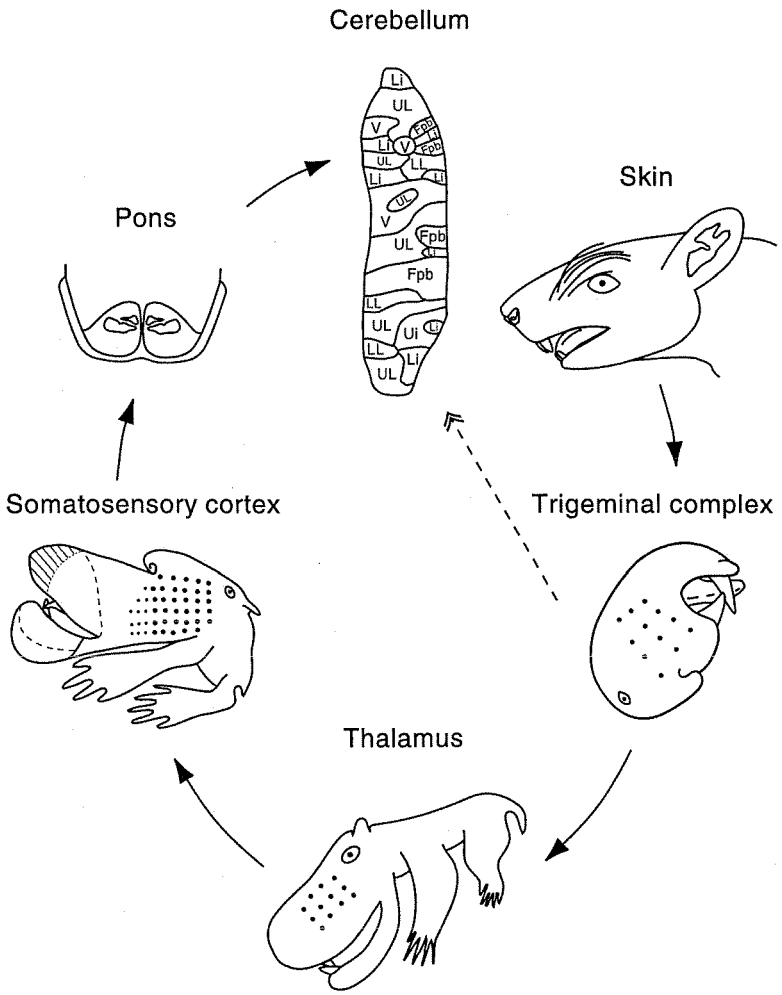

Figure 6.1 Simplified diagram showing two major mossy fiber projections to crus IIa, a direct trigeminocerebellar (dashed line) and an indirect cerebrocerebellar pathway (solid line). Ratunculi are shown for the somatotopically organized nuclei (trigeminal nucleus shown in a coronal plane, adapted from Nord 1967; thalamus shown in a coronal plane, adapted from Emmers 1965; SI shown in a horizontal plane, adapted from Welker 1971). The cerebellar fractured tactile map is shown in a horizontal plane. Dots represent vibrissae; hatched area, furry buccal pad; and broken lines, parts of the upper and lower lip that curve inside the mouth. The organization of the sensory representation in the pons is not known, thus only the outline of a transverse section through the pontine nuclei is shown.

Several other areas not shown, such as the superior colliculus, also send mossy fiber projections to crus IIa (Brodal 1981; Huerta et al. 1983; Marfurt and Rajchert 1991). *Abbreviations*: Fbp: furry buccal pad; Li: lower incisor; LL: lower lip; Ui: upper incisor; UL: upper lip; V: vibrissae.

Somatotopic sensory maps are also found in the thalamus (Emmers 1965; Sugitani et al. 1990). The thalamus projects topographically to SI, which is also somatotopically organized (Welker 1971; Chapin and Lin 1984). SI then projects through the pontine nuclei to the ipsilateral cerebellum. No sensory representation is shown for the pons in Figure 6.1 since that information is not yet known in detail.

It has been shown previously that the tactile inputs from the direct trigeminocerebellar and the indirect cerebrocerebellar pathways are in register spatially, i.e., a trigeminal location responding to tactile stimulation of a certain vibrissa influences cerebellar regions receiving projections from SI location responding to the same vibrissa (Bower et al. 1981; Woolston et al. 1981).

6.4 Model description

Our main interest is in the reorganization of the cerebellar tactile areas following peripheral injury. The modeling effort described here is a first step toward using systems level topographic models to explore plasticity in the somatosensory system of the rat. Although it is a simplified representation, the current model is based on features of the anatomy and physiology of the real system. It is, however, not "physiological" in the sense of capturing detailed single cell physiology (De Schutter and Bower 1994) or of representing a large-scale network of cells (Wilson and Bower 1992); rather, it is "connectional."

6.4.1 Projections

In this model, we have specifically focused on the *major* cerebellar-related somatosensory pathways. Thus, not all known projections are represented; for example, projections from the superior colliculus (Kassel 1980) are not included in our model. The brain areas shown in Figure 6.1 contain one or more representations of the face and the various nuclei are richly interconnected. The subset of the known projections that have been included in the model is shown in Figure 6.2. The model begins with a representation of the rat's face (Skin). In the model, the afferents from the face project to the trigeminal nucleus Principalis (Pr5) and the spinal trigeminal subnucleus Interpolaris (Sp5I) which each contain an organized representation of tactile inputs from the face. Both nuclei project to the thalamus and to the cerebellum (Mantle-St.John and Tracey 1987).

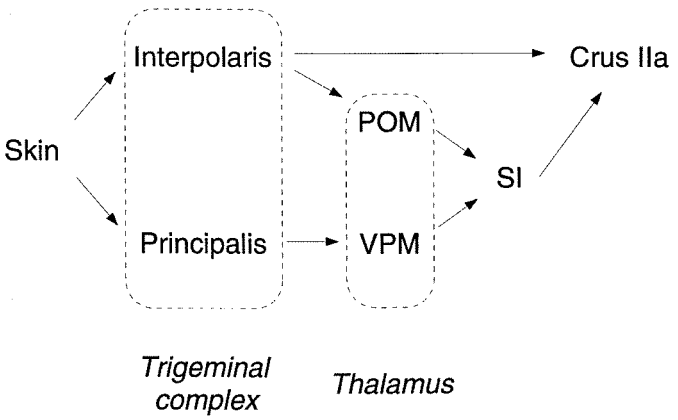

Figure 6.2 Diagram of the tactile projections to crus IIa that are included in the model.

There are two separate representations of the face in the thalamus: one in the medial ventroposterior nucleus (VPM) and the other in the medial posterior nucleus (POM). The

main projection of Pr5 is to the thalamus, in particular to VPM (Chiaia et al. 1991a). The sparse projection from Pr5 to POM and to the cerebellum (Mantle-St.John and Tracey 1987; Chiaia et al. 1991a) is not represented in this model. The Sp5I projects mainly to the cerebellum (Watson and Switzer 1978; Mantle-St.John and Tracey 1987) and also to the thalamus (Mantle-St.John and Tracey 1987; Chiaia et al. 1991a). It has been shown anatomically (Mantle-St.John and Tracey 1987; Phelan and Falls 1991) and physiologically (Woolston et al. 1982) that different populations of Sp5I neurons project to each structure. Thus, in the model we simulate two different cell populations in Sp5I that we refer to as Interpolaris-Th and Interpolaris-Cb (population projecting to the thalamus and to the cerebellum, respectively).

Both VPM and POM project topographically to the somatosensory cortex (SI) but to different regions. Inputs from VPM terminate mainly in the barrel centers in layer IV (SI-IV barrel), while POM projects to the septa regions around the barrels (SI-IV septa) (Koralek et al. 1988).

Corticopontine afferents arise from layer V of SI , (SI-V), (Legg et al. 1989) and the pontine nuclei project to the cerebellum (Mihailoff 1983). Since the organization of tactile sensory inputs and the receptive field properties have not been established in the pons, the model represents the pontine nuclei as a relay station (i.e., it is not explicitly simulated).

In summary, as shown in Figure 6.2, we model the projections from the face of the rat to SI as two separate pathways: 1) a "lemniscal" pathway relayed by the trigeminal nucleus Principalis and the thalamic VPM to the centers of barrels in layer IV of SI, and 2) a "paralemniscal" pathway relayed by the trigeminal subnucleus Interpolaris and the thalamic POM to the septal regions in layer IV of SI. Then, layer V of SI projects, through the pons (a direct relay in our model since not enough is known about the organization of the pontine nuclei), to crus IIa. Finally, the model also includes a direct trigeminocerebellar projection from a distinct population of the Interpolaris (Interpolaris-Cb).

6.4.2 Model architecture

Basic assumptions

Several features of the model are based on physiological and anatomical features of the real system, but not all aspects of the system are known or implemented in detail. Our simplified representation of the system is based on the following assumptions:

- *Each of the brain areas modeled is represented as a 2-D layer of units.*

The initial topography of the different structures, i.e., the proportion of units with a particular receptive field, the neighborhood relationship, etc., was obtained from maps published for the various brain areas. Each of the ten structures included in this model are represented by 100 "topographical units" each intended to represent the inputs and outputs from a particular region of the structure in question. Thus, each unit receives inputs from units in its afferent structure(s) and sends outputs to units in its efferent structure(s). In effect, these connections carry information on the location of the periphery (skin surface) projecting to that region. Exclusively *excitatory* interactions and *feedforward* projections are simulated.

- *The specific pattern of connections between simulated units is established based on the receptive field size distribution determined physiologically in the real system.*

The detailed anatomical patterns of divergence and convergence have not been determined experimentally for most of the structures in the model. Therefore, the connection patterns in the model were established based on the distribution of the size of the physiological receptive fields of individual neurons (or multiunit in the case of the cerebellum) in each structure as determined experimentally.

- *The distribution of receptive field size observed experimentally for the vibrissae is generalized to other face areas.*

The receptive field size for the vibrissae has been well studied physiologically. The discrete nature of the mystacial vibrissae makes it easy to quantify the size of a receptive field; one only needs to count how many vibrissae, when deflected, produce a response in the brain area under study. In contrast, very little data are available on the receptive field size of other face areas such as the upper lip, lower lip, or teeth. We thus generalized the known distribution of receptive field size for the vibrissae to the other perioral structures represented in our model. The experimental data incorporated in the model are described for each brain area in subsequent sections and summarized in Figure 6.3.

Trigeminal complex

Cerebellar-projecting Interpolaris cells (Interpolaris-Cb) have been shown experimentally to respond to the deflection of an average of five vibrissae (Woolston et al. 1982; Jacquin et al. 1989). The probability distribution of receptive field size for Interpolaris-Cb units in the model is taken from the proportion of cells responding to one, two, three, etc., vibrissae that was reported by Woolston et al. (1982); see Figure 6.3. In the simulations shown in Figure 6.3, the average receptive field size of the Interpolaris-Cb units is 4.6 vibrissae. To date, the receptive field size distribution of the population of Interpolaris neurons that project to POM (Interpolaris-Th) has not been determined experimentally. Accordingly, in the model, we used the same distribution as that of their efferent structure POM, which is described below. Most of the neurons in the Principalis respond to the deflection of a single vibrissa (Rhoades et al. 1987; Doherty et al. 1993; Jacquin et al. 1993). Doherty et al. (1993), for example, report that over three-quarters of the Principalis cells respond to one vibrissa; however, the distribution of the receptive field size for the remaining cells is not given. Thus, in the simulations shown in Figure 6.3, the receptive field of each Principalis unit consists of a single vibrissa.

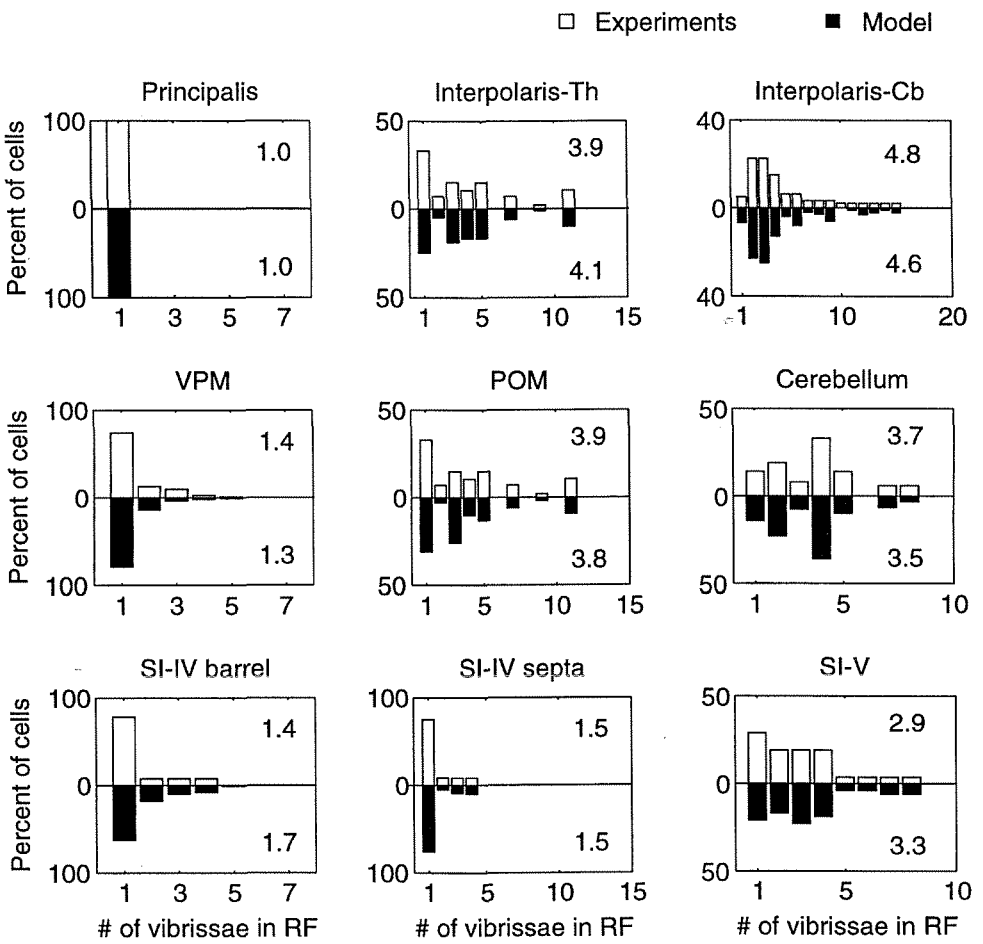

Figure 6.3 Distribution of receptive field size for each structure in the model. The percentage of cells that respond to deflection of different numbers of vibrissae is shown for experiments (white bars) and for a typical simulation (black bars). The data were obtained from the following papers: Principalis: Jacquin et al. 1993; Interpolaris-Cb: Woolston et al. 1982; VPM and POM: Chiaia et al. 1991b; SI-IV barrel, SI-IV septa, and SI-V: Armstrong-James and Fox 1987. No experimental data on receptive field size were available for Interpolaris-Th; the same distribution as for POM was used. Cerebellar receptive field size distribution is from our experimental data. The numbers in the upper and lower right corners of each histogram are the average number of vibrissae in the peripheral receptive field (upper corner: experimental average, lower corner: average in the simulation). RF: receptive field.

Thalamus

The receptive field size of VPM neurons, on average 1.4 vibrissae, is much smaller than that of POM neurons, 3.9 vibrissae (Chiaia et al. 1991b). The probability distribution of receptive field size for VPM and POM units in the model is obtained from the distribution of receptive field sizes reported by Chiaia et al. (1991b) based on their extracellular recordings of neurons in VPM and POM. Thus, in the simulations shown in Figure 6.3, VPM and POM units respond to an average of 1.3 and 3.8 vibrissae.

SI cortex

The somatosensory cortex is represented in the model as three separate populations of units, the barrel population in layer IV (SI-IV barrel) that receives projections from Pr5, the septa population also in layer IV (SI-IV septa) that receives projections from Interpolaris-Th, and the layer V population (SI-V) that projects to the cerebellum through the pons. The receptive field size of SI neurons and the distribution of the receptive field sizes was obtained from the data of Armstrong-James and Fox (1987). They report an average receptive field size of 1.4 vibrissae for the barrel regions of layer IV, 1.5 for the septa regions of layer IV, and 2.9 for layer V (1.7, 1.5, and 3.3 vibrissae, respectively, for the simulations shown in Figure 6.3).

Cerebellum

Finally, the distribution of receptive field size for vibrissae in crus IIa is from our extracellular recordings in the granule cell layer. Because single granule cells have not been recorded from, the distribution of receptive field sizes in the model was based on field potential recordings in the granule cell layer as described in Chapters 3, 4, and 5. In the real system, locations in the granule cell layer responded to an average of 3.7 vibrissae (cerebellar units responded to an average of 3.5 vibrissae in the simulations shown in Figure 6.3).

Thus, the distribution of receptive field size obtained from published data for each structure is encoded in the model as a probability distribution (there is a specific probability distribution for each structure; see Figure 6.3). The receptive field size for each unit in a given structure is assigned based on the experimentally-derived probability distribution (Figure 6.3, white bars) and the resulting average receptive field size for each structure is given for a typical simulation (Figure 6.3, black bars).

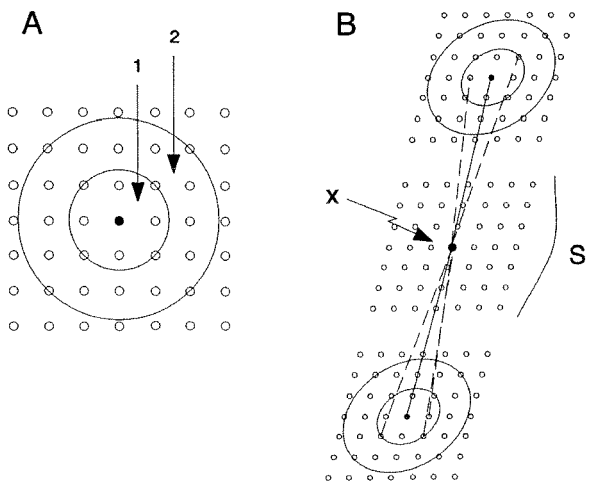

Figure 6.4 Depiction of the rings (1st and 2nd) used to assign connections. **A:** The rings shown here are for the "center" unit (filled circle). Every unit (small open circle) within, or intersecting, a given ring is considered to be at the same distance from the center unit. Only part of the network is shown. **B:** Unit "x" in structure S receives connections from afferent structure and sends connections to efferent structure (solid and dotted lines). Filled circles show units (centers) from S's afferent and efferent structures that correspond to "x". Solid lines show the connections between the corresponding units.

6.4.3 Establishing connections

As already described, the 100 units representing each structure were assigned receptive fields based on the published data (section 6.4.2). The specific pattern of connections is established in order to match the experimental receptive field size (RFsize) distribution. The connections were not "hand drawn;" instead, specific connection rules were implemented. The connections were automatically established in the simulations following the steps outlined below.

A. Topographic connections from skin to trigeminal complex

1. Unit "x" in structure S is randomly assigned a target receptive field size (trf(x)) based on the experimentally observed probability distribution for that structure.
2. Topographic connection is established from the corresponding unit (center) in the afferent layer (skin in this case) to "x" (Figure 6.4B).
3. Connect (trf(x) – 1) Skin units, randomly chosen from center's 1st ring, to "x". If all 1st ring units are connected and RFsize(x) < trf(x), start choosing from 2nd ring and so on until RFsize(x) = trf(x) (Figure 6.4).
4. Determine receptive field type for unit "x" (RF(x)) by adding number of connections from each different receptive type (such as vibrissae, upper lip, upper incisor, etc.), RF(x) is the face area providing the most connections. For example, let's imagine unit "x" in Interpolaris-Th receives projections from vibrissae E4, E5, and E6 from the Skin and unit "y" receives projections from vibrissae D5 and E4 as well as from one upper lip unit; both units "x" and "y" have an RF(x) = RF(y) = vibrissae and RFsize(x) = RFsize(y) = 3. If "x" and "y" project to unit "z" in POM, then RF(z) is also vibrissae and RFsize(z) = 5. In this example, not all projections to "y" or "z" were from vibrissae; we call the second largest number of connections from a certain face area the subdominant RF (subRF). Thus, subRF(y) = subRF(z) = upper lip; "x" does not have a subRF as all of its connections were from vibrissae. In some cases, the center has more weight than other connections in determining the resulting receptive field.

B. Topographic connections between trigeminal, thalamus, and SI

1. Same as A1.
2. Same as A2.

3. If RFsize(x) ≥ trf(x), no more connections are established.
   If RFsize(x) < trf(x), survey center's immediate neighbors (1^{st} ring) and connect to optimal combination to attain trf(x). If all 1^{st} ring units are connected and RFsize(x) < trf(x), start choosing from 2^{nd} ring and so on until RFsize(x) = trf(x).
4. Same as A4.

C. Nontopographic connections to cerebellum

1. Same as A1.
2. For each cerebellar patch, randomly select a "seed" unit in both SI-V and Interpolaris-Cb that has the same RF. Seed plays the same role as center did for topographic connections. Connection is established from the seed unit (center) in afferent layers to "x".
3. Same as B3.
4. Same as A4.

In making these connections, interesting observations came to light. For example, structures with large receptive fields project to structures with a smaller average receptive field size. This is characteristic of the paralemniscal pathway, for example, POM to SI-IV septa (Figure 6.3). It was not possible to make connections between such structures as the simulated units could not match the experimental receptive field size distribution. It was necessary to add "silent" connections between some of the structures to match experimental receptive field size. Under these conditions, when a unit receptive field size is greater than its target receptive field size, i.e., when RFsize > trf, then (RFsize – trf) connections chosen at random become silent. The silent connections are "physically" still there but do not contribute to the establishment of the receptive field size or type of their target units. Following disturbance of the simulated system, however, such as when simulating a peripheral injury (as considered in the results section), these connections might influence the reorganization.

6.4.4 Simulation of infraorbital nerve lesion

Once connections were established, we first simulated a peripheral lesion by replacing the "normal" trigeminal representations by the "reorganized" one that has been

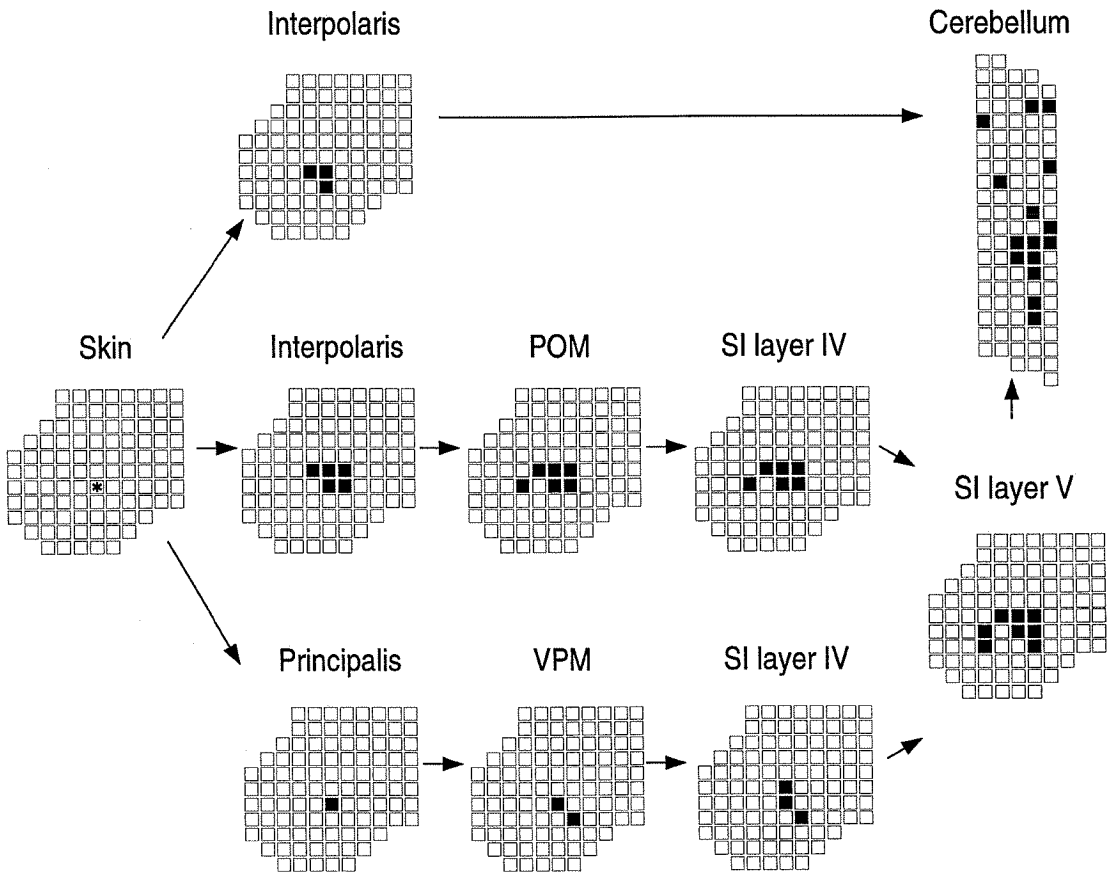

Figure 6.5 Locations in the simulated somatosensory system related to the particular position on the skin shown as a white square with a black asterisk. All the units in each structure are shown as squares. Black squares indicate units that receive information (directly or indirectly) from that specific face area. Arrows indicate the direction of the projections between two structures.

described by Waite (1984) under similar conditions to the experiments described in this thesis. Unfortunately, the published data on trigeminal reorganization following peripheral lesion of the infraorbital branch of the trigeminal nerve treated LL, Li, and Ui as the single structure "lower jaw and inside mouth" (Waite 1984) and made no differentiation between these three structures (Waite, personal communication). The simulated trigeminal reorganized maps are based on Waite's data with some extrapolations subject to the following constraints: 1) The total area of Ui, Li, and LL is equivalent to Waite's "lower jaw and inside mouth." 2) The reorganized map is somatotopic. 3) Adjacent intact representations expand into the denervated area. 4) The reorganized trigeminal map should be such that it leads to an SI upper incisor representation that expands approximately six-fold from its normal value because we showed in Chapter 5 that the Ui representation expands by such a factor in experiments with lesioned rats.

Fixed connections

In our simulations, once the connections were established based on data from normal animals and using the algorithms described in section 6.4.3, they were kept fixed. After reorganization of the afferent structures to mimic the effect of infraorbital nerve lesion as just described, the new information was propagated throughout the entire system (the connections were kept the same but the information they carried changed) and the effects on the cerebellum organization were studied.

6.4.5 Computer simulations

Simulations were performed on a SPARCstation 10 (Sun Microsystems), using the neural simulator GENESIS (Wilson et al. 1989; Bower and Beeman 1995). Typically, for a network consisting of 1000 units, it took 12 minutes to establish the network connections and less than 2 minutes to simulate the effects of nerve lesion.

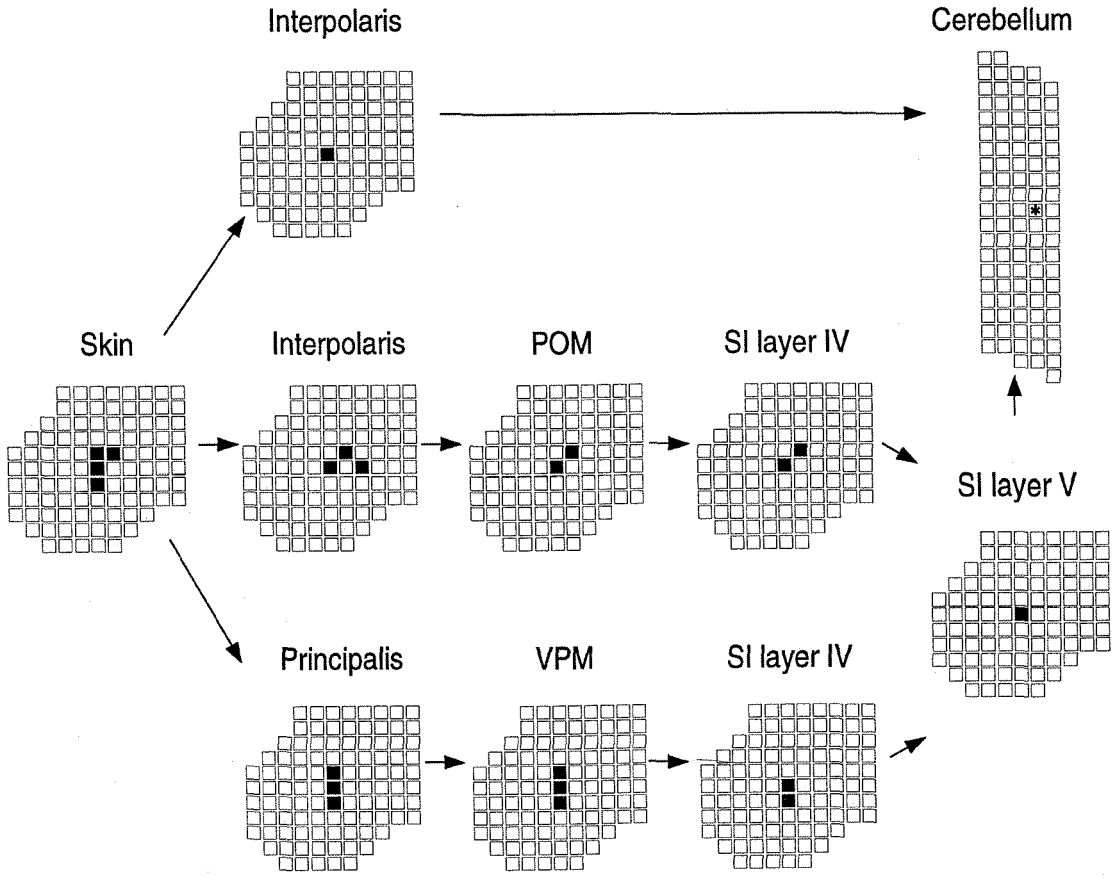

Figure 6.6 Locations in the simulated somatosensory system related to the particular position in crus IIa shown as a white square with a black asterisk. All the units in each structure are shown as squares. Black squares indicate units that send information (directly and indirectly) to that specific cerebellar area. Arrows indicate the direction of the projections between two structures.

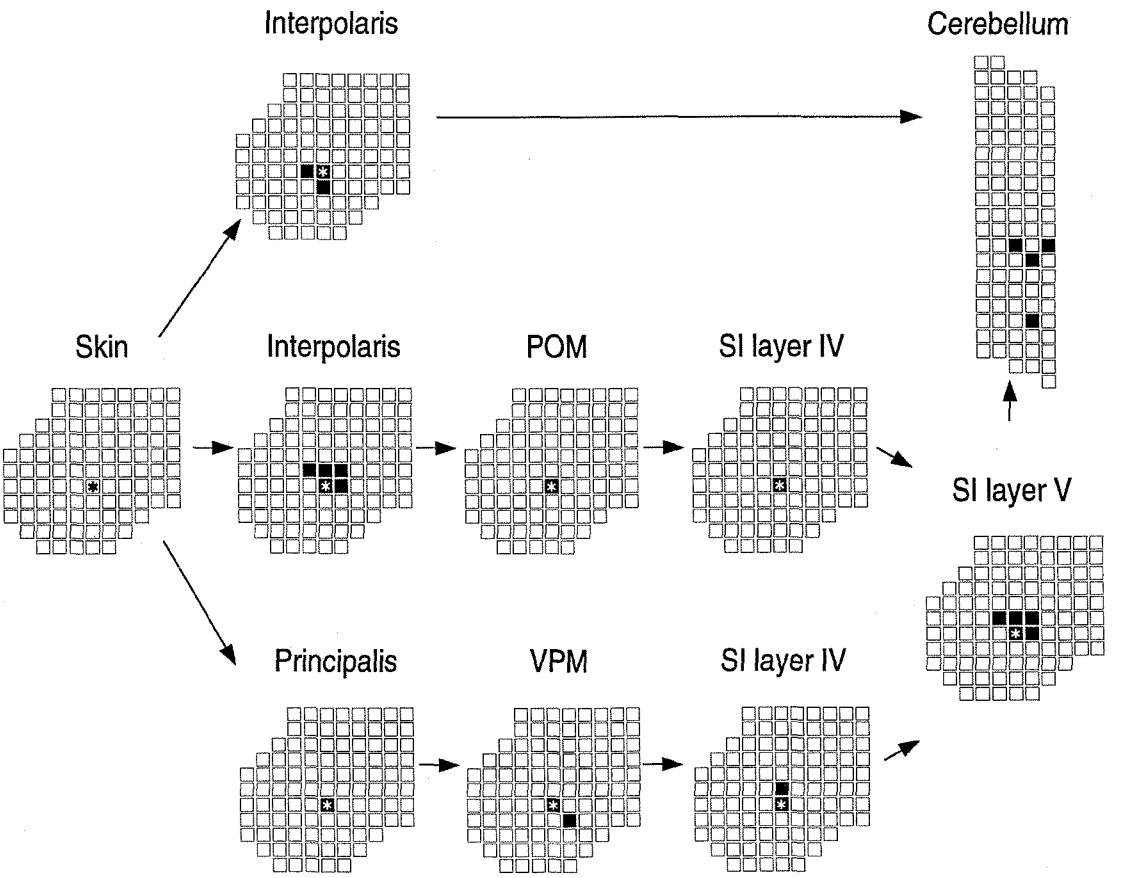

Figure 6.7 Connection pattern in simulated system. All the units in each structure are shown as squares. An arrow indicates projections from the square with an asterisk (in the structure at the tail of the arrow) to the black squares and the square with an asterisk (in the structure at the head of the arrow).

6.5 Results

6.5.1 Intact somatosensory system

Once the connections are established based on the principles described in section 6.4, one can look at divergence and convergence in the system. This is implied in the receptive field and mapping data used to build the model, but the simulation brings together all of the separate data and allows visualization. Figure 6.5 shows all the regions in the simulated somatosensory system that are activated by tactile stimulation of a small location on the skin. A large cerebellar area receives input from that skin location. Conversely, one can look at all the regions that send information, directly or indirectly, to a small area of crus IIa. A single cerebellar location receives inputs from several skin locations (Figure 6.6). Finally, Figure 6.7 shows the connection pattern at each level from a single location of the afferent structures.

Subdominant receptive fields

The data presented in Chapter 4 showed that over 70% of all cerebellar recording sites had receptive fields associated with weaker responses (subdominant receptive fields) in the granule cell layer. The presence and type of such weaker responses were also explored in the model. On average, about half of the simulated cerebellar units had subdominant receptive fields (see section 6.4.3 for definition). Most of the subdominant receptive fields were responsive to upper lip and upper lip-related structures and, as in the experimental case, the upper incisor was not represented more frequently than other perioral structures (Figure 6.8).

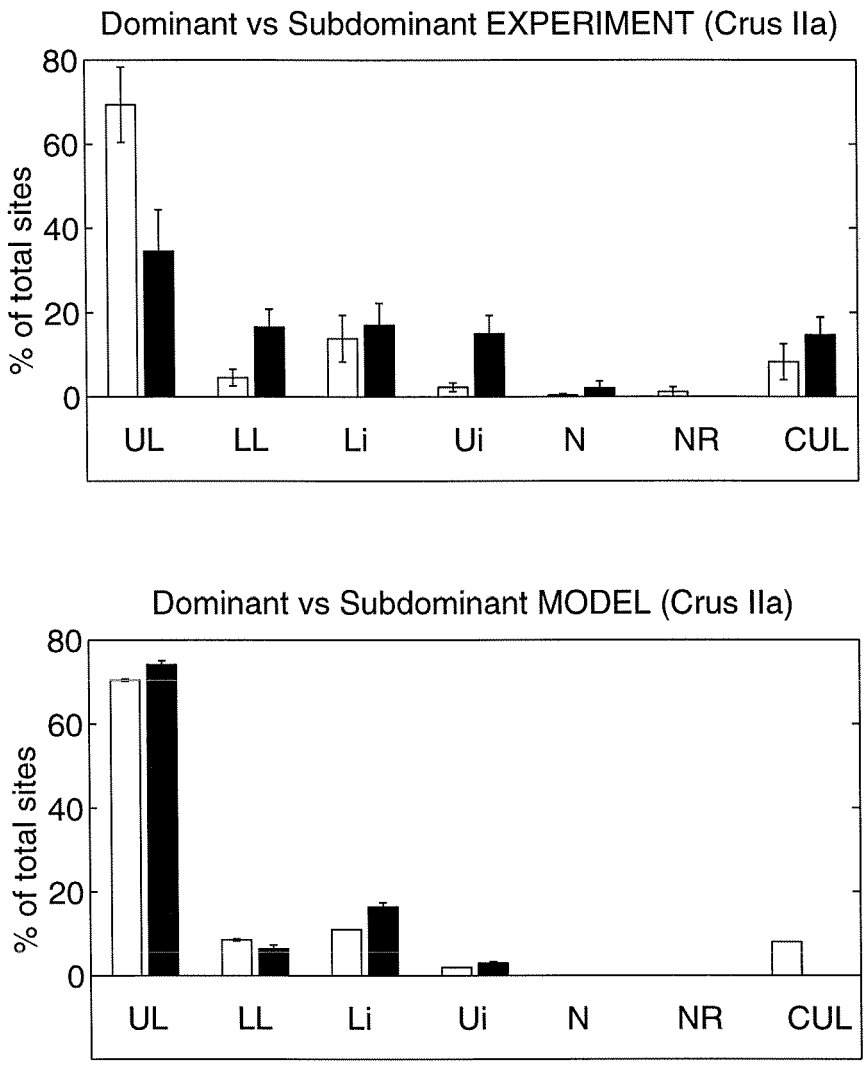

Figure 6.8 Comparison of dominant (white bars) and subdominant (black bars) cerebellar representation of the various face areas observed experimentally and in the simulated system. Each bar represents the mean percent ± SE of total number of electrode penetrations or units with a given receptive field type. Top: experimental results from six normal animals. Bottom: simulation results, n = 18. *Abbreviations for these and subsequent histograms*: UL: upper lip and related structures (i.e., vibrissae, furry buccal pad, and anterior sinus hair); LL: lower lip; Li: lower incisor; Ui: upper incisor; N: nose; NR: nonresponsive; CUL: contralateral upper lip and related structures (i.e., vibrissae, furry buccal pad, and anterior sinus hair).

6.5.2 Change in representation of face areas following simulated nerve lesion

As shown in Figures 6.9 and 6.10, when the maps in the trigeminal nuclei alone are changed based on existing data (Waite 1984), the reorganization seen both in SI and in the cerebellum were remarkably similar to real maps. For example, the reorganized cerebellar map maintained a fractured somatotopy and the upper incisor representation expanded significantly in the reorganized crus IIa (Figure 6.9B). In SI, the upper incisor also replaced the upper lip representation. This is quantified in the histograms in Figure 6.10. It can be seen that a six-fold expansion of the upper incisor in the trigeminal complex led to a six-fold expansion in SI and a twenty-one-fold expansion in crus IIa. The simulated reorganized cerebellar maps were very similar to experimental maps, with significant increase in the representation of upper incisor and lower lip (Figure 6.11).

In order to assess the robustness of the results presented in Figure 6.11, we did two things. First, we used normal cerebellar topography from a different animal as a starting point to establish the normal connection pattern, since cerebellar tactile map organization, in particular the positional relationships between different body part representation, has been demonstrated to vary among normal animals (Bower and Kassel 1990). The simulated cerebellar reorganization patterns were still similar to real patterns. Second, we explored the possible range of trigeminal reorganization and looked at the effect of different trigeminal reorganized maps on cerebellar reorganization. As described in section 6.4.4, the organization of the Interpolaris in lesioned animals is not known precisely. Thus, even based on Waite's data and with the constraints described in section 6.4.4, there was some flexibility in determining the reorganized Interpolaris maps used in the model. We tried many possible combinations, with most giving results similar to Figure 6.11. To give an idea of the range, Figure 6.12 shows results from simulations that were the most different from experimental data. In these simulations, the lower lip representation expanded more

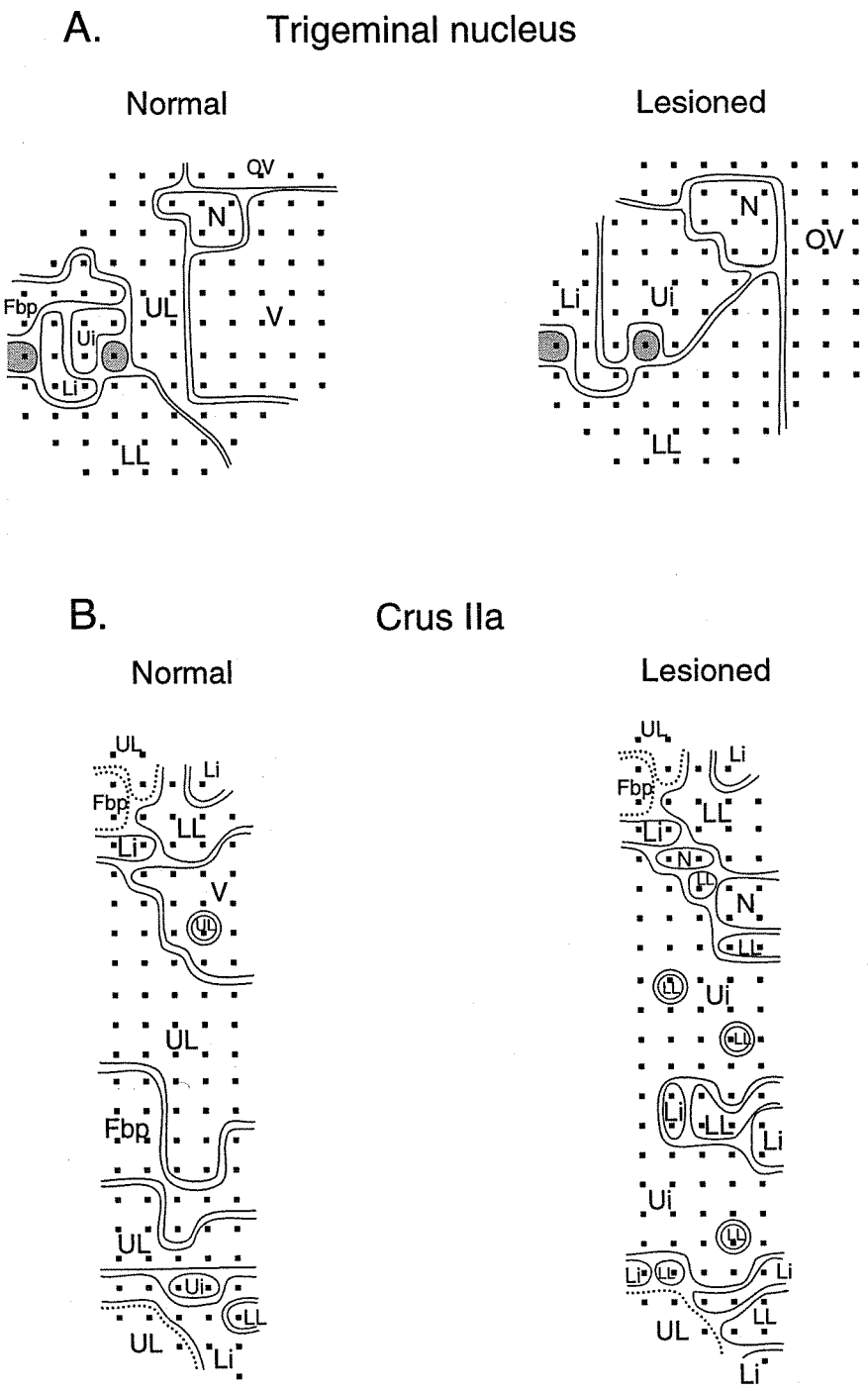
A.
Trigeminal nucleus
Normal
Lesioned
OV
N
Fbp
UL
V
Ui
Li
LL
B.
Crus IIa
Normal
Lesioned

Figure 6.9

Figure 6.9 Organization of the tactile inputs to the trigeminal nucleus Interpolaris and crus IIa in the model. **A:** Model representation of the trigeminal nucleus Interpolaris: normal (based on data from Waite 1984) and reorganized (based on data from Waite 1984 and subject to the constraints discussed in section 6.4.4). **B:** Model representation of crus IIa: normal (based on our experimental data) and reorganized (resulting from simulated infraorbital nerve lesion). Units are shown as squares. Enclosing boundaries are drawn around units with common receptive field type. Solid lines represent projections from ipsilateral body areas; dotted line, contralateral. Shaded areas indicate nonresponsive units. *Abbreviations:* Fbp: furry buccal pad; Li: lower incisor; LL: lower lip; Ui: upper incisor; UL: upper lip; N: nose; OV: vibrissae over the eye (not innervated by infraorbital nerve); V: vibrissae.

than the upper incisor did. This is not usually seen experimentally. It still, however, retained important similarities to experimental results, for example, the upper incisor representations did expand significantly and the lower incisor did not.

Cerebellar field potentials

As described in Chapter 2, in normal animals, cerebellar granule cell layer field potentials evoked by tactile stimulations usually consist of two components: a short-latency component (from the direct trigeminocerebellar pathway) peaking around 8 msec after the onset of the stimulation and a long-latency component (from the indirect cerebrocerebellar pathway) peaking around 20 msec. We have also shown in Chapters 3 and 4 that peripheral lesions affect these field potentials components differently. In animals deafferented later than two weeks after birth, between 5 to 30% of all cerebellar field potentials recorded lacked the short-latency component (only the long-latency component was present).

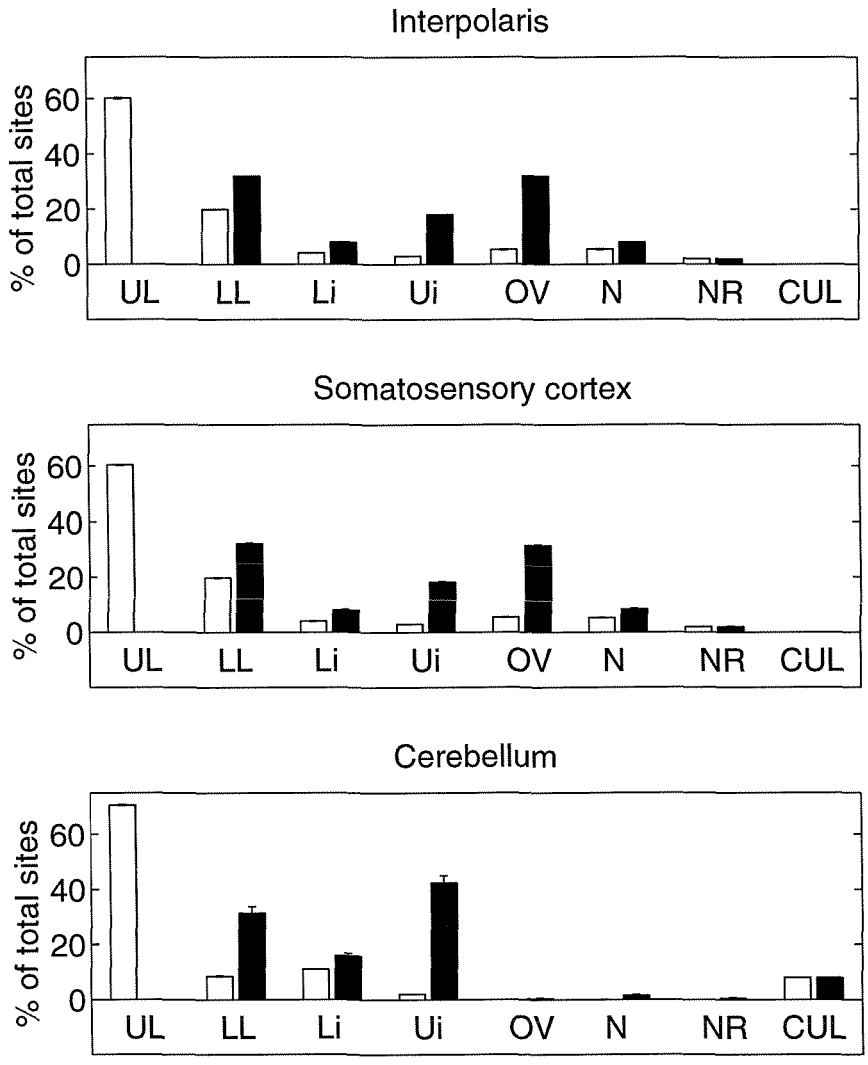

Figure 6.10 Representation of the various face areas before (white bars) and after (black bars) simulation of infraorbital nerve lesion using reorganized Interpolaris representation as described in section 6.4.4. Each bar represents the mean percent ± SE of total number of units with a given receptive field, n = 19. Abbreviations as in Figure 6.8. OV: vibrissae over the eye (not innervated by infraorbital nerve).

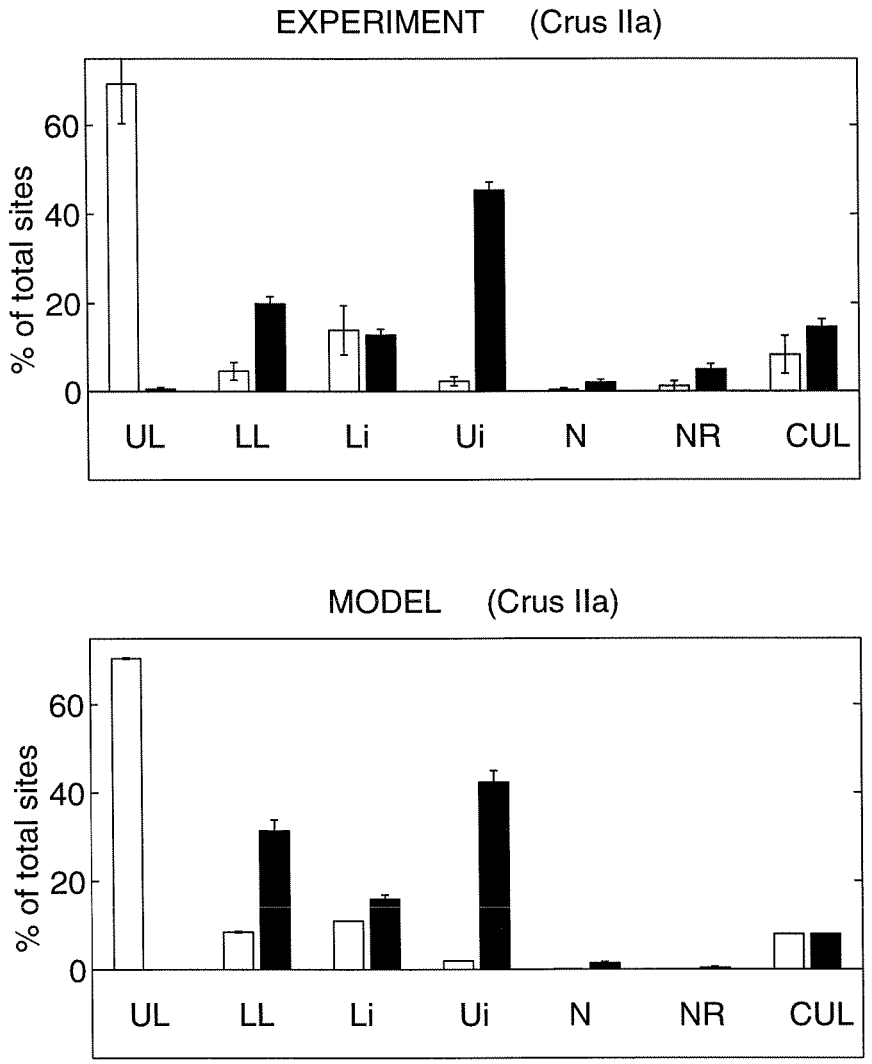

Figure 6.11 Comparison of cerebellar representation of the various face areas observed experimentally and in the simulated system. Each bar represents the mean percent ± SE of total number of electrode penetrations or units with a given receptive field type. Top: experimental results from 15 normal animals (white bars) and 31 animals lesioned from 1 to 89 days postnatally (black bars). Bottom: simulation results before (white bars) and after (black bars) simulation of infraorbital nerve lesion, n = 19 (same simulations as in Figure 6.10).

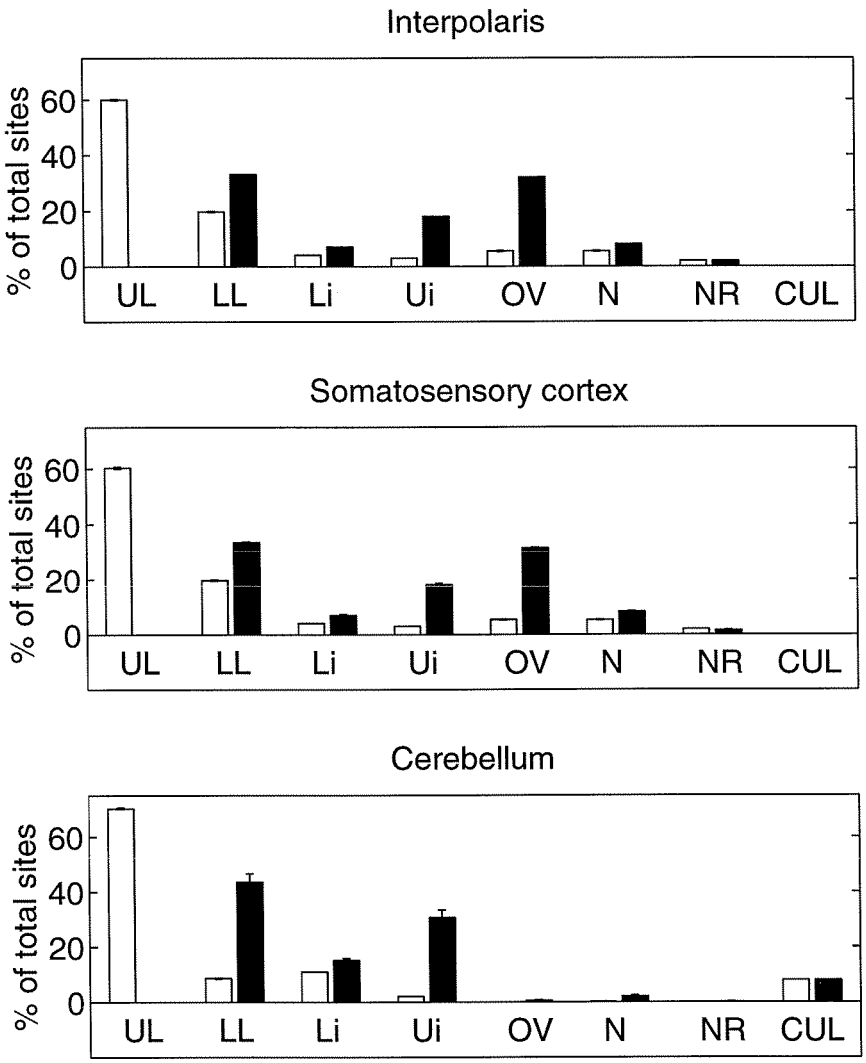

Figure 6.12 Representation of the various face areas before (white bars) and after (black bars) simulation of infraorbital nerve lesion using a different reorganized Interpolaris representation than in Figures 6.10 and 6.11; see text for details. Each bar represents the mean percent ± SE of total number of units with a given receptive field type, n = 16.

In our model, field potentials were not explicitly simulated, but a cerebellar unit was considered to have a "field potential" consisting of both components if it received responsive connections from both the direct trigeminocerebellar and the indirect cerebrocerebellar pathway. It had only the long-latency component if it received responsive connections from the cerebrocerebellar pathway but no connections or connections carrying no tactile information (RF = nonresponsive) from the trigeminocerebellar pathway. In order to test the effect of lesions on field potentials, we assumed in this particular instance of the model that some regions of the trigeminal nuclei did not reactivate following peripheral injury. Thus, a small number of units (black circle in Figure 6.13) from the trigeminal map based on Waite's data (Figure 6.9) were made nonresponsive to tactile stimulation. This is a reasonable assumption since Waite (1984) showed that nonresponsive areas in the trigeminal nuclei of animals lesioned as adults remained several months after peripheral injury.

We found that following simulation of an infraorbital nerve lesion, several locations throughout the reorganized cerebellar map had only the long-latency component of the field potential. The simulation results share many features of the real system. For the simulation results presented in Figure 6.13, 8% of the cerebellar units lacked the short-latency component of the field potentials; this is within the range observed experimentally. In addition, it was not unusual for the same patch (real or simulated) to contain units exhibiting the normal two-peaked response as well as units with only the long-latency component. Finally, as in the real system, the field potentials consisting of only the long-latency component are not regionally localized but are spread throughout the folium. Note that both the direct trigeminocerebellar and the indirect thalamocerebropontocerebellar projections synapse through the trigeminal nuclei on their way to the cerebellum. These results suggest that the difference in the convergence and divergence of connections in the two pathways might explain the emergence of cerebellar locations with long-latency response only.

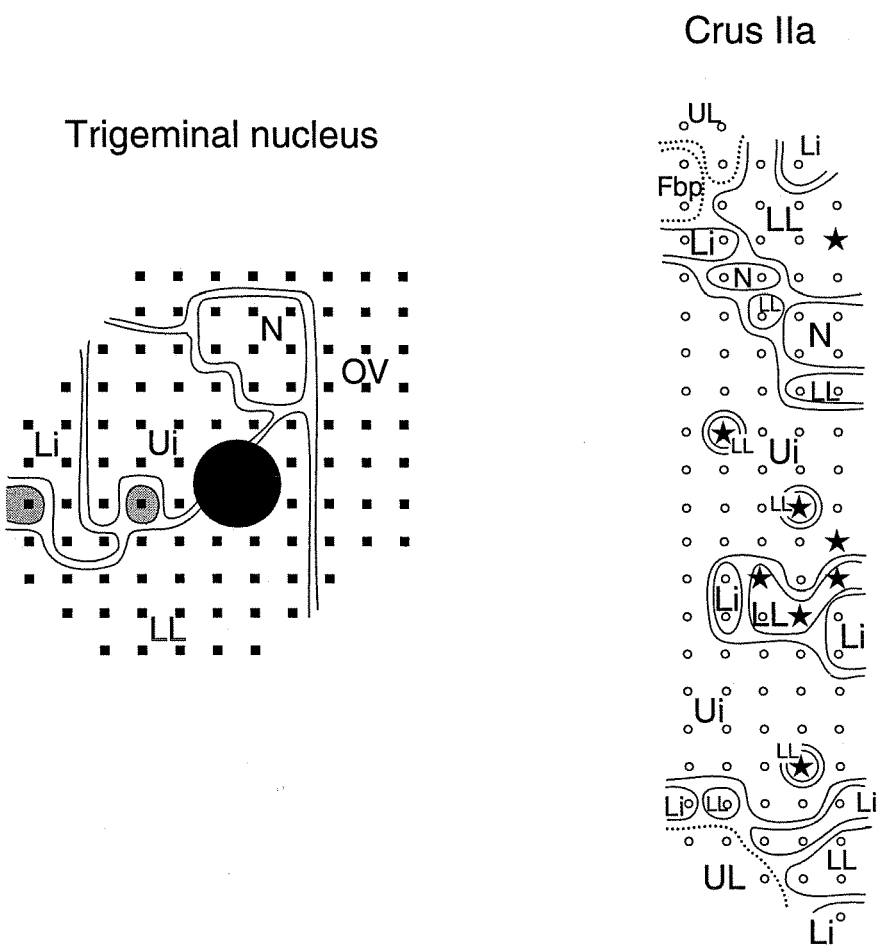

Figure 6.13 Simulated reorganization of trigeminal and cerebellar tactile maps: location of cerebellar units with field potentials consisting of only the long-latency component of the response to tactile stimulation (from indirect SI pathway). **Trigeminal nucleus:** Reorganized Interpolaris was based on data from Waite 1984 and constraints discussed in section 6.4.4. A small patch in the middle of the denervated area of Interpolaris was made nonresponsive following peripheral lesion (black area) and the effect on cerebellar reorganization was studied. Units are represented as squares. **Crus IIa:** Effects of simulated infraorbital nerve lesion on the cerebellar field potentials are shown. Open circles represent units with field potentials similar to those seen in normal animals, with both a short-latency (from direct trigeminocerebellar pathway) and a long-latency component (from the indirect cerebropontocerebellar pathway). Stars denote units for which the

field potentials consisted of only the long-latency component. Enclosing boundaries are drawn around units with common receptive field type. Solid lines represent projections from ipsilateral body areas; dotted lines, contralateral. Shaded areas indicate nonresponsive units. Abbreviations as in Figure 6.9.

6.6 Discussion

The trigeminal nuclei, thalamus, SI, and crus IIa have been shown experimentally to reorganize following peripheral nerve lesion (Chapters 3, 4, and 5; Waite 1984; Garraghty and Kaas 1991b; González et al. 1993). One of the goals of this modeling effort was to explore the possibility that cerebellar reorganization might be a reflection of reorganization occurring in its afferent pathways. In this chapter, we described a systems level topographic model we developed to explore the possibility that the connection patterns to the cerebellum are hardwired and that the site of reorganization is extrinsic to the cerebellum. There has been some recent experimental evidence for genetic specificity of cerebellar projections (Sotelo 1995) that support our assumption of fixed, non activity dependent cerebellar projections.

Our simulation results show that cerebellar reorganization patterns remarkably similar to experimentally observed ones can be generated by assuming plasticity, i.e., active reorganization, only in the cerebellar afferent pathways. For example, the significant increase in the upper incisor representation and the smaller, but also significant, increase in the lower lip representation following simulation of an infraorbital nerve lesion (Figure 6.11) were comparable to the increase observed experimentally following infraorbital nerve lesion (Chapters 3, 4, and 5). In addition, as described in Chapters 3 and 4, a number of cerebellar field potentials evoked by tactile stimulation in lesioned rats lacked the short-latency component. In the model, cerebellar locations with evoked field potentials consisting of only the long-latency component (representing the indirect

trigeminal-thalamus-SI-pons pathway), thus lacking the short-latency (direct trigeminal input) component of the response, were observed after a small area in the middle of the reorganized trigeminal maps (based on Waite's data) was made nonresponsive. Waite reported such nonresponsive areas in the trigeminal nuclei of animals deafferented as adults (Waite 1984). These simulation results suggest that a small continuous nonresponsive area in the reorganized trigeminal map could lead to the experimentally observed emergence of cerebellar field potentials with only the long-latency component in widely spread locations of crus IIa.

Models allow for visualization and synthesis of a large amount of experimental data; they can also provide motivation and serve as context for additional data collection. With the available experimental data, our model could be refined and made more physiological. It is also clear, however, that there is a need for additional experimental data in order to build a detailed, physiologically and anatomically realistic model of the somatosensory system. For example, more information about the organization and the receptive field properties of pontine nuclei neurons would allow the explicit modeling of this part of the pathway. Detailed analysis of the receptive field properties of the population of cells in the spinal trigeminal nucleus Interpolaris that project to the thalamic POM would allow simulation of a more realistic paralemniscal pathway. More detailed and complete maps of reorganized trigeminal and SI representations following nerve lesion would reduce the degrees of freedom in our simulations. This model is a first step and provides a basis for future work to create more realistic and sophisticated models of the somatosensory system.

7

Conclusions

La science est comme une corde que nous tenons par un bout que nous voyons; l'autre bout est dans l'eau et il tient à l'inconnu. Toutes les fois que l'on prétendra présenter un travail complet ou rien ne reste obscur, on pourra dire que cela est faux.

Claude Bernard

The main contributions of this research will be summarized in this chapter; detailed discussions can be found at the end of each individual chapter. A discussion of related areas for future research is also presented.

7.1 Contribution of this work

7.1.1 Plasticity in cerebellar somatosensory maps

The results presented in this thesis provide the first demonstration of plasticity in a cerebellar somatosensory map following peripheral nerve lesion. Our detailed electrophysiological mapping of the crown of crus IIa shows that cerebellar tactile maps, like somatotopic sensory maps in other parts of the brain, are capable of reorganizing following peripheral injury. Moreover, these cerebellar somatosensory maps reorganized

following deafferentation *at all ages* tested, from the first day after birth to adulthood (PND 1 to PND 89). There was no critical period after which the peripheral lesion did not produce reorganization, unlike anatomical studies reported for other somatosensory areas of the rat (for reviews see Belford and Killackey 1980; Woolsey 1990). All reorganized maps, independent of the animal's age at deafferentation, maintained a fractured somatotopy as well as several features of normal maps. Animals deafferented as adults, though, showed a significant increase in the number of cerebellar recording sites not responsive to any tactile stimulation compared to animals deafferented earlier in development.

The cerebellar denervated upper lip area was consistently and predominantly invaded by the upper incisor representation and to a lesser extent by the lower lip representation. This pattern of reactivation is considerably different from other somatosensory regions, since the upper incisor representation is often not adjacent to the upper lip and sometimes not even represented in crus IIa of normal adult rats. In addition, our results showed that neither the immediate unmasking of silent projections nor previously weak (subdominant) projections appeared to be responsible for the dominance of the upper incisor in the reorganized maps. We found no evidence that intrinsic cerebellar mechanisms were responsible for the observed patterns of map reorganization.

7.1.2 Influence of cerebellar afferent projections

The detailed analysis of the temporal structure of the cerebellar field potentials presented in this thesis provides a new tool to study the influence of afferent projections without having to simultaneously record in many brain areas. The evoked field potentials recorded in the granule cell layer of crus IIa of normal animals consist of two components at different latencies within the first 50 msec following brief peripheral tactile stimulations. By simultaneously recording in both the somatosensory cortex (SI) and crus IIa, we demonstrated that the latency of the second peak in the cerebellar response, or long-latency component, is strongly correlated to the latency of the SI response to tactile stimulation.

Moreover, using several methods to interfere with the physiological integrity of SI, we showed that the long-latency component of the cerebellar response is primarily due to inputs from SI. The short-latency component of the cerebellar response to tactile stimulation was already known to result from the direct trigeminal projection (Watson and Switzer 1978; Woolston et al. 1981). Thus, the effects of peripheral injury on the trigeminocerebellar pathway (reflected by the short-latency cerebellar component) and the cerebroponto-cerebellar pathway (reflected by the long-latency cerebellar component) can be inferred from a detailed analysis of the cerebellar field potentials. Our results showed that the age of the animal at deafferentation affected the short-latency but not the long-latency component of the cerebellar field potential, suggesting a difference in the developmental sensitivity of the trigeminocerebellar and the cerebropontocerebellar pathways. In addition, we directly explored SI reorganization following peripheral lesions and demonstrated that the upper incisor representation, which we showed is adjacent to the upper lip in SI of normal rats, increased significantly in size. Our results suggest that the site of plasticity following deafferentation is not in the cerebellum itself but in its afferent pathways. This hypothesis was tested with a network connectivity model of the rat somatosensory system that we developed. In these simulations, it was possible to obtain cerebellar reorganization similar to what was observed experimentally without assuming any intrinsic plasticity in the cerebellum. This model provides a framework upon which more detailed simulations can be built.

7.2 Future research

7.2.1 Intracortical microstimulation in the cerebellum

We found no evidence for an intrinsic mechanism underlying the cerebellar reorganization following peripheral injury. In order to further explore the possibility of

intrinsic mechanisms of reorganization, the cerebellar representation could be examined following microstimulation in the cerebellar granule cell layer. Although this stimulus is not natural, stimulating the cerebellum directly would bypass any role of peripheral inputs in driving cerebellar reorganization and could therefore help rule out, or support, the possibility of intrinsic cerebellar mechanisms of reorganization. Such microstimulation in the middle layers of SI in monkeys led to an expansion of the cortical representation of a skin area and was interpreted as demonstrating a capacity for intrinsic plasticity in SI (Recanzone et al. 1992a).

7.2.2 Plasticity of patch boundaries, transformation from a topographic map to a fractured one

Studies of individual differences in somatotopic cerebral maps and fractured cerebellar maps have shown that these two maps have different patterns of variability. In the normal cerebral cortex, the greatest variability is in the spatial pattern across somatotopically-related body surfaces, in particular, size and shape; neighborhood relations are among the least variable, i.e., there is a constant overall general somatotopy (Merzenich et al. 1987; Riddle and Purves 1995). In the normal cerebellar cortex, in contrast, the main variability is in the positional relationships between different body surfaces, while the relative proportions of representations do not appear to change significantly (Bower and Kassel 1990). Future studies could examine the plasticity of patch boundaries in crus IIa to determine if a boundary between two different body structures can be extended or reduced following an alteration in the spatial relationship or use of these body structures. It is also important to understand how the topographic information from the somatotopic SI cortex is transformed into the fractured information found in the cerebrocerebellar projection, and where such a transformation occurs; similarly with the somatotopic trigeminal nuclei and the trigeminocerebellar projection.

7.2.3 Behavioral correlate to peripheral lesion

Ultimately, a full understanding of the role of the cerebellum, the significance of afferents circuits in cerebellar function, and the functional consequences of brain reorganization will require a close examination of neural activity in behaving animals. The observations in this thesis have resulted in a new series of behavioral studies; preliminary results from awake behaving rats show cerebellar field potentials with short- and long-latency components similar to the ones reported here (Hartmann and Bower 1993, 1995).

Awake behaving rats use their vibrissae extensively to explore their environment. When the input from these sensory structures is destroyed, as when the infraorbital branch of the trigeminal nerve is lesioned, the sensory maps in crus IIa and SI reorganized (Chapters 3, 4, and 5; Waite 1984); Waite also demonstrated reorganization in the trigeminal nuclei. We therefore undertook a series of preliminary experiments to search for a behavioral correlate to the neural reorganization associated with deafferentation of the upper lip and vibrissae[1]. We were also interested in comparing the behavioral results of deafferentation with those resulting from lesions of crus II.

Seventeen normal adult female rats were trained to put their head through a hole in a plexiglass wall in order to drink from a nozzle. The hole was only large enough for either the head or the paws, but not both. Animals were water deprived for several hours before each experiment. Their exploratory behavior was videotaped and later analyzed frame by frame. After establishing a typical and repeatable drinking behavior for each rat (about 10 days), we deafferented the infraorbital branch of the trigeminal nerve of 5 rats, lesioned crus II of 4 animals, and performed sham surgeries on the remaining animals. We then resumed videotaping the exploratory behaviors for 1 week to 3 months.

In normal rats, a typical drinking sequence began with the rat exploring the hole in the plexiglass wall. As its head crossed the midplane of the hole, the rat's snout gradually

[1] These experiments were done in collaboration with Mitra Hartmann and Mike Lin.

approached the nozzle; the vibrissae palpated the nozzle, and curled and uncurled around it. The mouth stayed closed for the entire exploratory sequence until the tongue protruded to lick the nozzle (Zeigler et al. 1984).

Cerebellar lesions have been shown to cause slowing of voluntary movement and to disrupt the completion of fast actions, such as saccadic eye movements (Dichgans 1984) but merely produce temporary deficits in grooming sequences (Berridge and Whishaw 1992). We found that cerebellar lesions only transiently affected the drinking sequence; the lesioned animals appeared to miss the nozzle more frequently than the controls (sham surgery). Moreover, they often exhibited rhythmic licking activity in the air next to the nozzle. Some of the lesioned rats put their paws through the hole to explore the nozzle before drinking, a behavior never exhibited by normal animals.

Infraorbital nerve section caused an increase in the duration of perioral contact and disrupted drinking in the days following surgery. But again, this was a transient effect; no significant difference was observed in the drinking behavior of deafferented animals several weeks after the lesion. Zeigler and his colleagues reported similar effects for infraorbital lesions in their thorough study of the effect of trigeminal denervation on ingestive behavior (Zeigler et al. 1984, for review see Zeigler et al. 1985). The rats appeared to continue using both sides of their upper lip for nozzle exploration, even when unilateral infraorbital nerve sections were performed. We were unable to determine whether sensory information was transferred from the upper lip to the upper incisors, or whether the drinking task could be done in the absence of upper lip and vibrissae sensory information.

Berridge and Fentress published a series of experiments in which they studied the effect of trigeminal nerve lesion (Berridge and Fentress 1985, 1986, 1987). Their behavioral testing of lesioned animals was performed within two weeks of the deafferentation. In their study, lesions were much more extensive than ours. They sectioned the inferior alveolar, lingual, and auriculotemporal nerves of the mandibular

branch as well as the anterior superior alveolar and infraorbital nerves of the maxillary branch; in effect, removing sensation from the upper and lower lip, gums, incisors, lower molars, chin, anterior tongue, oral mucous membrane, vibrissae, and furry buccal pads. Such lesions have been shown to severely disrupt food and water intake in the rat (Jacquin and Zeigler 1983) and the pigeon (Zeigler 1973). Berridge and Fentress (1985) showed that these trigeminal lesions selectively reduced the ingestive actions elicited by preferred tastes but left the aversive actions elicited by unpreferred tastes unchanged. They also showed that such lesions disrupted the *form* of individual action during grooming, such as forelimb stroke across the face (Berridge and Fentress 1986) but the *sequential* organization of the actions during grooming were not affected (Berridge and Fentress 1987).

The effects of sensory map reorganization on perception and performance is not clear. In some cases, the reorganization appears to relate to behavioral recovery and increase in perceptual ability such as in the demonstration of hypersensitivity to tactile stimulation of intact representation adjacent to a denervated cortical area (Wall and Kaas 1985). Also, after training that improved the performance of monkeys at detecting change in the frequency of a tactile stimulation to a particular skin area, the cortical representation of that skin area had significantly increased (Recanzone et al. 1992b). In other cases, deafferentation of sensory input resulted in mislocalization of tactile stimuli (Wall and Kaas 1985). A striking example of such mislocalization of tactile stimuli was provided by Ramachandran et al. (1992). They showed that following amputation of an upper limb, tactile stimulation of the face of human patients evoked sensation in precise locations of their missing limb. Pons et al. (1991) have shown that following similar injuries in monkeys, the face representation expanded in the denervated forelimb area of SI.

7.2.4 Gating mechanisms

Finally, our simultaneous recordings of SI and crus IIa produced an interesting and unexpected result. We showed that the failure rate for SI and SI-related cerebellar

responses increased when the interstimulus interval within a pair of stimuli was less than 100 msec (10 Hz). At 75 msec interstimulus interval (13 Hz), failure in these responses was nearly complete, even though the short-latency component of the cerebellar response remained unchanged. In the olfactory system, these frequencies correspond to the sniffing rate of the animal which effectively gates cortical afferent input (Bressler 1984). Thus, our studies also lay the groundwork for future studies of the interaction between SI and the cerebellum in normal animals.

Bibliography

Albus JS (1971) A theory of cerebellar function. *Math Biosci* **10**: 25–61.

Allard T, Clark SA, Jenkins WM, and Merzenich MM (1991) Reorganization of somatosensory area 3b representations in adult owl monkeys after digital syndactyly. *J Neurophysiol* **66**: 1048–1058.

Allen GI and Tsukahara N (1974) Cerebrocerebellar communication systems. *Physiol Rev* **54** (4): 957–1006.

Allen GI, Azzena GB, and Ohno T (1974) Somatotopically organized inputs from fore- and hindlimb areas of sensorimotor cortex to cerebellar Purkyne cells. *Exp Brain Res* **20**: 255–272.

Allen GI, Azzena GB, and Ohno T (1979) Pontine and non-pontine pathways mediating early mossy fiber responses from sensorimotor cortex to cerebellum in the cat. *Exp Brain Res* **36**: 359–374.

Altman J (1972) Postnatal development of the cerebellar cortex in the rat. III: Maturation of the components of the granular layer. *J Comp Neurol* **145**: 465–514.

Altman J (1982) Morphological development of the rat cerebellum and some of its mechanisms. In: *The cerebellum: new vistas* (Series: *Exp Brain Res Suppl 6*), Palay SL and Chan-Palay V (eds), Berlin, New York: Springer-Verlag, pp. 8–49.

Angaut P and Sotelo C (1975) Diversity of mossy fibres in the cerebellar cortex in relation to different afferent systems: an experimental electron microscopic study in the cat. *Brain Res* **95**: 179–189.

Armstrong-James M and Fox K (1987) Spatiotemporal convergence and divergence in the rat S1 "barrel" cortex. *J Comp Neurol* **263**: 265–281.

Bantli H and Bloedel JR (1977) Spinal input to the lateral cerebellum mediated by infratentorial structures. *Neuroscience* **2**: 555–568.

Bayer SA and Altman J (1991) Neocortical development. New York: Raven Press.

Belford GR and Killackey HP (1979) The development of vibrissae representation in

subcortical trigeminal centers of the neonatal rat. *J Comp Neurol* **188**: 3–74.

Belford GR and Killackey HP (1980) The sensitive period in the development of the trigeminal system of the neonatal rat. *J Comp Neurol* **193**: 335–350.

Berridge KC and Fentress JC (1985) Trigeminal-taste interaction in palatability processing. *Science* **228**: 747–750.

Berridge KC and Fentress JC (1986) Contextual control of trigeminal sensorimotor function. *J Neurosci* **6** (2): 325–330.

Berridge KC and Fentress JC (1987) Deafferentation does not disrupt natural rules of action syntax. *Behav Brain Res* **23**: 69–76.

Berridge KC and Whishaw IQ (1992) Cortex, striatum and cerebellum: control of serial order in a grooming sequence. *Exp Brain Res* **90**: 275–290.

Bloedel JR (1973) Cerebellar afferent systems: a review. *Prog Neurobiol* **2**: 1–68.

Bloedel JR and Courville J (1981) Cerebellar afferent systems. In: *Handbook of physiology: The nervous system, vol II*, Brooks VB (ed), Bethesda: American Physiological Society, pp. 735–829.

Bower JM (1993) Is the cerebellum a motor control device? Commentary on "Functional heterogeneity with structural homogeneity: how does the cerebellum operate?" by JR Bloedel. *Behav Brain Sci* **15**: 714–715.

Bower JM, Beermann DH, Gibson JM, Shambes GM, and Welker W (1981) Principles of organization of a cerebro-cerebellar circuit. Micromapping the projections from cerebral (S1) to cerebellar (granule cell layer) tactile areas of rats. *Brain Behav Evol* **18**: 1–18.

Bower JM and Woolston DC (1983) Congruence of spatial organization of tactile projections to granule cell and Purkinje cell layers of cerebellar hemispheres of the albino rat: vertical organization of cerebellar cortex. *J Neurophysiol* **49**: 745–766.

Bower JM and Kassel J (1990) Variability in tactile projection patterns to cerebellar folia crus IIa of the Norway rat. *J Comp Neurol* **302**: 768–778.

Bower JM and Beeman D (1995) The Book of GENESIS. New York: Springer-Verlag.

Bressler SL (1984) Spatial organization of EEGs from olfactory bulb and cortex.

Electroenceph Clin Neurophysiol **57**: 270–276.

Brodal A (1981) Neurological anatomy in relation to clinical medicine. New York: Oxford University Press.

Brodal P (1979) The pontocerebellar projections in the rhesus monkey: an experimental study with retrograde axonal transport of horseradish peroxidase. *Neuroscience* **4**: 193–208.

Brodal P (1982) The cerebropontocerebellar pathway: salient features of its organization. In: *The cerebellum: new vistas* (Series: *Exp Brain Res Suppl 6*), Palay SL and Chan-Palay V (eds), Berlin, New York: Springer-Verlag, pp. 108–133.

Brodal P and Bjaalie JG (1992) Organization of the pontine nuclei. *Neurosci Res* **13**: 83–118.

Byrne JA and Calford MB (1991) Short-term expansion of receptive fields in rat primary somatosensory cortex after hindpaw digit denervation. *Brain Res* **565**: 218–224.

Calford MB and Tweedale R (1988) Immediate and chronic changes in responses of somatosensory cortex in adult flying-fox after digit amputation. *Nature* **332**: 446–448.

Calford MB and Tweedale R (1991) Acute changes in cutaneous receptive fields in primary somatosensory cortex after digit denervation in adult flying fox. *J Neurophysiol* **65**: 178–187.

Chapin JK and Lin C (1984) Mapping the body representation in the SI cortex of anesthetized and awake rats. *J Comp Neurol* **229**: 199–213.

Chiaia NL, Rhoades RW, Bennett-Clarke CA, Fish SE, and Killackey HP (1991a) Thalamic processing of vibrissal information in the rat. I. Afferent input to the medial ventral posterior and posterior nuclei. *J Comp Neurol* **314**: 201–216.

Chiaia NL, Rhoades RW, Fish SE, and Killackey HP (1991b) Thalamic processing of vibrissal information in the rat. II. Morphological and functional properties of medial ventral posterior nucleus and posterior nucleus neurons. *J Comp Neurol* **314**: 217–236.

Chubbuck JG (1966) Small-motion biological stimulator. *APL Tech Dig* **5**: 18–23.

Clendenin M, Ekerot C-F, Oscarsson O, and Rosén I (1974) The lateral reticular nucleus in the cat. I. Mossy fibre distribution in cerebellar cortex. *Exp Brain Res* **21**: 473–486.

Cusick CG, Wall JT, and Kaas JH (1986) Representations of the face, teeth and oral cavity in areas 3b and 1 of somatosensory cortex in squirrel monkeys. *Brain Res* **370**: 359–364.

Cusick CG, Wall JT, Whiting JH, and Wiley RG (1990) Temporal progression of cortical reorganization following nerve injury. *Brain Res* **537**: 355–358.

Darian-Smith C and Gilbert CD (1994) Axonal sprouting accompanies functional reorganization in adult cat striate cortex. *Nature* **368**: 737–740.

Dean P, Redgrave P, and Mitchell IJ (1988) Organization of efferent projections from superior colliculus to brainstem in rat: evidence for functional output channels. In: *Vision within extrageniculo-striate systems* (Series: *Prog Brain Res, vol 75*), Hicks TP and Benedek G (eds), Amsterdam, New York: Elsevier, pp. 27–36.

Delacour J, Houcine O, and Talbi B (1987) "Learned" changes in the responses of the rat barrel field neurons. *Neuroscience* **23** (1): 63–71.

De Schutter E and Bower JM (1994) An active membrane model of the cerebellar Purkinje cell. II. Simulation of synatic responses. *J Neurophysiol* **71** (1): 401–419.

Devor M (1987) On mechanisms of somatotopic plasticity. In: *Effects of injury on trigeminal and spinal somatosensory systems*, Pubols LM and Sessle BJ (eds), New York: Liss, pp. 215–225.

Diamond ME, Armstrong-James M, and Ebner FF (1993) Experience-dependent plasticity in adult rat barrel cortex. *Proc Natl Acad Sci USA* **90**: 2082–2086.

Dichgans J (1984) Clinical symptoms of cerebellar dysfunction and their topodiagnostic significance. *Human Neurobiol* **2**: 269–279.

Doherty DW, Jacquin MF, and Killackey HP (1993) Quantitative analysis of receptive field properties in the rat nucleus Principalis. *Soc Neurosci Abstr* **19**: 327.

Durham D and Woolsey TA (1978) Acute whisker removal reduces neuronal activity in barrels of mouse SmI cortex. *J Comp Neurol* **178**: 629–644.

Elias SA, Taylor A, and Somjen G (1987) Direct and relayed projection of periodontal receptor afferents to the cerebellum in the ferret. *Proc R Soc Lond B* **231**: 199–216.

Emmers R (1965) Organization of the first and the second somesthetic regions (SI and SII) in the rat thalamus. *J Comp Neurol* **124**: 215–228.

Erzurumlu RS, Bates CA, and Killackey HP (1980) Differential organization of the thalamic projection cells in the brainstem trigeminal complex of the rat. *Brain Res* **198**: 427–433.

Florence SL, Garraghty PE, Carlson M, and Kaas JH (1993) Sprouting of peripheral nerve axons in the spinal cord of monkeys. *Brain Res* **601**: 343–348.

Frank JL (1980) Functional reorganization of cat somatic sensory-motor cortex (SmI) after selective dorsal root rhizotomies. *Brain Res* **186**: 458–462.

Fraser SE (1985) Cell interactions involved in neuronal patterning: an experimental and theoretical approach. In: *Molecular bases of neural development*, Edelman GM, Gall WE, and Cowan WM (eds), New York: Wiley, pp. 481–507.

Fraser SE and Hunt RK (1980) Retinotectal specificity: models and experiments in search of a mapping function. *Annu Rev Neurosci* **3**: 319–352.

Gao J-H, Parsons LM, Bower JM, Xiong J, Li J, Brannon S, and Fox PT (1995) Cerebellar dentate-nucleus activated by sensory and perceptual discrimination, imagined hand movement, and mental rotation of objects. *Soc Neurosci Abstr* **21**: 270.

Garraghty PE and Sur M (1990) Morphology of single intracellularly stained axons terminating in area 3b of macaque monkeys. *J Comp Neurol* **294**: 583–593.

Garraghty PE and Kaas JH (1991a) Large-scale functional reorganization in adult monkey cortex after peripheral nerve injury. *Proc Natl Acad Sci USA* **88**: 6976–6980.

Garraghty PE and Kaas JH (1991b) Functional reorganization in adult monkey thalamus after peripheral nerve injury. *NeuroReport* **2**: 747–750.

Gilbert CD and Wiesel TN (1992) Receptive-field dynamics in adult primary visual cortex. *Nature* **356**: 150–152.

González L, Shumway C, Morissette J, and Bower JM (1993) Developmental plasticity in cerebellar tactile maps: fractured maps retain a fractured organization. *J Comp Neurol* **332**: 487–498.

Hartmann MJ and Bower JM (1993) Rat cerebellar granule cell activity monitored with

chronic implants. *Soc Neurosci Abstr* **19**: 1588.

Hartmann MJ and Bower JM (1995) Cerebellar granule cell responses in the awake, freely-moving rat: the importance of tactile input. *Soc Neurosci Abstr* **21**: 1910.

Houk JC (1988) Schema for motor control utilizing a network model of the cerebellum. In: *Neural Information Processing Systems*, Anderson DZ (ed), New York: Amer Inst Physics, pp. 367–376.

Huerta MF, Frankfurter A, and Harting JK (1983) Studies of the principal sensory and spinal trigeminal nuclei of the rat: projections to the superior colliculus, inferior olive, and cerebellum. *J Comp Neurol* **220**: 147–167.

Jacquin MF and Zeigler PH (1983) Trigeminal orosensation and ingestive behavior in the rat. *Behav Neurosci* **97** (1): 62–97.

Jacquin MF, Barcia M, and Rhoades RW (1989) Structure-function relationships in rat brainstem subnucleus Interpolaris: IV. Projection neurons. *J Comp Neurol* **282**: 45–62.

Jacquin MF, Renehan WE, Rhoades RW, and Panneton WM (1993) Morphology and topography of identified primary afferents in trigeminal subnuclei Principalis and Oralis. *J Neurophysiol* **70** (5): 1911–1936.

Jaeger D and Bower JM (1994) Prolonged responses in rat cerebellar Purkinje cells following activation of the granule cell layer: an intracellular *in vitro* and *in vivo* investigation. *Exp Brain Res* **100**: 200–214.

Jain N, Florence SL, and Kaas JH (1995) Limits on plasticity in somatosensory cortex of adult rats: hindlimb cortex is not reactivated after dorsal column section. *J Neurophysiol* **73** (4):1537–1546.

Jenkins WM and Merzenich MM (1987) Reorganization of neocortical representations after brain injury: a neurophysiological model of the bases of recovery from stroke. In: *Neural regeneration* (Series: *Prog Brain Res, vol 71*), Seil FJ, Herbert E, and Carlson BM (eds), Amsterdam, New York: Elsevier, pp. 249–266.

Jenkins WM, Merzenich MM, Ochs MT, Allard T, and Guíc-Robles E (1990) Functional reorganization of primary somatosensory cortex in adult owl monkeys after behaviorally controlled tactile stimulation. *J Neurophysiol* **63** (1): 82–104.

Jensen KF and Killackey HP (1987) Terminal arbors of axons projecting to the

somatosensory cortex of the adult rat. I. The normal morphology of specific thalamocortical afferents. *J Neurosci* **7** (11): 3529–3543.

Jolicoeur P, Pirlot P, Baron G, and Stephan H (1984) Brain structure and correlation patterns in insectivora, chiroptera, and primates. *Syst Zool* **33** (1): 14–29.

Joseph JW, Shambes GM, Gibson JM, and Welker W (1978) Tactile projections to granule cells in caudal vermis of the rat's cerebellum. *Brain Behav Evol* **15**: 141–149.

Kaas JH (1991) Plasticity of sensory and motor maps in adult mammals. *Annu Rev Neurosci* **14**: 137–167.

Kaas JH (1994) The reorganization of sensory and motor maps in adult mammals. In: *The cognitive neurosciences*, Gazzaniga MS (ed), Cambridge, MA: MIT Press, pp. 51–71.

Kaas JH, Merzenich MM, and Killackey HP (1983) The reorganization of somatosensory cortex following peripheral nerve damage in adult and developing mammals. *Annu Rev Neurosci* **6**: 325–356.

Kalaska J and Pomeranz B (1979) Chronic paw denervation causes an age-dependent appearance of novel responses from forearm in "paw cortex" of kittens and adult cats. *J Neurophysiol* **42**: 618–633.

Kassel J (1980) Superior colliculus projections to tactile areas of rat cerebellar hemispheres. *Brain Res* **202**: 291–305.

Kassel J, Shambes GM, and Welker W (1984) Fractured cutaneous projections to the granule cell layer of the posterior cerebellar hemisphere of the domestic cat. *J Comp Neurol* **225**: 458–468.

Kelahan AM, Ray RH, Carson LV, and Doetsch GS (1981) Functional reorganization of adult raccoon somatosensory cerebral cortex following neonatal digit amputation. *Brain Res* **223**: 152–159.

Kelahan AM and Doetsch GS (1984) Time-dependent changes in the functional organization of somatosensory cerebral cortex following digit amputation in adult raccoons. *Somatosensory Res* **2**: 48–81.

Kennedy TT, Grimm RJ, and Towe AL (1966) The role of cerebral cortex in evoked somatosensory activity in cat cerebellum. *Exp Neurol* **14**: 13–32.

Killackey HP (1989) Static and dynamic aspects of cortical somatotopy: a critical evaluation. *J Cogn Neurosci* **1** (1): 3–11.

Killackey HP, Rhoades RW, and Bennett-Clarke CA (1995) The formation of a cortical somatotopic map. *TINS* **18** (9): 402–407.

Knudsen EI (1983a) Auditory and visual maps of space in the optic tectum of the owl. *J Neurosci* **2**: 1177–1194.

Knudsen EI (1983b) Early auditory experience aligns the auditory map of space in the optic tectum of the barn owl. *Science* **222**: 939–942.

Knudsen EI (1985) Experience alters the spatial tuning of auditory units in the optic tectum during a sensitive period in the barn owl. *J Neurosci* **5**: 3094–3109.

Knudsen EI, du Lac S, and Esterly D (1987) Computational maps in the brain. *Annu Rev Neurosci* **10**: 41–65.

Koralek K-A, Jensen KF, and Killackey HP (1988) Evidence for two complementary patterns of thalamic input to the rat somatosensory cortex. *Brain Res* **463**: 346–351.

Kossut M (1992) Plasticity of the barrel cortex neurons. *Prog Neurobiol* **39** (4): 389–422.

Landry P and Deschenes M (1981) Intracortical arborizations and receptive fields of identified ventrobasal thalamocortical afferents to the primary somatic sensory cortex in the cat. *J Comp Neurol* **199**: 354–371.

Legg CR, Mercier B, and Glickstein M (1989) Corticopontine projection in the rat: the distribution of labelled cortical shells after large injections of horseradish peroxidase in the pontine nuclei. *J Comp Neurol* **286**: 427–441.

Mantle-St.John LA and Tracey DJ (1987) Somatosensory nuclei in the brainstem of the rat: independent projections to the thalamus and cerebellum. *J Comp Neurol* **255**: 259–271.

Marfurt CF and Rajchert DM (1991) Trigeminal primary afferent projections to "non-trigeminal" areas of the rat central nervous system. *J Comp Neurol* **303**: 489–511.

Marr D (1969) A theory of cerebellar cortex. *J Physiol Lond* **202**: 437–470.

Mason CA (1987) The development of cerebellar mossy fibers and climbing fibers: embryonic and postnatal features. In: *New concepts in cerebellar neurobiology*, King JS

(ed), New York: Liss, pp. 57–88.

Mason CA and Gregory E (1984) Postnatal maturation of cerebellar mossy and climbing fibers: transient expression of dual features on single axons. *J Neurosci* **4** (7): 1715–1735.

McCandlish CA, Li CX, and Waters RS (1993) Early development of the SI cortical barrel field representation in neonatal rats follows a lateral-to-medial gradient: an electrophysiological study. *Exp Brain Res* **92** (3): 369–374.

McKinley PA and Smith JL (1990) Age-dependent differences in reorganization of primary somatosensory cortex following low thoracic (T12) spinal cord transection in cats. *J Neurosci* **10** (5): 1429–1443.

McMahan SB and Wall PD (1983) Plasticity in the nucleus gracilis of the rat. *Exp Neurol* **80**: 195–207.

Merrill EG and Wall PD (1978) Plasticity of connection in the adult nervous system. In: *Neuronal plasticity*, Cotman CW (ed), New York: Raven Press, pp. 97–111.

Merzenich MM (1987) Dynamic neocortical processes and the origins of higher brain functions. In: *The neural and molecular bases of learning*, Changeux J-P and Konishi M (eds), Chichester, New York: Wiley, pp. 337–358.

Merzenich MM, Kaas JH, Wall JT, Nelson RJ, Sur M, and Felleman D (1983a) Topographic reorganization of somatosensory cortical areas 3b and 1 in adult monkeys following restricted deafferentation. *Neuroscience* **8** (1): 33–55.

Merzenich MM, Kaas JH, Wall JT, Sur M, Nelson RJ, and Felleman D (1983b) Progression of change following median nerve section in the cortical representation of the hand in areas 3b and 1 in adult owl and squirrel monkeys. *Neuroscience* **10** (3): 639–665.

Merzenich MM, Nelson RJ, Stryker MP, Cynader MS, Schoppmann A, and Zook JM (1984a) Somatosensory cortical map changes following digit amputation in adult monkeys. *J Comp Neurol* **224**: 591–605.

Merzenich MM, Jenkins WM, and Middlebrooks JC (1984b) Observations and hypotheses on special organizational features of the central auditory nervous system. In: *Dynamic aspects of neocortical function*, Edelman GM, Gall WE, and Cowan WM (eds), New York: Wiley, pp. 397–424.

Merzenich MM, Nelson RJ, Kaas JH, Stryker MP, Jenkins WM, Zook JM, Cynader MS, and Schoppmann A (1987) Variability in hand surface representations in areas 3b and 1 in adult owl and squirrel monkeys. *J Comp Neurol* **258**: 281–296.

Metzler J and Marks PS (1979) Functional changes in cat somatic sensory-motor cortex during short term reversible epidermal blocks. *Brain Res* **177**: 379–383.

Mihailoff GA (1983) Intra- and interhemispheric collateral branching in the rat pontocerebellar system, a fluorescence double-label study. *Neuroscience* **10** (1): 141–160.

Mihailoff GA, Lee H, Watt CB, and Yates R (1985) Projections to the basilar pontine nuclei from face sensory and motor regions of the cerebral cortex in the rat. *J Comp Neurol* **237**: 251–263.

Morissette J, Posakony LG, Shumway CA, Paulin MG, and Bower JM (1990) Fractured tactile maps retain fractured somatotopy following deafferentation at different stages of development. *Soc Neurosci Abstr* **16**: 896.

Morissette J, Lee M, and Bower JM (1991) Temporal relationships between cerebral cortical and cerebellar responses to tactile stimulation in the rat. *Soc Neurosci Abstr* **17**: 1383.

Morissette J and Bower JM (1996) The contribution of somatosensory cortex to responses in the rat cerebellar granule cell layer following peripheral tactile stimulation. *Exp Brain Res* (in press).

Nakahama H, Nishioka S, and Otsuka T (1966) Excitation and inhibition in ventrobasal thalamic neurons before and after cutaneous input deprivation. *Prog Brain Res* **21A**: 180–196.

Newman DB and Ginsberg CY (1992) Brainstem reticular nuclei that project to the cerebellum in rats: a retrograde tracer study. *Brain Behav Evol* **39**: 24–68.

Nicolelis MAL, Lin RCS, Woodward DJ, and Chapin JK (1993) Induction of immediate spatiotemporal changes in thalamic networks by peripheral block of ascending cutaneous information. *Nature* **361**: 533–536.

Nord SG (1967) Somatotopic organization in the spinal trigeminal nucleus, the dorsal column nuclei and related structures in the rat. *J Comp Neurol* **130**: 343–356.

Orlovsky GN (1972) Activity of rubrospinal neurons during locomotion. *Brain Res* **46**: 99–112.

Paulin MG and Bower JM (1988) Trigeminal nerve section in neonates leaves holes in cerebellar granule cell layer tactile maps of adult rats. *Soc Neurosci Abstr* **14**: 1238.

Paulin MG, Nelson ME, and Bower JM (1989a) Neural control of sensory acquisition: the vestibulo-ocular reflex. In: *Advances in Neural Information Processing Systems, vol 1*, Touretzky D (ed), San Mateo: Morgan Kaufmann, pp. 410–418.

Paulin MG, Nelson ME, and Bower JM (1989b) Dynamics of compensatory eye movement control: an optimal estimation analysis of the vestibulo-ocular reflex. *Int J Neur Syst* **1**: 23–29.

Penfield W and Rasmussen T (1950) The cerebral cortex of man: a clinical study of localization of function. New York: Macmillan.

Phelan KD and Falls WM (1991) A comparison of the distribution and morphology of thalamic, cerebellar and spinal projection neurons in rat trigeminal nucleus Interpolaris. *Neuroscience* **40** (2): 497–511.

Pons TP, Wall JT, Garraghty PE, Cusick CG, and Kaas JH (1987) Consistent features in the representation of the hand in area 3b of macaque monkeys. *Somatosensory Res* 309–331.

Pons TP, Garraghty PE, and Mishkin M (1988) Lesion-induced plasticity in the second somatosensory cortex of adult macaques. *Proc Natl Acad Sci USA* **85**: 5279–5281.

Pons TP, Garraghty PE, Ommaya AK, Kaas JH, Taub E, and Mishkin M (1991) Massive cortical reorganization after sensory deafferentation in adult macaques. *Science* **252**: 1857–1860.

Provini L, Redman S, and Strata P (1968) Mossy and climbing fibre organization on the anterior lobe of the cerebellum activated by forelimb and hindlimb areas of the sensorimotor cortex. *Exp Brain Res* **6**: 216–233.

Ramachandran VS, Rogers-Ramachandran D, and Stewart M (1992) Perceptual correlates of massive cortical reorganization. *Science* **258**: 1159–1160.

Rasmusson DD (1982) Reorganization of raccoon somatosensory cortex following removal of the fifth digit. *J Comp Neurol* **205**: 313–316.

Rasnow B, Assad C, Nelson ME, and Bower JM (1989) Simulation and measurement of the electric fields generated by weakly electric fish. In: *Advances in Neural Information Processing Systems, vol 1*, Touretzky D (ed), San Mateo: Morgan Kaufmann, pp. 436–443.

Recanzone GH, Allard TT, Jenkins WM, and Merzenich MM (1990) Receptive-field changes induced by peripheral nerve stimulation in SI of adult cats. *J Neurophysiol* **63**: 1213–1225.

Recanzone GH, Merzenich MM, and Dinse HR (1992a) Expansion of the cortical representation of a specific skin field in primary somatosensory cortex by intracortical microstimulation. *Cerebral Cortex* **2**: 181–196.

Recanzone GH, Merzenich MM, Jenkins WM, Grajski KA, and Dinse HR (1992b) Topographic reorganization of the hand representation in cortical area 3b of owl monkeys trained in a frequency-discrimination task. *J Neurophysiol* **67**: 1031–1056.

Rhoades RW, Belford GR, and Killackey HP (1987) Receptive-field properties of rat ventral posterior medial neurons before and after selective kainic acid lesions of the trigeminal brain stem complex. *J Neurophysiol* **57**: 1577–1600.

Rhoades RW, Chiaia NL, Macdonald GJ, and Jacquin MF (1989) Effect of fetal infraorbital nerve transection upon trigeminal primary afferent projections in the rat. *J Comp Neurol* **287**: 82–97.

Rhoades RW, Wall JT, Chiaia NL, Bennet-Clarke CA, and Killackey HP (1993) Anatomical and functional changes in the organization of the cuneate nucleus of adult rats after fetal forelimb amputation. *J Neurosci* **13**: 1106–1119.

Riddle DR and Purves D (1995) Individual variation and lateral asymmetry of the rat primary somatosensory cortex. *J Neurosci* **15** (6): 4184–4195.

Robertson LT (1982) Organization of climbing fiber input from mechanoreceptors to lobule V vermal cortex of cats. *Exp Brain Res* **46**: 281–291.

Robertson LT (1987) Organization of climbing fiber representation in the anterior lobe. In: *New Concepts in Cerebellar Neurobiology*, King JS (ed), New York: Liss, pp. 281–320.

Ross SM (1987) Introduction to probability and statistics for engineers and scientists. New York: Wiley.

Schmid LM, Rosa MGP, and Calford MB (1995) Retinal detachment induces massive immediate reorganization in visual cortex. *NeuroReport* **6**: 1349–1353.

Schoen SW, Graeber MB, Toth L, and Kreutzberg JW (1991) Synaptic 5'-nucleotidase is transient and indicative of climbing fiber plasticity during the postnatal development of rat cerebellum. *Dev Brain Res* **61**: 125–138.

Schroeder CE, Seto S, Arezzo JC, and Garraghty PE (1995) Electrophysiological evidence for overlapping dominant and latent inputs to somatosensory cortex in squirrel monkeys. *J Neurophysiol* **74**: 722–732.

Shambes GM, Beermann DH, and Welker W (1978a) Multiple tactile areas in cerebellar cortex: another patchy cutaneous projection to granule cell columns in rats. *Brain Res* **157**: 123–128.

Shambes GM, Gibson JM, and Welker W (1978b) Fractured somatotopy in granule cell tactile areas of rat cerebellar hemispheres revealed by micromapping. *Brain Behav Evol* **15**: 94–140.

Sharp FR and Evans K (1982) Regional (^{14}C) 2-deoxyglucose uptake during vibrissae movements evoked by rat motor cortex stimulation. *J Comp Neurol* **208**: 255–287.

Shumway CA, Posakony LG, Morissette J, and Bower JM (1990) Possible mechanisms underlying reorganization in fractured cerebellar maps: correlations with S-1 cortical plasticity. *Soc Neurosci Abstr* **16**: 896.

Snider RS and Stowell A (1944) Receiving areas of the tactile, auditory, and visual systems in the cerebellum. *J Neurophysiol* **7**: 331–357.

Snow PJ and Wilson P (1991) Plasticity in the somatosensory system of developing and mature mammals – The effects of injury to the central and peripheral nervous system. In: *Progress in Sensory Physiology, vol 11*, Ottoson D (ed), New York: Springer-Verlag.

Snyder SH (1984) Drug and neurotransmitter receptors in the brain. *Science* **224**: 22–31.

Sotelo C (1995) Early phase in the development of the olivocerebellar projection map. In: *The cerebellum: From structure to control (Conference Proceedings)*, De Zeeuw CI, Strata P, and Voogd J (eds), pp. 8.

Stephan H, Frahm H, and Baron G (1981) New and revised data on volumes of brain structures in insectivores and primates. *Folia Primatol* **35**: 1–29.

Sugitani M, Yano J, Sugai T, and Ooyama H (1990) Somatotopic organization and columnar structure of vibrissae representation in the rat ventrobasal complex. *Exp Brain Res* **81**: 346–352.

Thach WT, Goodkin HP, and Keating JG (1992) The cerebellum and the adaptive coordination of movement. *Annu Rev Neurosci* **15**: 403–442.

Tolbert DL, Alisky JM, and Clark BR (1993) Lower thoracic-upper lumbar spinocerebellar projections in rats: a complex topography revealed in computer reconstructions of the unfolded anterior lobe. *Neuroscience* **55**: 755–774.

Udin SB and Fawcett JW (1988) Formation of topographic maps. *Annu Rev Neurosci* **11**: 289–327.

Van der Loos H and Woolsey TA (1973) Somatosensory cortex: structural alterations following early injury to sense organs. *Science* **179**: 395–398.

Verley R (1986) Reorganization of the somatosensory cerebral cortex after peripheral damage. In: *Advances in Neural Information Processing Systems, vol 1*, Touretzky D (ed), San Mateo: Morgan Kaufmann, pp. 15–19.

Waite PME (1973) Somatotopic organization of vibrissal responses in the ventro-basal complex of the rat thalamus. *J Physiol* **228**: 527–540.

Waite PME (1978) Removal of whiskers in young rats causes functional changes in cerebral cortex. *Nature* **274**: 600–602.

Waite PME (1984) Rearrangement of neuronal responses in the trigeminal system of the rat following peripheral nerve section. *J Physiol* **352**: 425–445.

Waite PME and de Permentier P (1991) The rat's postero-orbital sinus hair: I. Brainstem projections and the effect of infraorbital nerve section at different ages. *J Comp Neurol* **312**: 325–340.

Waite PME and Tracey DJ (1995) Trigeminal sensory system. In: *The rat nervous system*, Paxinos G (ed), San Diego: Academic Press, pp. 705–724.

Wall JT (1988a) Variable organization in cortical maps of the skin as an indication of the

lifelong adaptive capacities of circuits in the mammalian brain. *TINS* **11** (12): 549–557.

Wall JT (1988b) Development and maintenance of somatotopic maps of the skin: a mosaic hypothesis based on peripheral and central contiguities. *Brain Behav Evol* **31**: 252–268.

Wall JT and Egger MD (1971) Formation of new connections in adult rat brains after partial deafferentation. *Nature* **232**: 542–545.

Wall JT, Felleman DJ, and Kaas JH (1983) Recovery of normal topography in the somatosensory cortex of monkeys after nerve crush and regeneration. *Science* **221**: 771–773.

Wall JT and Cusick CG (1984) Cutaneous responsiveness in primary somatosensory (S-I) hindpaw cortex before and after partial hindpaw deafferentation in adult rats. *J Neurosci* **4** (6): 1499–1515.

Wall JT and Kaas JH (1985) Cortical reorganization and sensory recovery following nerve damage and regeneration. In: *Synaptic plasticity*, Cotman CW (ed), New York: Guiford Press, pp. 231–259.

Wall JT and Cusick CG (1986) The representation of peripheral nerve inputs in the S-I hindpaw cortex of rats raised with incompletely innervated hindpaws. *J Neurosci* **6** (4): 1129–1147.

Wall JT, Kaas JH, Sur M, Nelson RJ, Felleman DJ, and Merzenich MM (1986) Functional reorganization in somatosensory cortical areas 3b and 1 of adult monkeys after median nerve repair: possible relationships to sensory recovery in humans. *J Neurosci* **6** (1): 218–233.

Watson CRR and Switzer III RC (1978) Trigeminal projections to cerebellar tactile areas in the rat origin mainly from N. Interpolaris and N. Principalis. *Neurosci Let* **10**: 77–82.

Welker C (1971) Microelectrode delineation of fine grain somatotopic organization of SmI cerebral neocortex in albino rats. *Brain Res* **26**: 259–275.

Welker W (1973) Principles of organization of the ventrobasal complex in mammals. *Brain Behav Evol* **7**: 253–336.

Welker W (1987) Spatial organization of somatosensory projections to granule cell cerebellar cortex: functional and connectional implications of fractured somatotopy (summary of Wisconsin studies). In: *New Concepts in Cerebellar Neurobiology*, King

JS (ed), New York: Liss, pp. 239–280.

Welker W and Shambes GM (1985) Tactile cutaneous representation in cerebellar granule cell layer of the opossum, *Didelphis virginiana*. *Brain Behav Evol* **27**: 57–79.

Welker W, Blair C, and Shambes GM (1988) Somatosensory projections to cerebellar granule cell layer of giant bushbaby, *Galago crassicaudatus*. *Brain Behav Evol* **31**: 150–160.

Weller WL and Johnson JI (1975) Barrels in cerebral cortex altered by disruption in newborn but not five-day-old mice. *Brain Res* **83**: 504–508.

Wilson MA, Bhalla US, Uhley JD, and Bower JM (1989) GENESIS: a system for simulating neural networks. In: *Advances in Neural Information Processing Systems, vol 1*, Touretzky D (ed), San Mateo: Morgan Kaufmann, pp. 485–492.

Wilson MA and Bower JM (1992) Cortical oscillations and temporal interactions in a computer simulation of piriform cortex. *J Neurophysiol* **67** (4): 981–995.

Wise SP and Jones EG (1977) Cells of origin and terminal distribution of descending projections of the rat somatic sensory cortex. *J Comp Neurol* **175**: 129–158.

Woolsey CN (1958) Organization of somatic sensory and motor areas of the cerebral cortex. In: *Biological and biochemical bases of behavior*, Harlow HF and Woolsey CN (eds), Madison: University of Wisconsin, pp. 63–82.

Woolsey TA (1990) Peripheral alteration and somatosensory development. In: *Development of sensory systems in mammals*, Coleman JR (ed), New York: Wiley, pp. 461–516.

Woolsey TA and Van der Loos H (1970) The structural organization of layer IV in the somatosensory region (SI) of mouse cerebral cortex. The description of a cortical field composed of discrete cytoarchitectonic units. *Brain Res* **17**: 205–242.

Woolsey TA and Wann JR (1976) Areal changes in mouse cortical barrels following vibrissal damage at different postnatal ages. *J Comp Neurol* **170**: 53–66.

Woolston DC, Kassel J, and Gibson JM (1981) Trigeminocerebellar mossy fiber branching to granule cell layer patches in the rat cerebellum. *Brain Res* **209**: 255–269.

Woolston DC, La Londe JR, and Gibson JM (1982) Comparison of response properties of cerebellar- and thalamic-projecting interpolaris neurons. *J Neurophysiol* **48**: 160–173.

Zeigler PH (1973) Trigeminal deafferentation and feeding in the pigeon: sensorimotor and motivational effects. *Science* **182**: 1155–1158.

Zeigler PH, Semba K, and Jacquin MF (1984) Trigeminal reflexes and ingestive behavior in the rat. *Behav Neurosci* **98** (6): 1023–1038.

Zeigler PH, Jacquin MF, and Miller MG (1985) Trigeminal orosensation and ingestive behavior in the rat. *Prog Psychobiol Physiol Psychol* **11**: 63–196.